NUI MAYNOOTH
Ollscoil na hÉireann Má Nuad

Fondúireacht Eolaíochta Éireann
Science Foundation Ireland

The role of the DEAD box Helicase DDX3X in Anti-Viral Signalling Pathways Mediated by the Kinase IKKα.

Anthony Fullam B.A. (mod)
October 2013

A thesis submitted to: The National University of Ireland, Maynooth for the degree of Doctor of Philosophy

Research carried out in the Department of Biology, National University of Ireland, Maynooth

Head of Department: Paul Moynagh
Supervisor: Dr. Martina Schröder

This work was funded by Science Foundation Ireland

(Research Frontiers Grant (09/RFP/BIC2188))

Contents

Table of Contents 2

Abstract 6

Acknowledgements 7

List of Tables 8

List of Figures 9

List of Abbreviations 14

1 Introduction 21

1.1 The Human Immune System 21

1.2 Immune response to viruses 24

1.2.1 Anti-Viral Pattern Recognition Receptors 25

1.3 TLR 3/7/8/9 – The Anti-Viral TLRs 36

1.4 NF-κB 40

1.4.1 Canonical NF-κB Pathway 43

1.4.2 The Alternative NF-κB Pathway 43

1.5 DExD/H-box RNA Helicases 47

1.5.1 Helicases in Innate Immunity 51

1.6 Aims of this Study 59

2 Materials And Methods 62

2.1 Standard Laboratory Procedures 63

2.2 Cell Culture 63

2.2.1 Long term storage of cells 64

2.2.2 Transfection 64

2.2.3 shRNA Cells 66

2.2.4 Cell treatments 66

2.3 Luciferase Reporter Gene Assay 67

2.4 Co-Immunoprecipitations 68

2.5 SDS-PAGE and Western Blotting 69

2.5.1 SDS-PAGE 69

2.5.2 Western Blotting 69

2.5.3 Chemiluminescence detection 70

2.6 Blue Native Page 71

2.7 Competent Cell Preparation 73

2.7.1 Transformation of chemically competent cells 73

2.7.2 Large scale DNA preparation 74

2.8 Protein Work 75

2.8.1 Production of recombinant 6His-tagged and GST-tagged proteins in BL21 Ecoli 75

2.8.2 Coomassie staining 76

2.8.3 In vitro pulldown assay 76

2.8.4 Kinase assay 76

2.9 Statistical analysis. 77

2.10 Antibodies 78

2.11 Recipies 79

2.11.1 Lysis Buffers 79

2.11.2 General Reagents 81

2.11.3 Reagents for protein work 85

2.11.4 Reagents for Blue-Native PAGE 87

2.11.5 SDS PAGE Gels 90

3 Results 91

3.1 DDX3 interacts directly with IKKα and enhances its activation 92

3.1.1 Summary 97

3.2 DDX3 enhances IKKα activation 98

3.2.1 Summary 103

3.3 The effects of DDX3 on the alternative NF-κB pathway 104

3.3.1 DDX3 enhances processing of p100 104

3.3.2 DDX3 interacts with NF-κB subunits 110

3.3.3 Summary 112

3.4 Effects of DDX3 on TLR7 signalling 113

3.4.1 DDX3 is involved in IFN induction downstream of TLR7 113

3.4.2 DDX3 enhances IRF7 activation 117

3.4.3 Summary 121

3.5 DDX3 enhances the IKKα interaction with NIK and IRF7 122

3.5.1 Summary 125

3.6 DDX3 phosphorylation by the IKKs and IKK related kinases 126

3.6.1 Summary 147

3.7 Using Blue-Native PAGE for the isolation of Multi-Protein complexes .. 148

3.7.1 Introduction 148

3.7.2 Establishing conditions for BN-PAGE experiments 152

3.7.3 Aim 156

3.7.4 Results 157

3.7.5 Summary 162

4 Discussion 163

4.1 The effect of DDX3 on IKKα activity 164

4.2 DDX3 enhances signalling downstream of IKKα 167

4.3 DDX3 acts as a scaffold protein? 170

4.4 The effect of IKKα on DDX3 175

4.5 Relevance of the IKKα-DDX3 interaction in disease 178

4.6 Conclusion 181

5 References 182

6 Appendix 201

6.1 Publications 202

6.2 DDX3 siRNA sequence 203

Abstract

The human DEAD-box RNA helicase DDX3X has previously been shown to be involved in innate immune signalling in pathways mediated by IKKε and TBK1. In this work we show that DDX3X is also involved in pathways independent of these kinases, and functions by interacting with two related kinases IKKα and NIK. DDX3X enhances the activation of IKKα and subsequently, augments the activation of pathways that IKKα regulates. We show that DDX3 is involved in two important signalling pathways that are mediated by IKKα – the alternative NF-κB pathway and the TLR7 signalling pathway to type I IFN induction. We propose that DDX3X acts as a scaffolding protein that brings together IKKα and its substrates.

Acknowledgements

First of all I have to thank Dr. Martina Schröder for her unending help and guidance, I could not have gotten to this stage without you, I can't thank you enough for putting up with me for four whole years!

I also have to thank everyone in the lab – Ruth, Daniella, Yvette, Lili and the newbies Rossella and Susan – everyone in the cell-signalling lab. Without you guys to annoy and to listen to my constant whining I probably would have quit a long time ago ☺.

Of course I can't forget Mam and Dad who have never stopped supporting me all these many years, Thanks guys!

Am Ende möchte ich mich bei Romina bedanken. In den letzten 4 Jahren hattest du mehr Geduld, als ich es jemals für möglich gehalten hätte. Deine Motivation und dein Rat waren mir eine unglaublich große Hilfe.

List of Tables

Table 1: List of the ten known human Toll-Like Receptors. 26

Table 2 The typical motifs of DEAD-box helicases and their function. 49

Table 3: Composition of Stacking SDS-PAGE gel. 90

Table 4: Composition of Resolving SDS-PAGE gel 90

Table 5: DDX3 is phosphorylated by IKKα on distinct residues from IKKε. 141

Table 6: siRNA sequence and Identifier (Invitrogen) 203

List of Figures

Figure 1: Overview of the main signalling pathways induced by the key anti-viral pattern recognition receptors. 29

Figure 2: The TLR 7/8/9 signalling pathways to NF-κB and IRF activation. 37

Figure 3: Overview of NF-κB activation, showing the canonical NF-κB pathway (left), the "hybrid" pathway (centre) and the alternative NF-κB signalling pathway (right). 41

Figure 4 The nine motifs typical of DEAD-box helicases (Cordin et al. 2006). .. 47

Figure 5 Sequence of DDX3 showing 9 conserved motifs highlighted in red with the D-E-A-D motif in yellow (Cordin et al. 2006; Ota et al. 2004). 52

Figure 6: IKKα is a key kinase involved in both the alternative NF-κB pathway and TLR 7/8/9 signalling to IFN activation. 61

Figure 7: DDX3 co-immunoprecipitates with IKKα. 92

Figure 8: DDX3 co-immunoprecipitates with NIK. 93

Figure 9: DDX3 directly interacts with IKKα. 94

Figure 10: IKKα interacts with the N-terminal region of DDX3. 95

Figure 11: IKKα interacts with the region between aa 139 to 172 of DDX3. 96

Figure 12: Endogenous DDX3 and IKKα interaction induced by the TLR7/8 ligand CLO75. 97

Figure 13: DDX3 enhances IKKα auto-phosphorylation in its activation loop. 98

Figure 14: DDX3 enhances IKKα phosphorylation in its activation loop. 99

Figure 15: Knockdown of DDX3 both reduces and delays IKKα activation....102

Figure 16: The alternative NF-κB pathway can be induced by CLO75, SeV and TNFα.....104

Figure 17: DDX3 induces a smear in p100 and increases levels of p52.....105

Figure 18: DDX3 enhances p100 processing.....107

Figure 19: DDX3 knockdown reduces NIK-IKKα induced phosphorylation and processing of p100. 108

Figure 20: Knockdown of DDX3 reduces CLO75 induced p100 phosphorylation.....109

Figure 21: DDX3 interacts with p52 and p65. 110

Figure 22: DDX3 constitutively interacts with p100 and p65. 111

Figure 23: DDX3 mediates induction of IFNα4 and IFNβ by NIK/IKKα. 114

Figure 24: DDX3 enhances IFNα4 and IFNβ induction following CLO75 stimulation. 115

Figure 25: Knockdown of DDX3 may decrease induction of IFNα4 and IFNβ. 116

Figure 26: DDX3 enhances phosphorylation of IRF7 by IKKα. 117

Figure 27: DDX3 enhances IRF7 Ser471/472 phosphorylation induced by NIK/IKKα. 118

Figure 28: DDX3 knockdown reduces IRF7 phosphorylation induced by NIK/IKKα. 119

Figure 29: Knockdown of DDX3 reduces IRF7 phosphorylation induced by CLO75. 120

Figure 30: DDX3 co-immunoprecipitates with IRF7.....121

Figure 31: K7 reduces the interaction between NIK and IKKα. 122

Figure 32: Knockdown of DDX3 reduces the interaction between NIK and IKKα. 123

Figure 33: K7 reduces the interaction between IKKα and IRF7.....124

Figure 34: Higher molecular weight forms of DDX3 are observed in the presence of the IKKs and IKK related kinases. 126

Figure 35: DDX3 is phosphorylated by IKKα, IKKβ and IKKε but not NIK. 127

Figure 36: K7 inhibits the phosphorylation of DDX3 by IKKα.....129

Figure 37: IKKα phosphorylates DDX3 on multiple sites.....131

Figure 38: IKKα still strongly phosphorylates the S102A DDX3 alanine mutant. 133

Figure 39: Both IKKα and IKKε phosphorylate DDX3 on serine 71. 134

Figure 40: Mutation of serines on DDX3 does not affect IFNβ induction downstream of NIK/IKKα.....136

Figure 41: Mutation of serines on DDX3 does not affect IFNβ induction downstream of CLO75 stimulation. 137

Figure 42: Mutation of serines on DDX3 does not affect IFNα4 induction downstream of NIK/IKKα.....138

Figure 43: Mutation of serines on DDX3 does not affect IFNα4 induction downstream of CLO75 stimulation. 139

Figure 44: Cartoon representation of phosphorylation sites in the N-terminal region of DDX3.....141

Figure 45: Mutation of serines on DDX3 affects IFNβ induction downstream of NIK/IKKα. 143

Figure 46: Mutation of serines on DDX3 affects IFNb induction downstream of CLO75 stimulation. 144

Figure 47: Mutation of serines on DDX3 affects IFNα4 induction downstream of NIK/IKKα. 145

Figure 48: Mutation of serines on DDX3 affects IFNa4 induction downstream of CLO75 stimulation. 146

Figure 49: Principle of first and second dimension BN-PAGE.....151

Figure 50: The effect of running a sample with a high ionic strength 153

Figure 51: The effect of having protein and/or detergent concentration that is too high. 154

Figure 52: Showing the best conditions for BN-PAGE for DDX3.....155

Figure 53: DDX3 redistributes into higher molecular weight bands upon Sendai virus stimulation. 157

Figure 54: DDX3 appears as two distinct bands in unstimulated cells. 158

Figure 55: DDX3 changes its banding pattern upon short SeV stimulation. ...159

Figure 56: The higher sized bands containing DDX3 disappear upon boiling samples with SDS. 160

Figure 57: DDX3 may exist as monomer, dimer, trimer and tetramer species. 161

List of Abbreviations

Abbreviation	Meaning
AIM2	Absent In Melanoma 2
AMP	Adenosine Mono-Phosphate
APC	Antigen Presenting Cell
ATP	Adenosine triphosphate
BAFF	B-cell activating factor of the TNF family
BAFFR	B-cell activating factor of the TNF family receptor
BN	Blue Native
BN-PAGE	Blue Native Polyacrylamide Gel Electrophoresis
BSA	Bovine Serum Albumin
CARD	Caspase Activation and Recruitment Domain
CBP	CREB Binding Protein
CD4	Cluster of Differentiation 4
CD40	Cluster of Differentiation 40
CD8	Cluster of Differentiation 8

CREB	cAMP response element-binding protein
CRM1	Chromosome Region Maintainance 1
DAI	DNA-dependent Activator of IFN regulatory factors
DC	Dendritic Cell
DDX	DEAD-box Helicase
DMEM	Dulbecco's Modified Eagle Medium
DMSO	Dimethyl sulfoxide
DNA	Deoxyribonucleic acid
dsDNa	Double-stranded Deoxyribonucleic acid
dsRNA	Double-stranded Ribonucleic acid
DTT	Dithiothreitol
ECL	Enhanced Chemoluminescence
EDTA	Ethylenediaminetetraacetic acid
EGTA	Ethylene Glycol Tetraacetic Acid
FCS	Foetal Calf Serum
GST	Glutathione *S*-transferases
GTP	Guanosine-5'-triphosphate

HBS	HEPES Buffered Saline
HBV	Hepatitis B Virus
HBV pol	HBV polymerase
HCC	Hepatocellular Carcinoma
HCL	Hydrochloric Acid
HCV	Hepatitis C Virus
HEK	Human Embryonic Kidney (cells)
HIV	Human Immunodeficiency Virus
HRP	Horse Radish Peroxidase
HSV	Herpes Simplex Virus
HVEM	HSV Entry Mediator
IFN	Interferon
IKK	IκB Kinase
IPS-1	MAVS
IPTG	Isopropyl β-D-1-thiogalactopyranoside
IRAK	IL-1R associated kinases
IRF	Interferon Regulatory Factor

ISG	Interferon Stimulated Gene
IκB	Inhibitor of κB
JAK	Janus Kinase
LB	Luria Bertani
LGP2	Laboratory of Genetics and Physiology 2
LIGHT	homologous to LT, inducible expression, competes with herpes simplex virus (HSV) glycoprotein D for HSV entry mediator (HVEM), a receptor expressed on T lymphocytes
LRRFIP1	Leucine-rich repeat flightless-interacting protein 1
LTβR	Lymphotoxin-β receptor
LTβR	Lymphotoxin-β
MAP	Mitogen Activated Protein
MAPK	Mitogen Activated Protein Kinase
MAVS	Mitochondrial antiviral-signalling protein (IPS-1)
MDA5	Melanoma Differentiation-Associated protein 5
mDC	Myeloid Dendritic Cell
MHC	Major Histocompatobility Complex
MKK	Mitogen Activated Protein Kinase Kinase

mRNA	Messenger RNA
MyD88	Myeloid Differentiation gene 88
NEMO	NF-kappa-B essential modulator
NES	Nuclear Export Signal
NF-κB	Nuclear Factor Kappa-light-chain-enhancer of activated B cells
NIK	NF-κB Inducing Kinase
NK	Natural Killer (cell)
NSC	Non-Silencing Control
NTP	Nucleoside triphosphate
OD	Optical Density
PAMP	Pathogen Associated Molecular Pattern
pDC	Plasmacytoid Dendcitic Cell
PRR	Pathogen Recognition Receptor
PVDF	Polyvinylidene fluoride
REN	Ring Expanded Nucleoside
RIG-I	Retinoic acid-Inducible Gene 1
RLH	RIG-I Like Helicase

RNA	Ribonucleic acid
RRE	Rev Responsive Element
SARM	Sterile-α and Armadillo Motif containing protein
SDS	Sodium Dodecyl Sulfate
SDS-PAGE	SDS- Polyacrylamide Gel Electrophoresis
SeV	Sendai Virus
SFM	Serum Free Medium
SHP-1	Src homology region 2 domain-containing phosphatase-1
shRNA	Short Hairpin RNA
siRNA	Small Interfering RNA
SOC	Super Optimal Broth with Catabolite repression
ssDNA	Single-stranded Deoxyribonucleic acid
ssRNA	Single-stranded Ribonucleic acid
STAT	Signal Transducer and Activator of Transcription
STING	Stimulator of Interferon Genes
TAB 1	TAK1 binding protein 1
TAB 2	TAK1 binding protein 2

TAD	Transactivation Domain
TAK	TGF-β activated kinase
TB	Transformation Buffer
TBK1	TANK-Binding Kinase-1
TBS	Tris Buffered Saline
TBST	TBS Tween
TIRAP	TIR domain containing Adaptor Protein (Mal)
TLR	Toll Like Receptor
TNF	Tumor Necrosis Factor
TNFα	Tumor Necrosis Factor alpha
TRAF	TNF Receptor Associated Factor
TRAM	TRIF-Related Adaptor Molecule
TRIF	TIR-domain-containing adaptor-inducing interferon-β
β-TrCP	β-Transducin repeat Containing Protein

1 Introduction

1.1 The Human Immune System

The human immune system is a complex multifaceted system that is able to adapt and adjust in response to almost any threat it may encounter, including bacterial, fungal, viral and parasitic infections. It must be able to distinguish between 'self' and 'non-self'. It must recognise when a pathogen is present, mount an effective, but regulated, response and finally bring that response to an end, with as little damage to self as possible. The immune system is generally considered to consist of two main parts: the innate and the adaptive system.

The innate response is non-specific in nature and is typically the first line of defence against pathogens. The skin and mucosal layers are the first physical barrier against incursion. They both function by attempting to prevent initial entry; the skin, by constantly shedding epithelial cells taking any bacteria present with them, and the mucosal layers, which are chemical barriers that protect epithelial layers, by stopping microorganisms from adhering.

The next level of defence, if the initial physical barriers have been broken through, is the complement system. Complement is a key part of both the innate and the adaptive immune response. It results in the destruction of pathogen, either directly by lysis of susceptible microbes, or indirectly by opsonisation, or enhancement of the antibody mediated response.

If the pathogen is not destroyed immediately by complement, the cells of the innate immune system come into play. There are a number of innate immune cells, including macrophages, dendritic cells, Natural Killer (NK) cells, neutrophils,

eosinophils, basophils and mast cells. Macrophages and dendritic cells (DCs) possess pattern recognition receptors (PRRs) which recognise conserved structures that are found on a wide range of pathogens, so-called "pathogen associated molecular patterns" (PAMPS). Each PRR specifically recognises particular PAMPs; this recognition induces signalling pathways and forms the basis for one of the most important parts of the innate immune system. These PRR-induced signalling pathways promote inflammation by inducing the production of inflammatory mediators which can establish a response to clear the infection. This is primarily done by attracting other leukocytes to the site of infection. This is achieved, for example, by dilating blood vessels to increase blood flow to the area and allowing extravasation of leukocytes from blood vessels into the surrounding tissue, or by releasing chemoattractants, which guide the leukocytes in, and by releasing cytokines that activate them. Neutrophils are the most common leukocyte and are usually the first cells to appear at the site of infection. They possess granules which contain toxic substances that can damage pathogens. They are known (along with macrophages and dendritic cells) as phagocytic cells, which can engulf the pathogen and degrade it. Eosinophils and basophils also contain granules, and are usually associated with parasitic infections and allergic reactions. As parasites are usually too large to be taken up by cells, these cells instead release their granules onto the parasite. Another important type of innate cell is the natural killer (NK) cell. The NK cell releases its granules onto the surface of the target cell; inducing apoptosis and thereby killing both the cell and any viruses inside.

While the innate immune system is an immediate response, it does not act alone: the adaptive response takes over when it has had the time to build up cell numbers specific to the antigen. Macrophages and DCs are professional antigen-presenting

cells (APCs) which serve as a bridge between the innate and adaptive systems. They can phagocytose microbes, break them down and present the peptides on Major Histocompatibility Complex (MHC) molecules to cells of the adaptive system for specific recognition, thereby amplifying the immune response. In addition, PRR stimulation upregulates co-stimulatory molecules that are needed for activation of T-cells and induces cytokines that shape T-cell differentiation.

The adaptive part of the immune system is important because it can give a more specific and stronger response to a particular antigen. A key aspect of the adaptive response is immunological memory, whereby the immune system 'remembers' a particular antigen and mounts a stronger and quicker response if re-infected. The major types of cells involved are B cells and T cells. If a CD8+ T-cell recognises an MHC-I/Peptide complex it will differentiate into a cytotoxic T-cell that can induce apoptosis and kill infected cells directly. Apoptosis of infected cells limits the time viruses have to replicate, reduces the number of virions produced and can interrupt cycles of latency and reactivation in persistent viruses. Recognition of an MHC-II/Peptide complex by CD4+ T-cells results in their differentiation into T helper cells, which can release cytokines and activate macrophages and B cells. B cells produce antibodies that are specific for a particular antigen. Once a B cell is presented with its specific antigen it differentiates into plasma cell, which will produce a great quantity of antibodies for the specific antigen. When activated, both T and B cells will also differentiate into memory cells that can be activated rapidly if re-infection occurs.

1.2 Immune response to viruses

Even though the immune system can be challenged by a wide range of pathogens, one that is of particular interest to us is viral infection. Viruses have co-evolved with their natural hosts for millions of years (Koonin et al. 2006) and, as such, have evolved many strategies to subvert host immune responses to allow their replication and proliferation (Holmes 2007). There are particular aspects of the immune system that are important in the response to viruses. Although the adaptive branch is significant, of particular interest to us is the initial innate response that is mediated primarily by PRRs. There are a number of families of PRRs, the most relevant to viral infections are the Toll like receptors (TLRs), RIG like Helicase receptors (RLHs) and cytoplasmic DNA receptors (Thompson et al. 2011). A common outcome from all these anti-viral PRRs is the activation of IKK family members which subsequently can activate transcription factors such as NF-κB family members or Interferon Regulatory Factors (IRFs) (Colonna 2007), that will induce production of anti-viral mediators.

The IKK family consists of 4 members, the canonical IKKs, IKKα and IKKβ, and the IKK-related kinases IKKε and TBK1. The IKK-related kinases are best known for their involvement in type 1 interferon induction by phosphorylating IRF3 and IRF7 (Hemmi et al. 2004; Sharma et al. 2003; Fitzgerald, McWhirter, et al. 2003), and the canonical kinases are best known for their role in the classical NF-κB pathway where they induce degradation of the inhibitory IκB subunit.

1.2.1 Anti-Viral Pattern Recognition Receptors

1.2.1.1 Toll-Like Receptors

There are 10 known TLR proteins found in humans, named TLR 1-10, these receptors each recognise a particular PAMP found on invading pathogens. TLRs are named after the *Drosophila melanogaster* protein Toll, which was first discovered in 1985 as being a key player in the establishment of dorsal-ventral polarity in embryo development (Anderson et al. 1985). Involvement of the Toll protein in host-defence only came to light in 1996 when it was shown to be involved in expression of the antifungal peptide, drosomycin (Lemaitre et al. 1996). At this time it was noted that there were similarities between Toll signalling and IL-1 signalling in humans and it wasn't long until a homologue for the Toll protein was found in humans (Medzhitov et al. 1997). Since then there has been an immense amount of work carried out identifying the other TLRs and characterising the pathways that they induce. The 10 TLRs and some of their ligands are listed in

Table 1.

Toll-Like receptor	Ligand	Cellular location	PAMP Possession
TLR1/2 dimer	Triacyl lipopeptide	Outer membrane	Bacteria/Fungi
TLR2/6 dimer	Diacyl lipopeptide	Outer membrane	Bacteria/Fungi
TLR3	Double stranded RNA	Endosomes	Viruses
TLR4	LPS	Outer membrane	Bacteria
TLR5	Flagellin	Outer membrane	Bacteria
TLR7	Single stranded RNA	Endosomes	Viruses
TLR8	Single stranded RNA	Endosomes	Viruses
TLR9	CpG DNA	Endosomes	Bacteria/Viruses
TLR10	Unknown		

Table 1: List of the ten known human Toll-Like Receptors.

The cellular location of each TLR is listed along with their cognate ligand and the pathogens that possess these ligands (Chang 2010; Kawai & Akira 2010).

1.2.1.1.1 TLR Adaptors

The TLRs belong to the IL-1R/TLR superfamily, all of which possess cytoplasmic Toll/IL-1R receptor (TIR) domains (Watters et al.). These domains are essential for mediating the downstream signals induced by TLR receptor engagement. They mediate a homotypic interaction between the receptors and TIR domain containing adaptor proteins. Differential recruitment of these adaptors confers the specificity of signalling pathways that are induced following TLR–ligand binding, by providing a linker between TLR and downstream kinases, forming a signalling complex (Ve et al. 2012). Myeloid Differentiation gene 88 (MyD88) was the first adaptor to be found and is related to the IL-1R and the drosophila *Toll* gene (Hultmark 1994). MyD88 possesses a C-terminal TIR domain, which mediates its interaction with the TLRs, and an N-terminal death domain that interacts with a family of kinases known as the IL-1R associated kinases (IRAKs) (Wesche et al. 1997; Muzio et al. 1997). MyD88 mediates signalling from all TLRs except TLR3 (Alexopoulou et al. 2001), which can induce downstream signalling events, including NF-κB activation, independent of MyD88. TLR3 instead uses the adaptor TIR-domain-containing adaptor-inducing interferon-β (TRIF) (Yamamoto et al. 2002). TLR4 also induces a MyD88-independent pathway, which uses TRIF along with another adaptor known as TRIF-related adaptor molecule (TRAM) (Fitzgerald, Rowe, et al. 2003). There are additional adaptor proteins, including Mal (also known as TIRAP, TIR domain containing adaptor protein), which associates with TLR4 and TLR2, and serves as a bridge to recruit MyD88 (O'Neill & Bowie 2007), and sterile-α and armadillo motif containing protein (SARM) (O'Neill et al. 2003), which is a negative regulator of TRIF dependent signalling (Fitzgerald et al. 2001; Horng et al. 2001; Bernard & O'Neill 2013; Carty et al. 2006).

1.2.1.1.2 TLR signalling to NF-κB activation

The recruitment of MyD88 via its TIR domain frees its death domain which allows it to act as a scaffold protein for IRAK proteins, including IRAK 1,4 and 2, via their own corresponding death domains (Neumann et al. 2008). A complex known as the Myddosome is formed (Motshwene et al. 2009) which consists of six MyD88, four IRAK4 and four IRAK2 death domains in a left-handed helix formation (Lin et al. 2010). This complex, as of yet only observed in vitro, appears to be sequentially formed, with MyD88 subunits oligomerising first, forming a platform allowing IRAK4 to bind and oligomerise followed by IRAK2 (Lin et al. 2010). As there are a number of MyD88 subunits involved, binding of more than one MyD88-dependent TLR may occur, which could allow synergistic signalling in response to varied stimuli (Gay et al. 2011). The regions of IRAK2 that interact with this structure are conserved in IRAK1 also, and it has been suggested that they may be interchangeable in this complex (Lin et al. 2010). IRAK4 is essential for signalling from TLR 7/8/9 (Yang et al. 2005) and its phosphorylation and activation of IRAK1 induces IRAK1 to dissociate from the complex and bind to TRAF6 (Li et al. 2002) (**Figure *1***). IRAK2 appears to be more important for sustained NF-κB and MAPK activation (Kawagoe et al. 2008) while IRAK 1 seems to be important for TLR 7/9 signalling to IFNα induction (Uematsu et al. 2005). IRAK proteins, with the exception of IRAK4, also contain at least one C-terminal domain that mediates an interaction with TRAF6 (Ye et al. 2002).

TRAF6 itself mediates an interaction with a complex consisting of TGF-β activated kinase (TAK1) and TAK1 binding proteins 1 and 2 (TAB 1 and 2) and, following ubiquitination of TRAF6 and TAK1 and a series of phosphorylation steps, TAK1 is activated (Wang et al. 2001). TAK1 can then phosphorylate IKKβ, which activates a

complex known as the IKK complex, resulting in the activation of NF-κB (**Figure *1***, section:1.4).

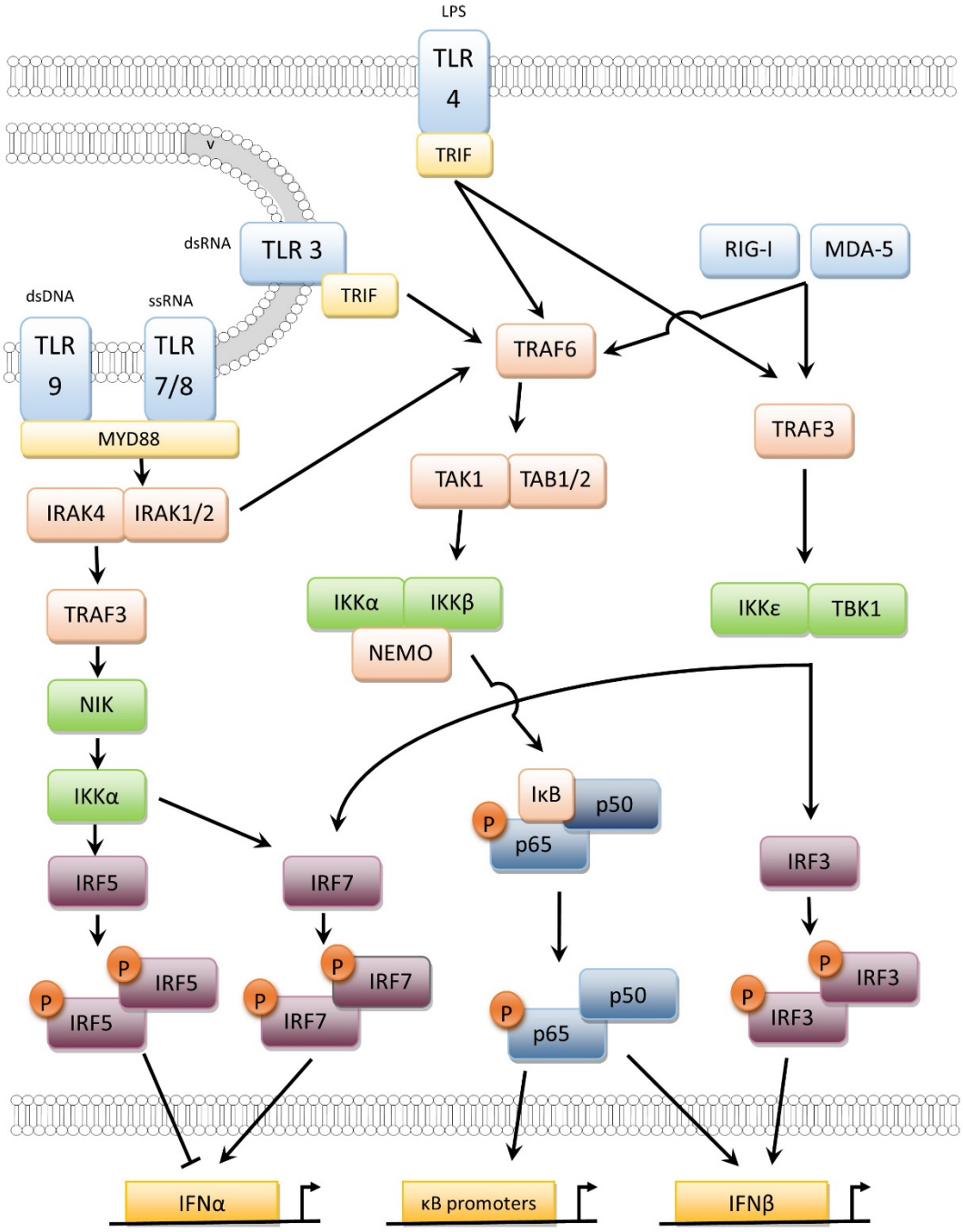

Figure 1: Overview of the main signalling pathways induced by the key anti-viral pattern recognition receptors.

1.2.1.1.3 TLR signalling to IRF activation

All TLRs signal to NF-κB activation (Doyle & O'Neill 2006), but it is not the only pathway that can be induced in response to TLR stimulation. For example, MAP kinase kinases like MKK4 and MKK3/6 can also be activated (Moriguchi et al. 1996), which results in p38 MAPK and JNK activation and subsequently activation of the transcription factor AP-1, which regulates the expression of effector cytokines such as IL-8 and TNFα (Zhong & Kyriakis 2007). Other key pathways that are induced downstream of TLRs are those that are mediated by the interferon regulatory factor (IRF) transcription factor family. The IRFs are important in the response to viruses and are responsible for the induction of a wide range of genes, especially those involved in mounting an anti-viral immune response, the most important of which, are the type 1 IFNs, IFNα and IFNβ.

IFNs can regulate both the innate and adaptive immune responses, and are one of the main mediators in the defence against viral infections (van den Broek et al. 1995). There are three main types of interferon: Type 1, which includes 13 subtypes of IFN-α, IFN-β, IFN-ω and IFN-τ; type 2, which only includes IFN-γ; and type 3, consisting of 3 subtypes of IFN-λ (Kotenko et al. 2003). Most cell types can produce IFN-α and IFN-β in response to viral infection, but IFN-γ is produced only by certain immune cells such as NK cells, CD4+ T helper 1 (T_h1) cells and CD8+ cytotoxic T cells (Katze et al. 2002). IFN-α and IFN-β are secreted by infected cells and bind to interferon receptors on surrounding cells. This triggers signalling by the Janus kinase/signal transducer and activator of transcription (JAK/STAT) pathway, inducing an antiviral state in uninfected cells. This will contribute to further IFN-α and IFN-β synthesis, generating a positive feedback loop (Marié et al. 1998). The effects that IFNs have are numerous; experiments have shown that they differentially

regulate hundreds of genes, which are known as interferon stimulated genes (ISGs) (Der et al. 1998). The ISGs mediate the anti-viral effects of IFNs, with their effects ranging from inhibition of viral replication to production of inflammatory mediators.

When IRF3, 5 or 7 have been activated by phosphorylation, a conformational change occurs which exposes their IRF association domain that is normally masked by an autoinhibitory domain (Chen & Royer 2010). This allows them to homo- or hetero-dimerise with another IRF (Barnes et al. 2003; Lin et al. 2000), translocate into the nucleus and, along with co-activators such as CBP and NF-κB, induce type 1 IFN. Each IRF induces a different set of genes depending on the cellular context (Barnes et al. 2004). IRF7 is one of the most important IRFs in the context of antiviral immunity along with IRF3 and IRF5. IRF3 is constitutively expressed while IRF7 is present at very low levels in all cells except pDCs, with a half-life of approximately 5 hours (and IRF3 with a half-life of greater than 60 hours) (Prakash & Levy 2006). In the early phase of an anti-viral response, IFNβ and IFNα4 are produced which form a positive feedback loop, further inducing production and activation of IRF7, which will itself go on to induce more IFNβ along with IFNα1,2,4,5 (Sato et al. 2000; Marié et al. 1998). However in the case of IRF7-IRF5 heterodimers this appears to be inhibitory for IFNα induction (Barnes et al. 2003).

IRF7 is involved in both IFNα and IFNβ expression, with IFNα4 being dependent on IRF7 and independent of IRF3, while IRF3 is mainly involved in controlling IFNβ (Sato et al. 2000). The IFNB promoter contains binding sites for NF-κB, IRF3/7 and ATF2/c-Jun. Stimulation of IFNβ induction requires both IRF3/7 and NF-κB activation which form an enhanceosome along with CBP/p300, ATF2/c-Jun and IRF1, that binds to the *IFNB* promoter in non-activated cells (Merika et al. 1998). The promoters of *IFNA* subtypes however do not contain NF-κB binding sites (Raj et

al. 1991), but have multiple sites that can be bound by IRF family members (Chelbi-Alix et al. 2007).

The activation of the IRFs can occur in a number of different ways, however, the best known pathway to IRF3/7 activation is via the kinases TBK1 and IKKε downstream of TLR3/4 (TRIF dependent pathway). IKKε and TBK1 are positioned at a convergence point downstream of a number of PRRs, including TLRs, RLHs and DNA receptors (Thompson et al. 2011) (Sections: 1.2.1.2, 1.2.1.3) (**Figure *1***). These two kinases can phosphorylate IRF3 on serine 396 inducing it to dimerise and translocate to the nucleus to induce type 1 IFN (Fitzgerald, McWhirter, et al. 2003) (**Figure *1***). TRAF3 is thought to function as the link between TLRs and IRF activation through interactions with regulatory kinases such as TBK1, IKKε and IRAK1 (Oganesyan et al. 2006). While IKKε and TBK1 act as positive regulators of these pathways IRAK1 appears to be a negative regulator, it has been shown that the phosphatase SHP-1 promoted type 1 IFN induction by inhibiting IRAK1 (An et al. 2008). It has more recently been demonstrated to be an IKKε regulator, where it acts to limit TAK1-IKKβ-NF-κB signalling downstream of TLR3 (Bruni et al. 2013).

There are however, reports of IKKε/TBK1 activation independent of TRAF3 in a Myd88-dependent pathway (Clark et al. 2011). The mechanism of activation of the IRF proteins downstream of TLR7/8/9 specifically in pDCs has not yet been revealed fully and is not nearly as well elucidated as the TRIF-dependent pathway. However it appears that the key kinases downstream of these receptors are IKKα, NIK and IRAK1 and not IKKε and TBK1. The importance of these kinases along with a more detailed discussion of TLR 7/8/9 signalling can be found in section 1.3.

1.2.1.2 RIG-I like Helicases

The RIG-like family of RNA helicases are a key example of helicases being involved in innate immunity and belong to the SF2 helicase superfamily. The three - known members are: retinoic acid-inducible gene I (RIG-I, DDX58) melanoma differentiation-associated gene 5 (MDA5), and laboratory of genetics and physiology 2 (LGP2, DHX58). Homologues of the RIG-family members are found in many different species and appear to be highly conserved in vertebrates (Zou et al. 2009). The family is named after the RIG-I protein itself, which was initially described to bind double-stranded RNA, an intermediate in the replication of a wide range of viruses, and to induce activation of IRF-3 and NF-κB (Yoneyama et al. 2004). It was discovered in a screen for factors that enhanced IFN-β induced by the dsRNA analogue poly(I:C) (Yoneyama et al. 2004). Following on from this, MDA5 and LGP2 were both identified by database searches for proteins showing a high amino acid identity with RIG-I (Yoneyama et al. 2004). Both RIG-I and MDA5 possess two CARD domains at their N-terminus which are involved in downstream signalling as it allows them to interact with the mitochondrial CARD-domain containing molecule MAVS (Seth et al. 2005). LGP2 however lacks the CARD domains and is thought to regulate both RIG-I and MDA5. Its exact function is still unclear as there are reports suggesting that it acts as both an inhibitor (Rothenfusser et al. 2005) and enhancer of the other two RLHs (Satoh et al. 2010). All three RLHs possess domains involved in the specific recognition of dsRNAs (Cui et al. 2008; Takahasi et al. 2009). RIG-I ligands include RNA possessing a 5'triphosphate followed by a short double stranded region (forming a panhandle like structure) (Schlee et al. 2009), and potentially, long dsRNA lacking the 5'triphosphate end (Binder et al. 2011). MDA5 and LGP2 are not as well characterised but it is thought

that they are involved in dsRNA recognition also. MDA5 has been described to recognise mRNA lacking 2'-O methylation (Züst et al. 2011) and branched dsRNA (Pichlmair et al. 2009). MDA5 and LGP2 bind dsRNA, but unlike RIG-I this binding is independent of the presence of 5'triphosphates (Pippig et al. 2009). The downstream pathway that is induced by the RLHs can result in activation of IKKε/TBK1, leading to IRF3/7 activation and induction of type 1 interferon (Section: 1.2.1.1.3) (**Figure *1***).

1.2.1.3 DNA Receptors

The receptors that recognise DNA are as of yet poorly characterised compared to the more clearly established RIG-I-like and TLR receptors. The existence of such receptors became apparent through studies using MyD88/TRIF knockout mouse embryonic fibroblasts, which lack signalling from all known TLRs (Ishii et al. 2006). TLR9 was previously the only known receptor for DNA but signalling still occurred in response to certain types of DNA, even when TLR9 signalling was not present (Ishii et al. 2006). Like the RLHs and TLRs, most known DNA sensing pathways appear to converge at the level of TBK1 and IKKε. The adaptor protein, stimulator of interferon genes (STING), which interacts with TBK1, appears to be important in DNA sensing pathways (Sauer et al. 2011; Ishikawa & Barber 2008). There have been a number of DNA sensing receptors discovered to date including the DNA-dependent activator of IFN-regulatory factors (DAI), RNA pol III, Leucine-rich repeat flightless-interacting protein 1 (LRRFIP1), and IFI16 (Unterholzner 2013).

DAI was one of the first to be discovered and is known to recognise Z- and B- form dsDNA (Takaoka et al. 2007). RNA pol III transcribes B-form dsRNA to 5'-ppp RNA which can subsequently be recognised by RIG-I to induce a response (Chiu et

al. 2009). LRRFIP1 was identified in a screen that showed its knockdown resulted in reduced IFNβ production in response to both dsRNA and dsDNA. It appears to not operate through activation of IRF3 but instead it enhances activation of β-catenin, a transcriptional co-activator involved in IFNβ induction (Yang et al. 2010). Knock down of IFI16 also resulted in a reduction of an IFN response to exogenous DNA and HSV-1 (Unterholzner et al. 2010). There are additional putative DNA receptors such as DDX41, DDX9 and DDX36, but it is still unclear as to their exact roles (Broz & Monack 2013). Recently cGAMP synthase (cGAS) has been reported to act as a sensor for cytosolic DNA and to trigger IRF3 activation via cGAMP and STING (Wu et al. 2013; Sun et al. 2013). In addition, activation of AIM2-inflammasome mediated activation of caspase1 has been shown to occur in response to cytosolic DNA (Shah et al. 2013).

1.3 TLR 3/7/8/9 – The Anti-Viral TLRs

The most relevant TLRs in the context of viral infection are those that are located within the cell, namely TLR3/7/8 and 9. These PRRs are ideally placed on endosomal membranes to detect viral nucleic acids from endocytosed virions after digestion of their viral envelope (Nishiya & DeFranco 2004), but can also detect actively replicating virus in the cytoplasm through an autophagy-dependent mechanism, where replication intermediates are transported into the lysosome (Lee et al. 2007). TLR9 was the first of this group to be revealed, as a receptor for CpG-rich unmethylated DNA (Hemmi et al. 2000); and was later implicated as having a role in viral recognition, when it was shown to be required for IFNα secretion following HSV infection (Lund et al. 2003). In 2001, TLR3 was found to recognise double-stranded RNA (which is synthesised as part of the replication cycle of many viruses (Jacobs & Langland 1996)) and to activate the NF-κB and type-1 IFN pathways (Alexopoulou et al. 2001). TLR7 was shown to mediate the antiviral response induced by imidazoquinoline compounds in a MyD88-dependent manner (Hemmi et al. 2002) and finally, in 2004, TLR7 along with TLR8 were shown to be involved in the recognition of HIV-1 derived ssRNA in DCs and Macrophages (Heil et al. 2004). Overall, the genes induced by the antiviral TLRs greatly depend on a number of factors, including the particular TLR being engaged and the cell type, for example TLR7 induces IFNα in pDCs and IL-12 in mDCs (Ito 2002). While TLR7 and 8 were initially thought of as being redundant, there are some differences emerging in their ligand specificities, cellular expression/localisation and preference for gene induction (Gorden et al. 2005; Cherfils-Vicini et al. 2010). A study using selective agonists for TLR7 and 8 showed that TLR7 agonists preferentially induced cytokine production from plasmacytoid DCs (pDCs), while the TLR8 selective

agonist activated myeloid DCs (mDCs), monocytes and monocyte-derived dendritic cells. The same study showed a differential profile of cytokine induction, with TLR7 agonists inducing higher levels of IFNα and IFN inducible chemokines, and TLR8 agonists being better at inducing proinflammatory cytokines, such as TNFα and IL-12 (Gorden et al. 2005).

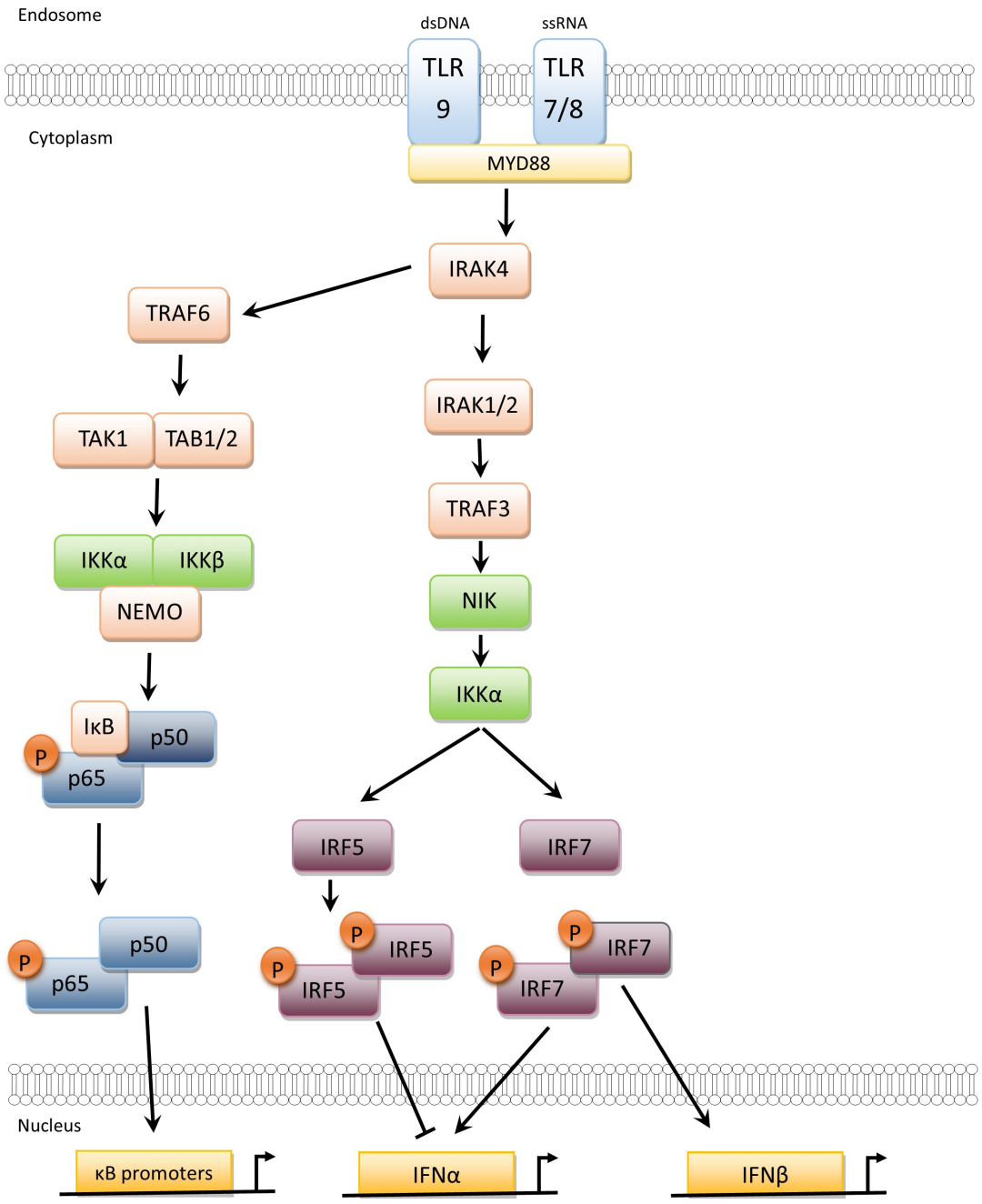

Figure 2: The TLR 7/8/9 signalling pathways to NF-κB and IRF activation.

While the signalling pathways downstream of TLR3, the RLHs and most DNA receptors utilise the IKK-related kinases TBK1 and IKKε for phosphorylation of IRF3/7 (Sharma et al. 2003) (section: 1.2.1), TLR7/8/9 signalling is independent of IKKε and TBK1 and instead uses the kinases IRAK1, NIK and IKKα to activate IRF7 (Wang et al. 2008).

The exact mechanisms of IRF7 activation are still not fully elucidated, however, IKKα appears to be a key kinase, both interacting with and phosphorylating IRF7 (Hoshino et al. 2006). There is severely decreased IFNα production in response to TLR7/9 ligands in IKKα-deficient bone marrow-derived dendritic cells (BMDCs) (Hoshino et al. 2006). However, IKKα does not act in isolation, it is phosphorylated by the kinase NIK on serines 176 and 180. Phosphorylation of serine 176 on IKKα results in activation of IRF3/7, but phosphorylation of serine 180 appears to negate this effect (Wang et al. 2008) implying a key role for NIK as both a positive and negative regulator of IKKα activity in this pathway (See also section: 1.4.2).

IKKβ has also recently been suggested to work cooperatively with IKKα to phosphorylate IRF3/7 in a TAK1 dependent manner (Pauls et al. 2012; Han et al. 2004). Additionally IKKα has recently been shown to interact with and phosphorylate IRF3 also. The authors showed that serine 396 phosphorylation is not sufficient for optimal IRF3 activity and that an additional phosphorylation by IKKα enhances IRF3 interaction with the coactivator CBP (Mancino et al. 2013). IKKα also has a role in the phosphorylation of IRF5. However, while IRF7 activity is enhanced following phosphorylation by IKKα (Hoshino et al. 2006), IRF5 is negatively regulated as a result of this modification (Schoenemeyer et al. 2005). IRAK1 may play a role, as in IRAK1-/- pDCs TLR7/9 induction of IFNα was

completely abolished, while NF-κB or MAPK activation were unaffected (Uematsu et al. 2005).

It is not yet clear if all these kinases are required for signalling to IFN induction and if they work cooperatively or in different contexts. The cellular context is quite important, as there is significant regulation of, and crosstalk between, TLRs and other pathways. The response upon TLR engagement can vary greatly depending on how the pathway is regulated. For example if a cell has received IFN signals from another infected cell, it is primed through the upregulation of signalling mediators like IRF7. Also there is a temporal aspect, the early response IFNs like IFNα4 and IFNβ are induced quite rapidly, while the late response IFNs IFNα 1,2,4,5 are produced later (Marié et al. 1998). The activity and involvement of particular upstream kinases may vary depending on factors such as the receptors engaged, the time since receptor engagement, and crosstalk from other signalling pathways.

1.4 NF-κB

In humans, there are 5 NF-κB family members; p50/p105 (NF-κB1), p52/P100 (NF-κB2), p65 (RelA), RelB and c-Rel (Nabel & Verma 1993). All members contain an N-terminal Rel homology domain (RHD) which mediates dimerization and binding to promoter elements known as κB elements. In resting cells NF-κB subunits are retained in the cytoplasm in an inactive state by proteins known as inhibitors of NF-κB (IκB). The 3 IκB proteins, IκBα, IκBβ, and IκBε contain ankyrin- repeat motifs, which mask a conserved nuclear localisation sequence found in the RHD, impairing the import of the NF-κB proteins into the nucleus. In addition, the precursors of p50 and p52 (p105 and p100 respectively) also act in a similar way to the IκBs. p105 and p100, like the IκBs, both contain ankyrin-repeat sequences in their C-termini, which are lost upon their processing to p50 and p52. Activation of NF-κB can occur in a number of ways, most of which involve activating IKK (IκB Kinase) complexes to phosphorylate the IκBs and induce their degradation (or in the case of p105 and p100, their processing) (Beg & Baldwin 1993). Degradation of the IκBs frees the NF-κB subunits, allowing them to translocate into the nucleus.

The best known pathway to NF-κB activation is the classical or "canonical" pathway typically associated with the activation of the p105/p50 and p65 NF-κB proteins. However, there is also an alternative or "non-canonical" pathway that characteristically results in activation of p100/52 and RelB and induces genes that are distinct from those induced by the canonical NF-κB pathway (Bonizzi & Karin 2004). A hybrid pathway also exists, which involves formation of a dimer of p52 from the alternative pathway with p65 from the canonical pathway (Wietek et al. 2006). This requires activation of both pathways simultaneously. In this case IKKε

can promote p52 transactivation via its interaction with p52 and phosphorylation of p65 (Wietek et al. 2006).

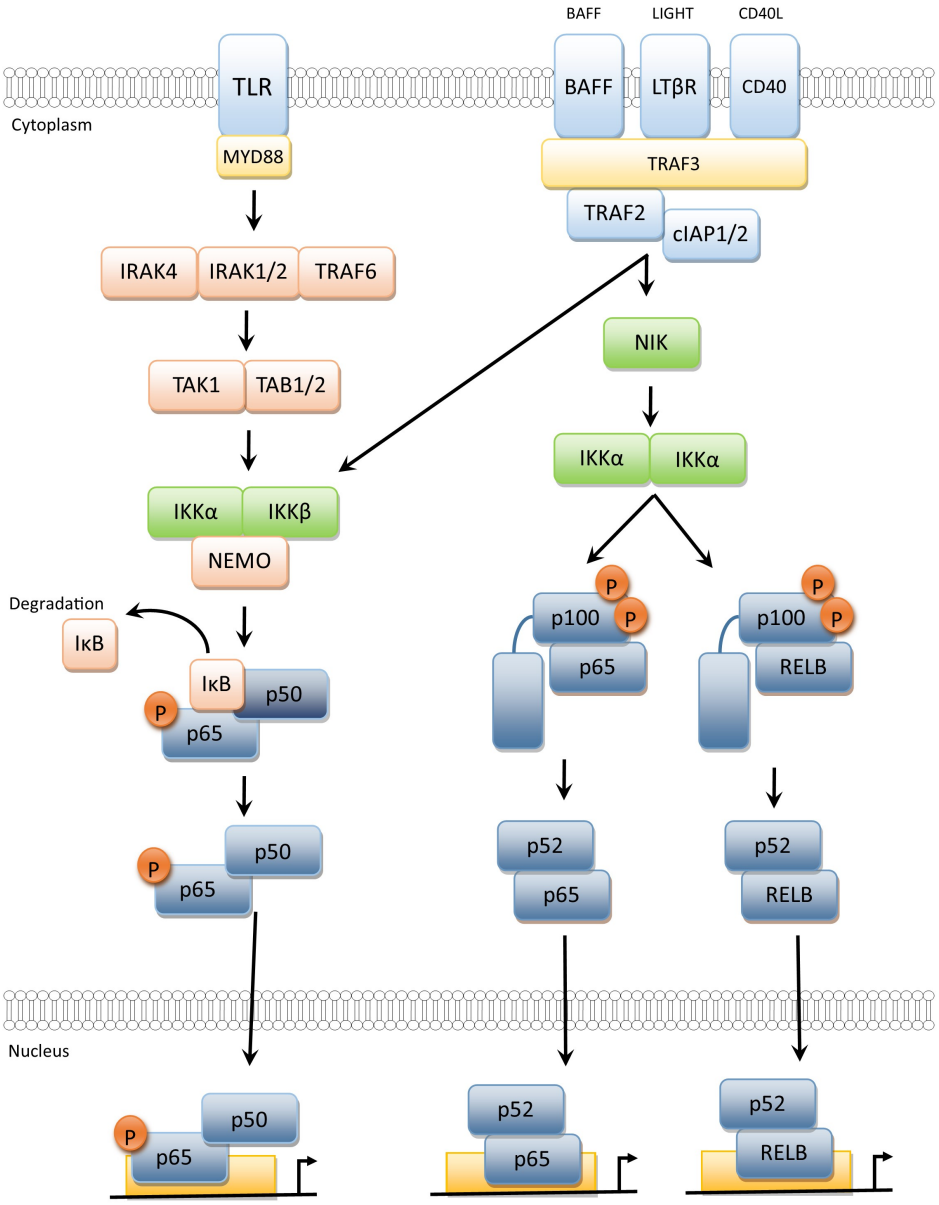

Figure 3: Overview of NF-κB activation, showing the canonical NF-κB pathway (left), the "hybrid" pathway (centre) and the alternative NF-κB signalling pathway (right).

The genes that are upregulated by NF-κB activation include TNFα (Shakhov et al. 1990), IL-1α (Mori & Prager 1996), IL-6 (Son et al. 2008), BAFF (Moon & Park 2007), IL-17 (Shen et al. 2006), lymphotoxin-α (Worm et al. 1998), RANTES (Moriuchi et al. 1997), Cyclin D1(Guttridge et al. 1999), and IRF7 (Lu et al. 2002). Indeed the genes affected by NF-κB are numerous and varied as it is involved in the regulation of a number of cellular processes, including apoptosis, adhesion, proliferation, stress response, innate and adaptive immunity and tissue remodelling (Perkins 2007). As a central mediator in such a wide range of cellular processes it is tightly regulated with many other pathways modulating the outcome of its activation (Perkins & Gilmore 2006).

1.4.1 Canonical NF-κB Pathway

The canonical IκB kinases IKKα and IKKβ are best known for their involvement in the canonical NF-κB activation pathway (Mercurio 1997), in which they form the IKK complex along with the regulatory subunit IKKγ (NEMO). The IKK-complex, once activated by Lys63-linked ubiquitination of NEMO by TRAF6 and subsequent activation of IKKα/β by recruitment of other kinases such as TAK1, will phosphorylate the inhibitory IκB bound to NF-κB subunits. In addition to this typical role for the IKKs, both of these kinases have been implicated in other NF-κB regulation activities, such as the direct phosphorylation of NF-κB subunits. NF-κB phosphorylation, for example the phosphorylation of p65 on serine 536 (Sakurai 1999) or serine 468 (Mattioli et al. 2006), is important for activating the transcription activity of the NF-κB subunits.

1.4.2 The Alternative NF-κB Pathway

IKKα, in addition to its role in canonical NF-κB signalling is also involved in the non-canonical NF-κB pathway. This non-canonical pathway has been shown to be important in a range of physiological functions, including the development of secondary lymphoid organs, bone metabolism, survival and maturation of B-cells and thymic deletion of autoimmune T-cells (Sun 2012). As such, lymphoid malignancies (Yu et al. 2012), osteoporosis (Seo et al. 2012), and autoimmune disorders (Brown et al. 2008) are just some of the diseases that have been associated with disregulation of this important signalling pathway.

The non-canonical pathway is typically activated by stimulation of CD40, lymphotoxin-β receptor (LTβR) (Müller & Siebenlist 2003) or B-cell activating factor of the TNF family receptor (BAFFR) (Claudio et al. 2002), among other

receptors (Sun 2011). LTβR is most highly expressed in lymphoid and epithelial cells and has been shown to also play a role in homeostasis of dendritic cells (De Trez 2012). LTβR has two ligands, lymphotoxin (including LTα and LTβ) and LIGHT (homologous to LT, inducible expression, competes with herpes simplex virus (HSV) glycoprotein D for HSV entry mediator (HVEM), a receptor expressed on T lymphocytes). CD40 is found on a wide variety of cell types including dendritic cells, B-cells, monocytes, neurons, fibroblasts and endothelial cells (Chatzigeorgiou et al. n.d.). The ligand for CD40 is CD154, which is expressed by activated T-cells, while BAFFR is found on B-cells and has BAFF as its ligand (Kayagaki et al. 2002). All three of these receptors possess TRAF binding motifs, which allows their interaction with different TRAF proteins, including TRAF3 and 2. However, while LTβR and CD40R can bind both TRAF2 and 3 (Sanjo et al. 2010; Werneburg et al. 2001), BAFFR can bind TRAF3 but not 2 (Morrison et al. 2005).

A key step in the alternative NF-κB pathway is the proteasome-mediated processing of the NF-κB protein p100 into p52. NIK is an essential component in the alternative NF-κB pathway, as all known pathways that induce p100 processing involve NIK (Sun 2010; Xiao et al. 2001). In unstimulated cells NIK is present at a very low level, which is due to its constitutive degradation mediated by TRAF3 (Liao et al. 2004). TRAF3, which is also involved in signalling downstream of TLR7/8/9 (Figure 2), bridges an interaction between NIK and TRAF2, which itself interacts with cIAP1/2. The roles of cIAP1 and 2 seem to overlap greatly, but their role in repression of NF-κB activation may depend on cell type (Giardino Torchia et al. 2013). The TRAF3-TRAF2-cIAP1/2 forms an E3 ligase complex resulting in K48-linked ubiquitination of NIK, thereby targeting it for degradation by the proteasome

(Liao et al. 2004; Zarnegar et al. 2008). In this way, the pathways regulated by NIK are kept suppressed by ensuring NIK levels are as low as possible.

Removal of this suppression is achieved yet again by controlling degradation of a protein, in this case TRAF3. TRAF3 degradation results in stabilisation of NIK levels, which means that induction of this pathway is dependent on *de novo* synthesis of NIK protein (Liang et al. 2006). When one of the alternative NF-κB-inducing receptors is stimulated, they bind TRAF3 and/or TRAF2 via their TRAF binding motif, which recruits the whole E3 complex to the receptor. This changes the target of the cIAP ligases from NIK to TRAF3, resulting in its degradation (Vallabhapurapu et al. 2008). With TRAF3 levels being reduced, this means that NIK can no longer be recruited to the TRAF2-cIAP1/2 complex.

NIK is unable to induce p100 phosphorylation alone but instead operates with IKKα. While NIK is known to phosphorylate and activate IKKα (Ling et al. 1998), it also promotes the interaction of IKKα with p100 independent of its kinase activity (Xiao et al. 2004). The phosphorylation of IKKα on serines 176 and 180 by NIK activates IKKα (Senftleben et al. 2001) and is required for its induction of p100 processing (Wang et al. 2008). However this is in contrast to IKKα regulation downstream of TLR7/8/9, where phosphorylation of these two serines shows different effects (Section: 1.3). NIK therefore, in addition to activating IKKα, seems to regulate IKKα activity. When serine 176 is phosphorylated, IKKα is primarily involved in IRF3/7 activation, but a further phosphorylation on serine 180 inhibits this and switches IKKα to be involved in the alternative NF-κB pathway (Wang et al. 2008). IKKα homodimers will then phosphorylate p100, which results in p100 being ubiquitinated and subsequently processed by the 26S proteasome to p52. NIK promotion of IKKα binding to p100 requires serines 866 and 870 of p100 (Xiao et al. 2004). Mutation of

these residues does not appear to reduce NIK binding to p100 but abolishes IKKα binding. IKKα phosphorylates a number of residues in p100 including serines 99, 108, 115, 123, 872. The mutation of these serines (also including serines 866 and 870) results in reduced processing of p100 to p52 by stopping recruitment of β-TrCP (β-Transducin repeat Containing Protein) (Xiao et al. 2004), the ubiquitin ligase that ubiquitinates p100 and thereby marks it for processing.

Following this processing, p52, as it possesses no transactivation domain (TAD) of its own, needs to dimerise with an NF-κB subunit possessing a TAD (typically RelB) to activate gene expression. The dimerised pair of NF-κB subunits translocate into the nucleus to induce specific gene transcription, for example genes involved in cell cycle progression like *skp2* (Schneider et al. 2006) and genes involved in development of lymphoid organs (Senftleben et al. 2001). However, activated NF-κB also needs to recruit co-activators to induce gene expression. Co-activators like CREB-binding protein (CBP) or p300 are involved in enhancing the activities of many transcription factors, like STATs, IRFs and NF-κB.

There are still some unanswered questions about the exact mechanism by which IKKα and NIK induce p100 degradation. For example it is unclear whether NIK needs to be activated and whether any other proteins are involved in this activation.

Elucidating the exact mechanisms of how NIK is activated and p100 processing is regulated may provide key insights into a number of disorders, as disregulation of the alternative NF-κB pathway is associated with a range of diseases (Sun 2011).

1.5 DExD/H-box RNA Helicases

Helicases are ATP-driven enzymes which unwind or remodel double-stranded DNA or RNA (Wu 2012); they are involved in nearly every aspect of nucleic acid metabolism (Pyle 2008). Based on their substrates they can be broadly separated into two groups - RNA and DNA helicases, however there are some helicases that can act on both (Wu 2012), and as such the family groupings of helicases are a bit more complex.

There are several superfamilies of helicase proteins, the main accepted groupings are the SF1, SF2 and SF3 superfamilies, however there is some debate over the group divisions (Gorbalenya & Koonin 1993; Fairman-Williams et al. 2010; Singleton et al. 2007). The SF1 and SF2 super families have similar conserved motifs but are distinct from each other; it has been suggested that they may share a common ancestor (Fairman-Williams et al. 2010; Gorbalenya et al. 1989). The SF3 superfamily consists of viral helicases from small DNA or RNA viruses which only contain 3 conserved motifs (including the Walker A and B motifs found in all helicases) (Hickman & Dyda 2005). The families comprise proteins from archaea, eubacteria, eukaryotes and viruses and have varying substrate specificity and unwinding activity. The grouping of these families is due to highly conserved regions in their sequences which are shared between all members of one particular family (Caruthers & McKay 2002). For example the DEAD-box family of RNA helicases are characterised by nine conserved motifs (**Figure *4***).

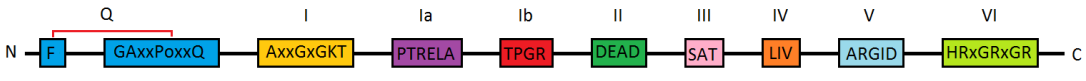

Figure 4 The nine motifs typical of DEAD-box helicases (Cordin et al. 2006)**.**

The DEAD-box family of putative RNA helicases belongs to the SF2 superfamily and is closely related to, but distinct from, the RIG-like helicases (Section: 1.2.1.2) (Gorbalenya & Koonin 1993). The family was first identified in 1989 by systematic sequence analysis of proteins containing a purine NTP binding motif (Linder et al. 1989). This new family consisted of 25 confirmed or suspected helicases and shared a number of conserved regions in their sequence. The 9 conserved motifs that characterise the DEAD box family are the Q-motif, motif 1 (Walker A motif), motif 1a, motif 1b, motif II (Walker B motif), motif III, motif IV, motif V, and motif VI (**Figure 4** and

Table 2) (Cordin et al. 2006). The name for this family is derived from motif II, which contains the amino acid sequence D-E-A-D.

MOTIF NAME	AMINO ACID SEQUENCE	FUNCTION	REFERENCE
Q-Motif	F-16aa-GFccPoPIQ-16 aa-motif I	**Regulate ATP Binding and Hydrolysis**	(Tanner et al. 2003; Tanner n.d.)
I (Walker A motif)	AxxGxGKT	**ATP Binding** MgATP/MgADP binding	
Ia	PTRELA	**Unknown (possibly RNA binding)**	(Caruthers & McKay 2002; Fuller-Pace 1994)
Ib	TPGR	**Unknown**	
ll (Walker B motif)	DEAD	**ATP Hydrolysis** MgATP/MgADP binding	(Caruthers & McKay 2002; Fuller-Pace 1994)
III	SAT	**ATP Hydrolysis/RNA Unwinding**	(Fuller-Pace 1994)
IV	LIV	**Unknown**	
V	ARGID	**Unknown**	
VI	HRxGRxGR	**ATP Hydrolysis/RNA Binding**	(Fuller-Pace 1994)

Table 2 The typical motifs of DEAD-box helicases and their function. An example of motifs used to classify a helicase family. C= charged group (D, E, H, K or R), o = alcohol (S or T) (Cordin et al. 2006).

Structures of various helicases of the SF1 and SF2 families have been shown to be almost identical within the RecA like core structure, which is a very highly conserved structural fold found in ATPases (Caruthers & McKay 2002; Johnson & McKay 1999). However, it is the surrounding unconserved C- and N-terminal domains that confer differences in substrate specificity and activity, possibly providing different binding domains, regulating enzyme activity or even allowing oligomerisation of the helicase (Fairman-Williams et al. 2010).

All helicases have the Walker A and B motifs, which are the most highly conserved regions and are involved in ATP binding and hydrolysis. They are located in a cleft that is formed between the two RecA-like globular domains. The Walker A motif is part of a classical phosphate-binding loop (P loop), which is commonly found in many proteins and is involved in binding and hydrolysing nucleoside triphosphates and ensures the triphosphate moiety is positioned correctly (Leipe et al. 2002). The Walker B motif has an aspartic acid, which is involved in Mg2+ binding and functions with the Walker A and Q motifs to help bind and hydrolyse ATP (Walker et al. 1982). The motifs involved in binding nucleic acid are the 1a, 1b, IV and V motifs and are situated on the opposite side to the NTP binding site (Fairman-Williams et al. 2010).

In addition to their roles in unwinding of nucleic acid structures, there is increasing evidence that helicase proteins perform functions that may be independent of their helicase properties (Fuller-Pace 2006; Schröder et al. 2008; Soulat et al. 2008), like involvement in transcriptional regulation (Fuller-Pace & Nicol 2012) or in innate immunity (section :1.5.1).

1.5.1 Helicases in Innate Immunity

Several helicases in the DExD/H-box family have been shown to be involved in the innate immune response to viruses including members of the DEAD, DEAH, DExD, and DExH (including RLHs) helicase families (Fullam & Schröder 2013). They have been implicated as sensors for viral nucleic acids as well as being involved in downstream signalling events. However, a number of helicases potentially play a dual role in this system: in addition to being involved in the innate anti-viral response itself, there are helicases that are also essential host factors needed by some viruses to support or enhance their own replication. While the RIG-like helicases (DExH family) are well known to be one of the most important groups of PRRs and are established as having a role in innate immune signalling (Schmidt et al. 2012) (section: 1.2.1.2), a few other members of the DExD/H family members have more recently been implicated as having roles in innate immunity too (Zhang, Yuan, Lu, et al. 2011; Zhang, Yuan, Bao, et al. 2011; Zhang, Kim, et al. 2011; Miyashita et al. 2011; Oshiumi, Sakai, et al. 2010; Kim et al. 2010), one of which is DDX3 (Schröder et al. 2008; Gu et al. 2013).

1.5.1.1 DDX3

DDX3 is a member of the DEAD-box helicase family. It is a 662 amino acid protein that is universally expressed in a wide range of human tissues (Kim et al. 2001). It has two homologues: DDX3X and DDX3Y, that were first described in 1997 in a study of the non-recombining region of the Y chromosome: DDX3X (hereafter referred to as DDX3) was one of several genes that escaped X-inactivation (Lahn 1997). DDX3 contains the 9 motifs that are characteristic of the DEAD-box RNA helicases (Linder et al. 1989) and as such, was placed in the family (**Figure *5***).

MSHVAVENALGLDQQFAGLDLNSSDNQSGGSTASKGRYIPPHLRNREATKGFYDKDSSGW

SSSKDKDAYSSFGSRSDSRGKSSFFSDRGSGSRGRFDDRGRSDYDGIGSRGDRSGFGKFE

RGGNSRWCDKSDEDDWSKPLPPSERLEQELFSGGNTGINFEKYDDIPVEATGNNCPPHIE

SFSDVEMGEIIMGNIELTRYTRPTPVQKHAIPIIKEKRDLMACAQTGSGKTAAFLLPILS

QIYSDGPGEALRAMKENGRYGRRKQYPISLVLAPTRELAVQIYEEARKFSYRSRVRPCVV

YGGADIGQQIRDLERGCHLLVATPGRLVDMMERGKIGLDFCKYLVLDEADRMLDMGFEPQ

IRRIVEQDTMPPKGVRHTMMFSATFPKEIQMLARDFLDEYIFLAVGRVGSTSENITQKVV

WVEESDKRSFLLDLLNATGKDSLTLVFVETKKGADSLEDFLYHEGYACTSIHGDRSQRDR

EEALHQFRSGKSPILVATAVAARGLDISNVKHVINFDLPSDIEEYVHRIGRTGRVGNLGL

ATSFFNERNINITKDLLDLLVEAKQEVPSWLENMAYEHHYKGSSRGRSKSSRFSGGFGAR

DYRQSSGASSSSFSSSRASSSRSGGGGHGSSRGFGGGGYGGFYNSDGYGGNYNSQGVDWW

GN

Figure 5 Sequence of DDX3 showing 9 conserved motifs highlighted in red with the D-E-A-D motif in yellow (Cordin et al. 2006; Ota et al. 2004)**.**

Since its initial discovery, DDX3 has been implicated in almost all aspects of RNA metabolism, including unwinding, splicing, import/export, transcription, translation and ribosome assembly (Schröder 2010; Geissler et al. 2012). Additionally, DDX3 has been suggested as having a role in the cell cycle (Chang et al. 2006; Choi & Lee 2012) and there have been several reports indicating an association with cancer progression (H. Liu et al. 2012; Sun et al. 2011). However, its exact function in this process is still unclear, as it has been suggested to be both a tumour suppressor (Chao et al. 2006; Wu et al. 2011; Chang et al. 2006) and an oncogene (Botlagunta et al. 2008; Botlagunta et al. 2011). In addition to these roles it has also been shown to be important in host responses to viral infection.

1.5.1.1.1 Role of DDX3 in Innate Anti-Viral Immune Signalling

Two simultaneous reports in 2008 provided the first evidence of DDX3 being involved in innate immune signalling pathways (Schröder et al. 2008; Soulat et al. 2008). The first identified DDX3 as a molecular host target of the vaccinia virus K7 protein. K7 inhibited *Ifnb* induction at the level of IKKε and TBK1, the two key kinases that are a point of convergence for TLR3/4 and the RLHs, and which phosphorylate and activate the transcription factors IRF7 and IRF3 that are required for type I IFN induction (Section: 1.2.1.1.3). In a search for K7-interacting proteins DDX3 was found. Further investigation showed that DDX3 interacts with IKKε after Sendai Virus stimulation and enhances induction of the *Ifnb* promoter. K7 was shown to block key residues of DDX3 possibly preventing its interaction with IKKε (Oda et al. 2009). The intrinsically unstructured N-terminal region of DDX3 was shown to be required for this activity, but it was independent of the ATPase and unwinding activities of DDX3. Additionally, exogenous expression of DDX3 aa 1-139 could act as a dominant negative to wt DDX3 (Schröder et al. 2008). The second report concurrently revealed that DDX3 interacts with, and is a phosphorylation target of, TBK1 (Soulat et al. 2008). TBK1 and DDX3 synergistically enhanced *Ifnb* induction, and DDX3 had to be phosphorylated by TBK1 for this synergism to occur. This report also supported a role for DDX3 in *Ifnb* promoter induction downstream of TBK1/IKKε. However, these authors also demonstrated that DDX3 is recruited to the *Ifnb* promoter enhancer region using chromatin immunoprecipitation (Soulat et al. 2008). Studies on HBV polymerase (pol) corroborated these results, showing that HBVpol inhibits type 1 IFN induction by preventing the DDX3 – IKKε/TBK1 interaction (Yu et al. 2010; Wang & Ryu 2010). DDX3 also seems to have a role in the response to dsDNA viruses, for example

HCMV (Human Cytomegalovirus), which is recognised by the cytoplasmic DNA receptor DAI (DNA-dependent Activator of IRFs) independent of MAVS. The IFNβ induction that is observed in response to this virus is greatly diminished upon knockdown of DDX3, further implicating it in the pathways to IFN production (DeFilippis et al. 2010). DDX3 has also been shown to be in a complex with RIG-I and MAVS. It has been suggested that DDX3 can act jointly with RIG-I and mda5 as a sensor for viral RNA and that it may induce IFNβ at the early stages of infection until sufficient RIG-I has been synthesised and can then take over viral recognition (Oshiumi et al. 2010).

The numerous reports that have been published implicating DDX3 in pathways leading to type-1 interferon induction, provide compelling evidence for its role in the innate immune response to viruses. However, despite the strength of the evidence the exact nature of DDX3's mechanism of action is not clear yet and its placement in the pathway is subject to some dispute as some of the data are contradictory. DDX3 has been suggested to act as a PRR at the early stages of infection (Oshiumi et al. 2010). It has also been implicated as being a key downstream mediator in the pathway, interacting with both IKKε and TBK1 and enhancing their action (Schröder et al. 2008; Soulat et al. 2008). Finally, it has also been shown to be bound to the *Ifnb* promoter directly, suggesting a role in transcriptional regulation, possibly acting as a transcription factor (Soulat et al. 2008). While the majority of evidence points to the interaction of DDX3 with IKKε/TBK1 as being its most important of these roles in the pathways, DDX3 may have multiple functions, adapting its role in response to differing conditions within the cell.

1.5.1.1.2 Role of DDX3 in Viral Replication

In the years following the initial description of the DDX3X gene, a number of reports have shown that several viruses target DDX3 and/or use it for their own benefit (Owsianka & Patel 1999; Yedavalli et al. 2004; Krishnan & Zeichner 2004; Ariumi et al. 2007; Ishaq et al. 2008; Jorba et al. 2008). In fact, it has been shown that Human Immunodeficiency Virus 1 (HIV-1) and Hepatitis C Virus (HCV) require DDX3 as an essential part of their replication cycle (Ariumi et al. 2007; Yedavalli et al. 2004; Randall et al. 2007).

In the case of HIV-1, DDX3 has been shown to be required for the export of unspliced and partially spliced HIV-1 RNA out of the nucleus. HIV-1 exports its incompletely spliced Rev Responsive Element (RRE) containing RNAs out of the nucleus via a Chromosome Maintenance Region 1 (CRM1)-mediated pathway (Yedavalli et al. 2004). CRM1 exports proteins that contain a leucine rich NES (Nuclear Export Signal) and can also export small nuclear RNAs and ribosomal RNA. This pathway apparently also requires DDX3, which was shown to bind to HIV-1 rev and CRM1, thereby facilitating export of RRE-containing HIV-1 RNAs out of the nucleus. It suggested that DDX3 is an effector of CRM-1 mediated transport rather than cargo as neither RanGTP binding nor its NES are required for DDX3 binding to CRM1 (Yedavalli et al. 2004). DDX3 binding to CRM1 does however seem to be dependent on its helicase activity, suggesting that RNA unwinding plays a role. Due to its requirement for HIV-1 replication, several studies have attempted to develop inhibitors for DDX3 that could potentially be used therapeutically against HIV-1. There have been several reports of groups attempting to target DDX3 to block HIV-1 replication using either shRNAs (Ishaq et al. 2008) or small molecule inhibitors (Yedavalli et al. 2008; Maga et al. 2008; Radi et al.

2012). Depletion of endogenous DDX3 using shRNA inhibited the export of HIV-1 RNAs and suppressed the replication of the virus while not affecting cell viability (Ishaq et al. 2008). Another group developed ring expanded nucleoside (REN) analogues that inhibited the ATP-dependent activities of DDX3, this also suppressed HIV-1 replication while still being non-toxic to the cells (Yedavalli et al. 2008). Yet another small molecule inhibitor was developed that can inhibit both the ATPase activity and the helicase functions of DDX3 (Radi et al. 2012). The emergence of resistance to antiretroviral drugs is a significant problem for HIV-1 treatment today. It is thought that targeting essential host factors of viral replication could be a better strategy, as the virus should find it harder to evolve ways of escaping these treatments (Kwong et al. 2005).

Several studies have shown that the HCV Core protein interacts with DDX3 (Owsianka & Patel 1999; Mamiya & Worman 1999; You et al. 1999) and that DDX3 is required for HCV replication (Ariumi et al. 2007; Randall et al. 2007). HCV contains both structural and non-structural proteins; HCV Core protein is one of the structural proteins. It, along with two envelope glycoproteins, forms the viral nucleocapsid (Owsianka & Patel 1999). The core protein was shown to disrupt the interaction between MAVS and DDX3 and to thereby block the induction of anti-viral IFNβ (Oshiumi et al. 2010). However in contrast, another study suggested the Core protein can induce IFN via DDX3 (Kang et al. 2012). In DDX3 knockdown studies a decrease in HCV RNA accumulation (80-90%) and colony formation was observed (Ariumi et al. 2007). Surprisingly, however, it is not the HCV Core interaction that causes this dependence. In a study that mutated a key residue in the HCV Core protein that abrogated the interaction with DDX3, no observable difference in viral replication or RNA accumulation was observed (Angus et al.

2010). The question as to why DDX3 is required for HCV replication therefore remains to be answered. HCV might have a dual effect in targeting DDX3, it uses DDX3 to enhance its replication, while simultaneously suppressing its antiviral role.

Hepatocellular carcinoma (HCC) is a highly prevalent cancer in the modern world and is linked with hepatitis virus infection (Alter 2007). In the analysis of human HCC tumour samples, DDX3 was down regulated in HCC samples from Hepatitis B Virus (HBV) positive patient samples, while no down-regulation was observed in those that were HCV positive (Chang et al. 2006). The same study linked DDX3 to the progression of the cancer with the observation that knock-down of DDX3 led to early entry into S-phase and an increased growth rate. Knockdown of DDX3 also resulted in an increase in cyclin D1 and a concurrent decrease in p21(waf1) both of which are cell cycle regulators (Chang et al. 2006). This deregulation in cell growth may enhance HBV's rate of replication and contribute to cancer progression. Another advantage for HBV to have DDX3 downregulation is due to the observation that HBV reverse transcription is inhibited by DDX3. A study by Wang *et al*. (2009) showed that DDX3 interacts with HBV pol, gets incorporated into nucleocapsids and inhibits viral reverse transcription. HCV, instead of downregulating DDX3 levels, seems to use its Core protein to disable some of DDX3's functions, as described above. Recent studies have also shown a requirement for DDX3 in the replication of additional viruses including noroviruses (Vashist et al. 2012) and West-Nile Virus (Chahar et al. 2013), further demonstrating it importance for the replication of a range of different viruses.

DDX3 is a remarkable example of the multifunctional nature of RNA helicases. In addition to its expected roles in various different aspects of RNA metabolism, it has also been shown to participate in anti-viral innate immune signalling. It is most interesting that DDX3 is also 'hijacked' by certain viruses to their own end, to the extent that it is an essential host factor for the replication of some viruses, such as HIV-1 and HCV. It has been suggested as a drug target in the treatment of viral infection (Kwong et al. 2005). However as studies have shown the multifunctional roles of DDX3 as both an inhibitor and an enabler of viral infection, and due to its possible involvement in tumorgenesis, it is vital that we understand more about its mechanism of action before it can be targeted safely.

1.6 Aims of this Study

The fact that DDX3 is manipulated by a number of viruses and the discovery of its role in anti-viral innate immune signalling emphasises its importance in viral infection and invites further investigation. While previous studies have shown that DDX3 is involved in pathways mediated by the kinases IKKε (Schröder et al. 2008) and TBK1 (Soulat et al. 2008) and work in our lab has shown that DDX3 directly interacts with IKKε and enhances its autophosphorylation (Gu et al. 2013), we asked whether DDX3 is also involved in pathways that are independent of these two kinases. While most of the main innate anti-viral signalling pathways to IFN induction signal via IKKε and TBK1, they have been shown to be dispensable for one of the most important IFN inducing pathways, namely the one triggered by TLR 7, 8 or 9 engagement (Hoshino et al. 2006) as they induce large amount of IFN upon recognition of viral nucleic acid. However, two other kinases that are closely related to IKKε and TBK1, NIK and IKKα, are involved instead. Therefore we aimed to investigate whether there was any involvement of DDX3 in the regulation of IKKα activity in a similar manner to what the lab had shown for IKKε (Schröder et al. 2008; Gu et al. 2013).

Therefore, in carrying out this work we aimed to:

- Investigate a possible interaction between DDX3 and IKKα or NIK.
- If an interaction exists, investigate the effects this interaction has on both proteins.
- If an effect is present, investigate what outcome this may have on pathways that are regulated by IKKα and NIK.

Both IKKα and NIK are involved in two key immune signalling pathways, the alternative NF-κB pathway and TLR 7/8 signalling to IFN production (Figure 6). In the TLR 7/8 signalling pathway. IKKα as been shown to interact with and phosphorylate IRF7, IRF3 and IRF5 (Hoshino et al. 2006; Wang et al. 2008; Mancino et al. 2013), key transcription factors in the anti-viral innate immune response. In the alternative NF-κB pathway NIK and IKKα have been shown to be involved in the induction of p100 processing to p52 (Xiao et al. 2004; Senftleben et al. 2001; Wang et al. 2008), a transcription factor known to be involved in lymphoid organ development, bone metabolism, survival and maturation of B-cells and thymic deletion of autoimmune T-cells (Sun 2012). However, while the involvement of these two kinases in activation of these important immune signalling pathways is clear, the full mechanisms of how they exert their effects is not yet known. Therefore in this study we also sought to gain further insight into the mechanisms that these kinases use to induce downstream signalling.

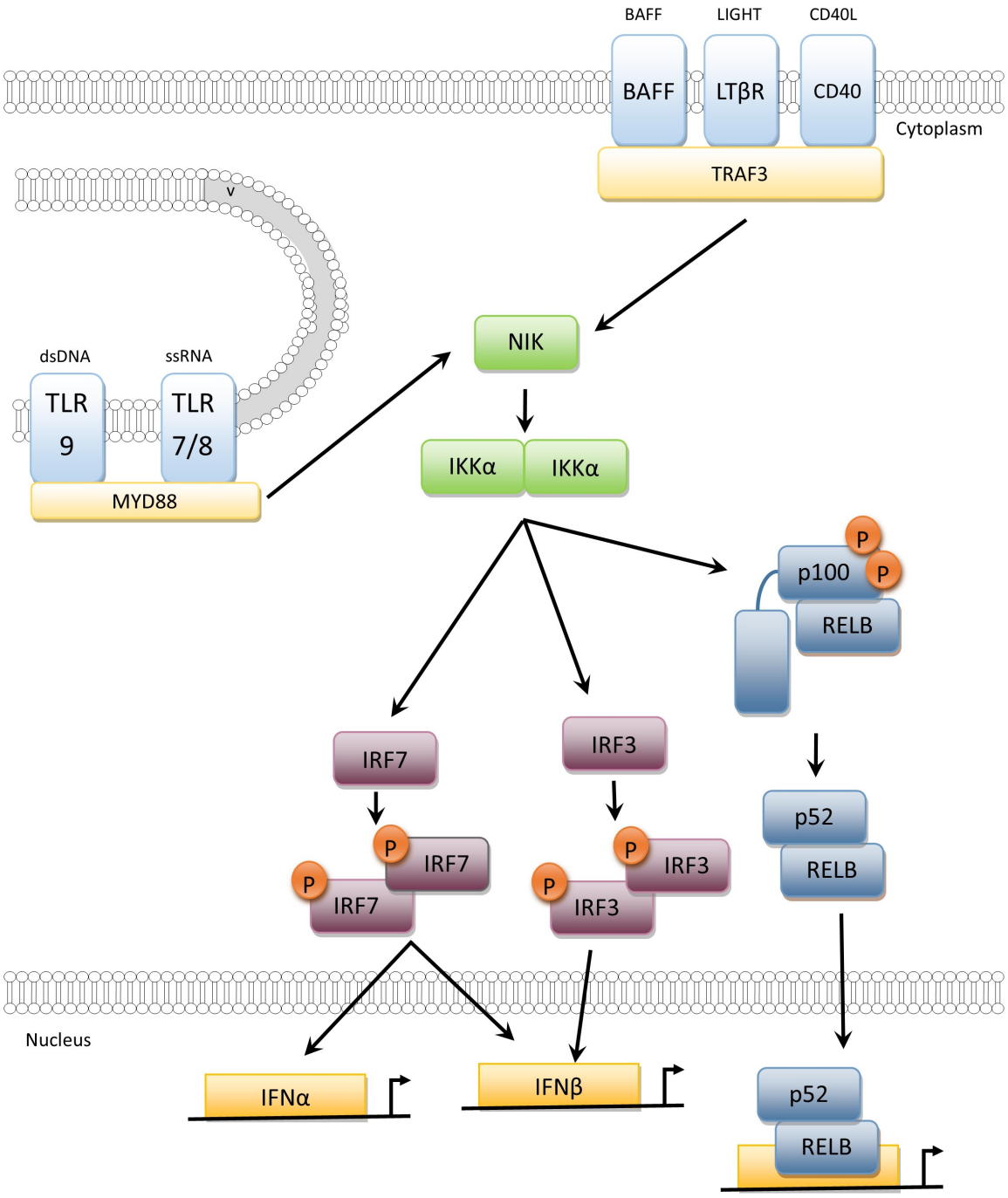

Figure 6: IKKα is a key kinase involved in both the alternative NF-κB pathway and TLR 7/8/9 signalling to IFN activation.

2 Materials And Methods

2.1 Standard Laboratory Procedures

Good laboratory practices were followed in all activities. All the tissue culture materials and reagents were kept sterile and used in a Class II (laminar flow) biological safety cabinet. Recipes for all reagents used are in appendix.

2.2 Cell Culture

HEK293T cell lines were cultured in Dulbecco's Modified Essential Medium (DMEM) (Invitrogen) supplemented with 10% (v/v) foetal calf serum (FCS) (Thermo Fisher Scientific) and antibiotics (10 µg/ml gentamicin (Sigma). Cells were maintained at 37°C at 5% CO2 in a humidified atmosphere. Confluent cultures were passed at 1:10 ratio for HEK293T in T 75cm2 tissue culture flasks (Corning) every 2-3 days. Cells were dissociated using 5% (w/v) trypsin-EDTA solution (Sigma) and resuspended in DMEM.

Cells	Description	Selection Antibiotic
HEK293T	Immortalised Human embryonic kidney cell line, containing the SV40 Large T-antigen	N/A
HEK293 R1	Immortalised Human embryonic kidney cell line, stably transfected with IL-1R1	N/A
HEK293-TLR7	Immortalised Human embryonic kidney cell line, stably transfected with TLR7	G418
HEK293-TLR8	Immortalised Human embryonic kidney cell line, stably transfected with TLR8	Blasticidin
HEK293-NSC	Immortalised Human embryonic kidney cell line, stably transfected with a random non-silencing shRNA control	Puromycin
HEK293-shDDX3	Immortalised Human embryonic kidney cell line, stably transfected with a doxycycline inducible shRNA directed towards DDX3	Puromycin

2.2.1 Long term storage of cells

Cells were frozen down at a density of $1x10^6$ cells/ml in FCS containing 10 % v/v DMSO (Sigma-Aldrich). Cells were pelleted by centrifugation at 1400 g and re-suspended in freezing medium at a concentration of $1x10^6$ cells/ml. Cells were then transferred to cryotubes (Nunc), placed into a chamber which allowed the temperature to drop at a rate of 1^oC/min in a -70°C freezer for 24 hours and then into liquid nitrogen.

Cells were recovered by thawing quickly at 37 °C and then added to warm complete culture medium; they were then centrifuged in order to remove the freezing medium. The cell pellet was re-suspended in warm medium and transferred to a sterile tissue culture flask.

2.2.2 Transfection

Cells were transfected with plasmids using either Calcium Phosphate, Lipofectamine™ (Invitrogen) or GeneJuice™ (Merck/Novagen) according to the manufacturer's protocol.

2.2.2.1 Calcium Phosphate Transfection

Cells were seeded at 2-2.5 x 10^5/ml and allowed to adhere for 24H prior to transfection. For a 10cm TC dish, 20 µg of plasmid DNA was aliquoted into a sterile 1.5 ml microfuge tubes. 2xHBS was added to bring the combined volume to 500µl. 30µl 2.5M CaCl2 was then added and mixed gently during the addition. After 20min incubation, solution was added dropwise to the cells. Cells were incubated at 37°C for 24-48 hours before harvesting. For a 6-well plate, 12- well plate or 24-well plate, reaction was scaled down appropriately.

2.2.2.2 Genejuice Transfection

Genejuice™ transfection (Merck/Novagen) was carried out when transfecting cells in a 96wp format to increase transfection efficiency with small cell numbers. Cells were seeded at 1-1.5 x 10^5/ml and allowed to adhere for 24H prior to transfection. Transfection was carried out as per the manufacturer's instructions. Genejuice was diluted in serum free medium (SFM) at a 1:25 dilution and left for 5min. This was added to DNA previously prepared in a (96well v-bottomed plate, the DNA/Genejuice mixture was left for 15 min before addition to the cells in a 96 well plate. A total amount of 230ng DNA in 10µl GeneJuice/SFM mixture was added to each well. Cells were incubated at 37°C for 24-48 hours before harvesting.

2.2.2.3 Lipofectamine/siRNA Transfection

Lipofectamine 200 was used in cases where siRNA was to be transfected into cells as recommended by the siRNA manufacturer (Invitrogen) instructions. Short Interfering RNA (siRNA) can be used to interfere with the expression of specific mRNAs containing complementary nucleotide sequences. Cells were seeded at 2-2.5 x 10^5/ml and allowed to adhere for 24H prior to transfection. Lipofectamine 2000 was used to transfect HEK293T cells with StealthTM RNAi oligonucleotides (*Invitrogen)* specific for DDX3 (Section 6.1) or a control siRNA with matched GC content. For a 6-well plate, 100pmole (5µl) of siDDX3 or si medium GC was added to 125µl of Optimem (*Gibco)* in a sterile eppendorf tube. 125µl of Optimem (*Gibco)* was mixed with 5µl Lipofectamine 2000 in a sterile eppendorf, and left for 15 min. The Lipofectamine/Optimem mix was added to the siRNA/Optimem eppendorf tube mixed with pipetting, and incubated for 15 min. 255µl of Lipofectamine/siRNA mix was added to cells. After 24 h, cells from each well were split into two new wells.

The following morning a second siRNA transfection was carried out, and 6 h later expression plasmids were transfected into cells using the calcium phosphate method as section 2.2.2.1. In the case of an experiment in a 96wp formant cell were harvested from the 6 well plate (wp) and transferred to a 96wp and left for 24H, cells were then transfected with genjuice as described in section 2.2.2.2. Knock-down was confirmed by Western blotting.

2.2.3 shRNA Cells

For some experimental conditions inducible DDX3 knockdown cells were used. These cells were produced by Dr. Yvette Hoehn (Host-Pathogen Interaction Lab, NUI Maynooth) using a TRIPZ inducible lentiviral shRNA system. HEK293 cells were transfected using lentivirus with a pTRIPZ vector that inducibly expressed shRNA targeted against either DDX3 or a Non-Silencing control shRNA. Cells were maintained in the presence of 10μg/ml puromycin to select for stable cells. Knockdown was induced by addition of 0.5μg/ml doxycycline when cells were being plated. Knockdown was assessed by western blotting.

2.2.4 Cell treatments

For Sendai virus (SeV, Charles River Laboratories) stimulation, Sendai virus was added at a 1:200 dilution from original stock (16,000/ml) at required time points. CLO75 was used at a final concentration of 1μg/ml of medium for the required time.

2.3 Luciferase Reporter Gene Assay

Cells were plated in flat bottomed 96wp and transfected with 80 ng of plasmid vectors containing a firefly luciferase gene under the control of the promoter region from either *ifnα4* or *ifnβ* gene as in section 2.2.2.2. In addition a control construct containing 20 ng of a renilla luciferase gene that is constitutively expressed was also transfected to allow normalisation of the data to take into account of transfection efficiency among other factors. Other constructs relevant to the experimental condition were also transfected, however, the total DNA concentration transfected into each well was brought to 230 ng with the appropriate empty vector. If cells were to be stimulated they were left for 24h at 37^{o}C at 5% Co2 and the treatment was applied for the appropriate time. 24 h after the transfection (or in the case of stimulation the appropriate time after stimulation), the medium was removed from the wells. 50 µl of 1X Reporter Lysis Buffer (from 5X Reporter Lysis Buffer diluted in water, Promega) was added to each well. The plate was then placed on a rocker at room temperature for 15 min and frozen. The cell lysates were then thawed at room temperature on a rocker. 20 µl of each lysate was pipetted into two separate white-bottom 96-wells plates. Firefly luciferase activity was assessed by adding 40 µl of firefly luciferase substrate to one white 96wp, whilst renilla luciferase activity was assayed diluting 0.1 µg/ml Coelenterazine in PBS straight before use (Promega). The luminescence was then measured in a luminometer. All experiments were carried out in triplicate.

2.4 Co-Immunoprecipitations

Protein G Sepharose Beads (*Sigma*), were prepared 24h in advance of cell lysis by incubating 20 µl of bead suspension per IP with 5% BSA in PBS-.1%Tween with an antibody for the protein to be immunoprecipitated, overnight at 4^{o}C with constant rotation.

Lysates for co-immunoprecipitation (co-ip) experiments were prepared by washing cells once with ice-cold 1X PBS and adding lysis buffer to each well. In all steps following addition of lysis buffer care was kept to keep samples on ice at all times. Lysates were transferred to pre cooled 1.5ml tubes and incubated for 45 mins on a rocker in ice. Lysates were then centrifuged at 13000g for 15 minutes. The supernatants were transferred into new 1.5 ml tubes. An aliquot of the lysates was added to the appropriate amount of 2X lamelli sample buffer and boiled for 5 mins. The rest of the lysate was used for the co-ip. The pre-prepared beads were washed twice with cold PBS and once with lysis buffer and aliquoted evenly into precooled 1.5ml tubes. Cell lystes were added to the beads and tubed were incubated overnight at 4^{o}C with constant rotation. Beads were washed three times with 1ml of cold lysis buffer and then then resuspended in 2x laemmli sample buffer and boiled for 10min at 100^{o}C. Co-immunoprecipitation samples were then subjected to SDS-PAGE and Western blotting (Section 2.5, 2.5.2).

2.5 SDS-PAGE and Western Blotting

2.5.1 SDS-PAGE

Samples to be subjected to SDS-page were prepared as in section 2.4 with cell lysates/protein samples being mixed with 2x lamelli sample buffer with subsequent boiling for 10mins. SDS-polyacrylamide gel electrophoresis (SDS-PAGE) was conducted in a Biorad Mini-Protean® Tetra System. The prepared samples were loaded into the wells of a pre-prepared gel (typically a 5% poly acrylamide stacking gel and a 10% resolving gel) along with a protein molecular weight marker *(Fermentas)*. Gels were then run in SDS- PAGE running buffer at 100-150 V constant voltage for 50-90 minutes, or until sufficiently resolved. (All buffers and gel composition is outlined in appendix)

2.5.2 Western Blotting

Once the proteins had been separated by SDS-PAGE, they were transferred electrophoretically to a polyvinylidene fluoride (PVDF) transfer membrane *(Millipore)* in a semi-dry electrophoretic transfer unit *(Biometra)* at 90mA/gel. Membrane was pre-soaked in methanol (*Sigma-Aldrich)* and cold transfer buffer for 10 min. After transfer, the membrane was allowed to dry at room temperature overnight while also being protected from light. The membrane was reactivated by being place shortly in methanol followed by a quick was in TBS 0.1% Tween. The membrane was then incubated in a blocking solution (5% semi-skimmed milk powder in TBS/0.01 % Tween *(Sigma))* at room temperature for 1h to prevent non-specific antibody binding. Subsequently, the membrane was incubated with a primary antibody, in 5% Milk TBS/Tween, at 4°C overnight. Following 3 x 5min washes with TBS/0.1%Tween, the membrane was then incubated with the

appropriate horseradish peroxidase conjugated secondary antibody for 1h at room temperature, and then washed again 3 x 5 min with TBS/0.1%Tween.

2.5.3 Chemiluminescence detection

Immunoreactive proteins were detected using Enhanced ChemiLuminescence (ECL). ECL was prepared and then added to the membrane for 30 secs. Membranes were placed between two layers of plastic and placed in a film cassette. In the dark room, Autorad film (UltraCruzTM Autoradiography Film, *Santa Cruz Biotechnology)* was placed on top of the membranes in the cassette for 1-30 min. Autorad film was then developed and fixed using a Fuji Medical film processor (*Fuji).*

2.6 Blue Native Page

HEK 293T cells were cultured in 10cm dishes and stimulated for the desired time. Cells were counted and a set number of cells were used for the experiment. The cell pellet was resuspended in cold Blue-Native (BN) -Lysis buffer. The sample was incubated on ice for 15 min and centrifuged at 13,000g for 15 min. The lysate was dialysed for 6 hours in cold BN-dialysis buffer at 4^{o}C with constant stirring.

All plates and equipment to be used in running the native gels were soaked in water overnight and cleaned thoroughly to ensure no trace of SDS was present. One of the most important things to be aware of is the presence of SDS. A lot of care must be taken to ensure no SDS is present on any of the equipment or in any of the reagents used in the experiment. If SDS gets in the sample it will disrupt any complexes that are still present. Best practice is to have a separate area for working with BN-PAGE gels in isolation from any areas where SDS is used.

Blue native gradient gels were poured and left to cool to 4^{o}C before loading the dialysed samples. The samples were loaded into dry wells along with a native molecular weight marker, empty wells were loaded with some BN-lysis buffer. The wells were then overlaid with cold cathode buffer, the inner chamber in the gel rig was then gently filled with cold cathode buffer while the outside was filled with the cold anode buffer. The gels were run overnight at 25 volts at 4^{o}C until the blue running front reached the bottom of the gel. A native marker mix was used to estimate the sizes of the complexes in the samples. In our experiments we used a range of proteins whose sizes covered the range of complexes that we were interested in. BSA (66 and 132kD), Catalase (232kD) and Ferritin (440 and 880kD) were used. An advantage of using BSA and Ferritin is that in addition to their

monomer form they also exist as dimers providing two size markers for the marker mix and possibly providing an indication of SDS contamination, if SDS is present it will disrupt the dimer of the marker in addition to the complexes in the samples, an additional advantage of ferritin is that it is coloured and can be seen while the gel is running providing an indication of how well the gel is progressing. The sizes of the detected complexes can vary from the predicted values however due to a number of factors for example detergent micelles may form around a membrane complex which would add to its observed size (Swamy, Siegers, et al. 2006) therefore the sizes given by the marker mix should be taken as a guide only.

For experiments that only required the first dimension the gel was transferred using the usual western blotting procedure. For samples that required a second dimension an SDS-Page gel was prepared with one small lane for the molecular weight marker and one long lane. The lanes on the blue native gel were cut out and the slices were placed into SDS sample buffer for 10 minutes followed by a quick boiling in the microwave for no more than 20 seconds. The slice was left in the sample buffer for another 10-15mins and it was then loaded into the long lane of the SDS-Page gel, overlaid with SDS sample buffer and run according to normal SDS PAGE protocols with subsequent western blotting.

A thorough and in-depth protocol for BN-PAGE with additional troubleshooting advice can be found in Swamy, M. et al. and Wittig, I. et al. (Swamy, Siegers, et al. 2006; Wittig et al. 2006).

2.7 Competent Cell Preparation

Chemically competent cells were prepared from *E.coli* strain Novablue (*Merck) (*endA1) or *E.coli* strain BL21/DE3 (*NEB)* with $CaCI_2$ solution, which facilitates transformation of the cells with DNA. 50 µl of Novablue competent cells were added to 5 ml of LB broth, and cultured overnight at 37°C. LB broth (100ml) was inoculated with 1ml of the *E.coli* overnight pre-culture and incubated at 37°C until the OD600 of the culture reached 0.4-0.8 (after approximately 6 hours). Then, the bacteria were pelleted by centrifugation at 4°C for 20 minutes at 3,000g. The pellet was immediately resuspended in 34ml of ice-cold transformation buffer (TB) and incubated on ice for 10 minutes. The cells were pelleted as before and resuspended in 8ml ice-cold TB. 600 µl of Dimethyl sulphoxide (DMSO, *Sigma-Aldrich)* was added and the cells were incubated on ice for a further 10 minutes. Aliquots of 200-300 µl were snap frozen in liquid nitrogen and stored immediately at - 80°C.

2.7.1 Transformation of chemically competent cells

Competent cells were thawed on ice. 50 µl of cells were transferred into a cold 1.5ml tube containing 50 ng of plasmid DNA and kept on ice for 10 mins before being heat- shocked for 30 seconds at 42°C, and then placed on ice for a further 2 minutes. The cells were immediately plated onto LB agar plates (LB broth with 1.5 % (w/v) agar) containing 100µg/ml ampicillin antibiotic and incubated at 37°C overnight.

For kanamycin resistant plasmids an additional outgrowth step was required. After heat-shock 100µl of SOC medium or LB broth was added to cells, and the tube was left shaking at 37°C in a bacterial incubator for 1h. Outgrowth at 37°C for 1 hour is best for cell recovery and maintenance of antibiotic resistance. Transformed cells

were then spread onto LB agar plates containing 100µg/ml kanamycin and incubated at 37°C overnight.

2.7.2 Large scale DNA preparation

Plasmid isolation and purification from bacterial cells was performed using the Nucelobond Xtra Midi Kit *(Macherey-Nagel)* according to the manufacturer's protocol. Briefly, a starter culture of LB broth (5ml) containing appropriate antibiotic was inoculated with a single transformed *E.coli* colony and incubated at 37°C with constant shaking for 3-6h. This was then added to LB broth (100ml) containing appropriate antibiotic and incubated over night at 37°C with constant shaking. The bacterial cells were centrifuged at 3000g for 20mins and subjected to lysis and purification as per the manufacturer's instructions. All plasmids were eluted in molecular grade water. DNA concentrations and purity were determined using a NanoDrop® ND-1000 Spectrophotometer according to the manufacturer's protocol.

2.8 Protein Work

2.8.1 Production of recombinant 6His-tagged and GST-tagged proteins in BL21 Ecoli

1 µl plasmid DNA (pHis-Parallel-2 expression plasmid) was transformed chemically into competent *E. coli* strain BL21/DE3 *(New England Biolabs)* as section 2.7.1. Overnight pre-culture was performed at 37°C by inoculating with one transformed colony in 12 ml of LB (AMP) overnight. Alternatively, 5 µl of a glycerol stock was used to inoculate the 12ml pre-culture of LB (AMP). 10 ml of the overnight pre-culture was inoculated into a 100 ml LB (AMP) culture and incubated at 37°C up to the logarithmic phase of growth. When OD600 =1.2, protein expression was induced by the addition of isopropyl β-D-1 thiogalactopyranoside (IPTG) to a final concentration of 100 µM at room temperature overnight. The *E.coli* cells were pelleted by centrifugation of 4000g for 15min at 4°C, and then resuspended in 1 ml native lysis buffer for 6His-tagged proteins (or for GST proteins in GST lysis buffer). Lysates were snap frozen in liquid nitrogen and thawed using a water bath. Three cycles of freeze-thawing were carried out. Additional sonication (30% power for 10sec x 3) were performed on the lysates to completely lyse the bacteria. The lysates were cleared by centrifugation at 13000g for 30 min. 100 µl Ni-NTA bead slurry (*Qiagene)* for his proteins (or Glutathione Sepharose (GS) bead slurry (70%, 1.4 ml, *GE Heathcare)* for GST proteins) was washed three times with His-Wash Buffer (or GST wash buffer), then added to the cleared lysates, and incubated at 4°C for overnight with constant rotation. The beads were then washed twice with 1.5 ml of the appropriate washing buffer I and II and the proteins were eluted by 100µl of

elution buffer. Aliquots of protein were run on SDS-PAGE and stained with Coomasie Blue to assess purity and amount of purified recombinant proteins.

2.8.2 Coomassie staining

SDS-PAGE gels were stained with Coomassie Blue Staining Solution for 5 minutes on a rocker, followed by destaining in de-stain solution until the background was clear.

2.8.3 In vitro pulldown assay

For pull-downs, equal amounts of the different His- or GST- tagged fusion proteins were used, as estimated by SDS–PAGE and Coomassie Blue staining prior to use. Cell lysates containing Myc-tagged proteins expressed in HEK293T cells or 0.5µg of recombinant protein were incubated with the purified His- or GST-tagged proteins coupled to Nickel-Agarose or Glutathione-Sepharose respectively, with constant rotation for 4h or overnight at 4°C. Beads were washed three times in 1.5ml lysis buffer, and then all the liquid drained. Beads were then resuspended in 2x Laemmli sample buffer and boiled for 10min at 95 oC. Sample were analysed for interactions by SDS-PAGE and Western blotting.

2.8.4 Kinase assay

Human N-terminal GST- HIS6-tagged IKK-epsilon, Human IKK-beta and human NF-kappaB-inducing kinase (NIK), proteins were purchased from ProQinase. Recombinant full- length human IKKα, containing an N-terminal GST-tag, was from Millipore.

In all experiments 55ng of recombinant kinase protein in 1 µl was used, to this, a master mix of 10 µl of 2X kinase assay buffer with 5 µg of substrate was added. An

ATP solution containing [γ-32P] ATP (5 μCi/tube, correspondent to 0.5 μl; Perkin-Elmer) and 200 μM ATP (2.5 μl/tube; Sigma- Aldrich) was prepared. 3 μl of this ATP mix were added to each tube. The tubes were incubated for 30 minutes at 30°C, then 3μl 6X sample buffer was added, and the tubes boiled at 95°C for 10 minutes; the boiled samples were then run on a 10% polyacrylamide gel. The incorporation of [γ- 32P] ATP was then evaluated by autoradiography of the gel (generally, 24h exposure). Non-radioactive kinases assay were also carried out where the addition of [γ-32P] ATP was omitted, visualisation of these result was obtained by carrying out western blotting on the gel followed by probing with appropriate antibodies.

GST-IRF7 (aa 468-503) peptides and constructs were kindly provided by Prof John Hiscott and Dr Qiang Sun (McGill University, Montreal).

2.9 Statistical analysis.

Data analysis was carried out using the unpaired Student *t* test using Microsoft Excel. Every experiment has been conducted at least three times, each time in triplicate, unless otherwise stated. Statistically significant differences are indicated by the asterisks: *, $P < 0.05$; **, $P < 0.01$; ***, $P < 0.001$.

2.10Antibodies

Antibody	Company	Species	Western Dilution
α-Ha	Cambridge Biosciences	Mouse	1:1000
α-Myc	Sigma	Mouse	1:1000
α-DDX3	Santa Cruz	Mouse	1:200
α-DDX3	Bethyl Laboratories	Rabbit	1:1000
α-polyHistidine HRP	Sigma	Mouse	1:1000
α-Tubulin	Abcam	Mouse	1:1000
α-GST HRP	GE Healthcare	Goat	1:2000
α-Flag	Sigma	Mouse	1:1000
α-IRF-7	Santa Cruz	Mouse	1:200
α-p52/p100	Millipore	Mouse	1:1000
α-IKKα/β P ser176/180	Cell Signalling	Rabbit	1:1000
α-NIK	Cell Signalling	Rabbit	1:1000
α-IKKα	Cell Signalling	Rabbit	1:1000
α-IRF7 P ser471/472	Cell Signalling	Rabbit	1:1000
α-p65 P ser468	Cell Signalling	Rabbit	1:1000
α-p100 P ser866/870	Cell Signalling	Rabbit	1:1000
α-IKKα/β ser176/180 II	Cell Signalling	Rabbit	1:1000
α-p65 ser536	Cell Signalling	Rabbit	1:1000
Control antibodies for Co-IPs			
Rabbit IgG	Bethyl Laboratories	Rabbit	
Mouse IgG2a	R&D Systems	Mouse	
Secondary antibodies			

Mouse Fab	Sigma		1:3000
Rabbit	Sigma		1:3000

2.11Recipies

2.11.1Lysis Buffers

Phospho-Lysis Buffer			
Reagent	**Final Conc.**	**Stock**	**For 6ml**
NaCl	150mM	1M	909.1 µl
Sodium Phos-Mono Ph 7.5	0.01M	1M	60 µl
IGEPAL	0.5%	100%	30 µl
NaF	50mM	0.5	75 µl
NaV	1mM	100mM	60 µl
DTT	1mM	100mM	60 µl
PMSF	1mM	100mM	60 µl
EDTA	2mM	500mM	24 µl
EGTA	1mM	100mM	60 µl
BGP	1M	100mM	60 µl
Aprotinin			60 µl
N-ethylmalemide	2mM	50 mg/ml	31.3 µl
Water			4612.6 µl

RIPA Lysis Buffer	50mM Tris-HCL pH 7.4 150mM NaCl 1mM EDTA 1% Triton-X 100 .5% Sodium Deoxycholate .1% SDS
Protease and phosphatase inhibitors	Aprotinin (20µl/ml) 1 mM sodium orthovanadate (10µl/ml) 1 mM PMSF (10µl/ml)
IP Lysis Buffer	50mM HEPES pH 7.5 (or Tris/HCl pH 7.5) 1mM EDTA 10% Glycerol 0.5% NP-40 (or 1% NP-40) 150mM NaCl

2.11.2 General Reagents

Resolving Gel Buffer **(1.5M Tris,pH8.8)**	90.75g Tris Add 400ml dH_20 Adjust pH 8.8 with HCl Make up to 500ml
Stacking Gel buffer **(0.5M Tris,pH6.8)**	15g Tris Add 150ml dH_20 Adjust to pH 6.8 with HCl Make up to 250ml
10% Resolving Gel **(2 gels)**	4.1ml dH_20 3.3ml 30% acrylamide 2.5ml 1.5Tris (pH 8.8) 100 µl 10% SDS 50µl APS Temed 5 µl
5% Stacking Gel **(2 gels)**	3.4ml dH_20 1ml 30% acrylamide 1.5ml 1.5Tris (pH 8.8) 60 µl 10% SDS 60µl APS Temed 6 µl

10x Running buffer	30.3g Trizma Base 144g Glycine 10g SDS Make up to1L with dH_20

10x Transfer Buffer	30.3 Tris 144g Glycine Make up to 1L with dH_20
1x Transfer Buffer	50ml 10X Transfer Bufer 75ml Methanol (15%) Make up to 500ml with dH_20

20x TBS pH 7.4	Tris 0.5M (48.4g) NaCl 1.5M (160g) To 1L with dH_2O

ECL development solution	24ml of 100mM Tris-HCL pH 8.5 7.6 µl of 30% H_2O_2 120 µl of 250mM luminol 53.2 µl of 90mM p-Coumaric acid

Transformation Buffer	55 mM $MnCl_2 \cdot 4H_2O$ 15 mM $CaCl_2 \cdot 2H_2O$ 250 mM KCl 10 mM PIPES (0.5M, pH 6.7) Chilled to 0ºC before use.

2X Kinase Assay buffer	40 mM HEPES pH 7.4 40 mM $MgCl_2$ 4 mM DTT 40 mM β-glycerophosphate 0.2mM Na_3VO_4 1 mM PMSF Complete Mini EDTA-free tablets, 1 tablet in 10ml 0 mM HEPES pH 7.4

Firefly luciferase substrate	470 mM Luciferine (Biosynth) 20 mM Tricine 2.67 mM Magnesium sulphate 0.1 mM EDTA (Promega) 2.0 mM DTT (Fisher) 5.0 mM ATP 270 μM Acetyl-CoA 1.07 mM Magnesium carbonate

2X HBS	42 mM HEPES 10 mM KCl 12 mM dextrose 1.5 mM $Na_2HPO_4 \cdot 7H_2O$ 280 mM NaCl 42 mM HEPES
2.5M CaCL2:	36.75g CaCL2.2H_20 to 100ml with dH_2O

10x PBS	85g NaCl 4.68g NaH_2PO_4 32.2g Na_2HPO_4 To 1L with dH_2O
PBS/Tween (PBST)	1xPBS 0.01% Tween

2x Laemmli sample buffer	2ml 0.5M Tris/Cl pH 6.8 2% SDS (use 10% stock) 10ml Glycerol 200µl bromophenol blue (1% stock in ethanol) 2ml 1M DTT Make up to 20ml with dH_20

2.11.3 Reagents for protein work

Coomassie Blue staining solution	0.25% (w/v) Coomassie Brilliant Blue 10% (v/v) glacial acetic acid 50% (v/v) methanol
De-stain solution	25% (v/v) methanol 2.5% (v/v) glacial acetic acid

GST lysis Buffer pH 8.0	**Reagent**	**Volume**	**Final Concentration**
	20x TBS	25ml	1x
	NaCl	4.38g	150mM
	1M MgCl2	2.5ml	5mM
	Sucrose		250mM
	Glycerol	50ml	10%
	Triton-X 100	5ml	1%
	Imidazole 1M	5ml	10mM
	B-mercaptoethanol	1.4 µl /ml	20mM
	To 500ml with dH_2O, mercaptoethanol and protease inhibitors added just before use.		
GST Wash Buffer 1		Lysis Buffer	1x
		Imidazole 1M	20mM
GST Wash Buffer 2		Lysis Buffer	1x
		Imidazole 1M	40mM
Elution Buffer		Imidazole 1M	250mM

His lysis Buffer pH 8.0	Reagent	Volume	Final Concentration
	NaH_2PO_4	3g	50mM
	NaCl	4.38g	150mM
	Imidazole 1M	5ml	10mM
	B-mercaptoethanol	1.4 µl /ml	20mM
	To 500ml with dH_2O, mercaptoethanol and protease inhibitors added just before use.		
His Wash Buffer 1		Lysis Buffer	1x
		Imidazole 1M	20mM
His Wash Buffer 2		Lysis Buffer	1x
		Imidazole 1M	40mM
Elution Buffer		Imidazole 1M	250mM

2.11.4 Reagents for Blue-Native PAGE

BN Native marker mix	BSA (66 / 132 kDa)	10mg/ml
	Catalase (232 kDa)	10mg/ml
	Ferritin (440 / 880 kDa)	10mg/ml
	Bis Tris	20mM
	NaCl	20mM
	Glycerol	10%
	Adjust pH to 7.0 with HCL	

BN Base Buffer	Bis-Tris	20mM
pH 7.0 (HCL)	E-Aminocaproic acid	500mM
	NaCl	20mM
	EDTA pH 8.0	2mM
	Glycerol	10%
For BN Lysis buffer add:	Triton-X 100	0.1%
	Na_3VO_4	0.5mM
	IAA	2.5mM
	PMSF	1mM
	NaF	0.5mM
	Protease inhibitor cocktail tablet	1
BN Dialysis Buffer pH 7.0	BN base buffer	
	Triton-X 100	0.1%
	PMSF	1mM
	NaV	0.5mM

3xBN-Gel Buffer	Bis-Tris	150mM
	E-Aminocaproic acid	200mM
	Adjust pH to 7.0 with HCL	
BN 3.2% upper gel	3x BN Gel Buffer	2ml
(4 gels)	Acrylamide-Bisacrylamide mix 32:1 40% acrylamide	0.48ml
	dH_2O	3.52ml
	10% APS	80 ul
	TEMED	8 µl
BN 4-12% gradient separating gel (1 gel)		
HIGH 12%	3x BN Gel Buffer	0.833ml
	Acrylamide-Bisacrylamide mix 32:1 40% acrylamide	0.750ml
	70% Glycerol	0.917ml
	10% APS	9.0 ul
	TEMED	1 µl
LOW 4%	3x BN Gel Buffer	0.833ml
	Acrylamide-Bisacrylamide mix 32:1 40% acrylamide	0.250ml
	dH_2O	1.417ml
	10% APS	9.0 ul
	TEMED	1 µl

BN Cathode Buffer	Bis-Tris	15mM
	Tricine	50mM
	Coomassie Blue G250	0.02%
	Prepare a 10x stock, pH to 7.0 with HCL before adding coomassie.	
BN Anode Buffer	Bis-Tris	50mM
	Prepare a 10x stock, pH to 7.0 with HCL before adding coomassie.	

2.11.5 SDS PAGE Gels

dH_2O (ml)	**30% Acrylamide (ml)**	**Gel Buffer* (ml)**	**10% w/v SDS (ml)**	**10% APS (µl)**	**TEMED (µl)**
3.4	1	1.5	.060	30	3

Table 3: Composition of Stacking SDS-PAGE gel. *0.5M Tris-HCL pH 6.8

% Gel	**dH_2O (ml)**	**30% Acrylamide (ml)**	**Gel Buffer* (ml)**	**10% w/v SDS (ml)**	**10% APS (µl)**	**TEMED (µl)**
7%	5.1	2.3	2.5	0.1	30	3
8%	4.7	2.7	2.5	0.1	30	3
9%	4.4	3.0	2.5	0.1	30	3
10%	4.1	3.3	2.5	0.1	30	3
11%	3.7	3.7	2.5	0.1	30	3
12%	3.4	4.0	2.5	0.1	30	3
13%	3.1	4.3	2.5	0.1	30	3

Table 4: Composition of Resolving SDS-PAGE GEL. *1.5M Tris-HCL pH 8.8

3 Results

3.1 DDX3 interacts directly with IKKα and enhances its activation

Initially, we sought to determine whether there was an interaction between DDX3 and IKKα. To this end, we carried out immunoprecipitation assays by co-expressing Myc-tagged DDX3 and Flag-tagged IKKα in HEK293T cells and using an anti-Flag antibody to immunoprecipitate IKKα. DDX3 showed a strong co-immunoprecipitation with IKKα in this case (**Figure** *7*).

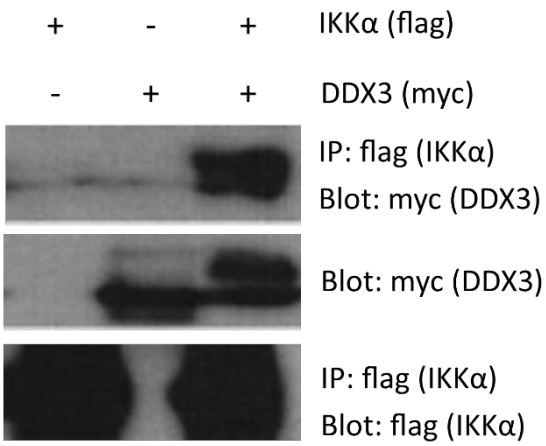

Figure 7: DDX3 co-immunoprecipitates with IKKα.

HEK293T cells were transfected with constructs for Flag-IKKα and/or Myc-DDX3. Cell lysates were subjected to immunoprecipitation (IP) with an anti-Flag antibody, followed by SDS-PAGE and WB analysis with the indicated antibodies (Shown is a representative experiment of 3 independent experiments).

This co-immunoprecipitation also showed a higher molecular weight form of DDX3 when both DDX3 and IKKα were expressed together, which is likely to be a phosphorylated form of DDX3. As NIK is a related kinase to IKKα and is known to work with IKKα in the signalling pathways we are interested in, we also carried out

similar co-immunoprecipitations with Myc-tagged DDX3 and Flag-tagged NIK. NIK also clearly immunoprecipitated with DDX3 (**Figure *8***). In this experiment, endogenous IKKα also showed strong co-immunoprecipitation with the NIK-DDX3 complex, suggesting that all three proteins might be in one complex together (**Figure *8***, bottom panel).

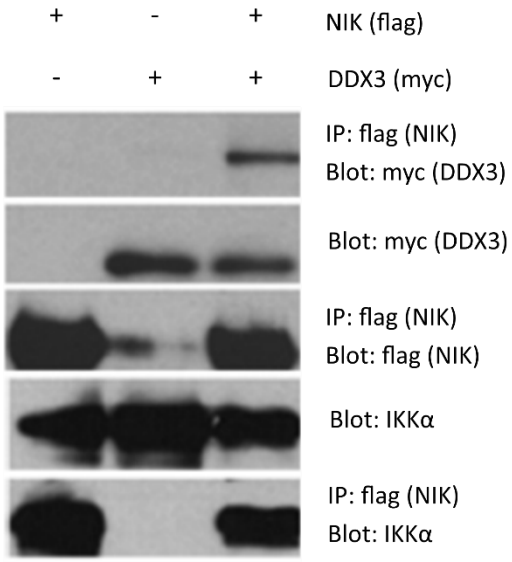

Figure 8: DDX3 co-immunoprecipitates with NIK.

HEK293T cells were transfected with constructs for Flag-NIK and/or Myc-DDX3. Cell lysates were subjected to immunoprecipitation (IP) with an anti-Flag antibody, followed by SDS-PAGE and WB analysis with the indicated antibodies (Shown is a representative experiment of 3 independent experiments).

With this experimental setup it was therefore not clear whether DDX3 interacted directly with both IKKα and NIK, as it is possible that IKKα might bridge the interaction between NIK and DDX3, and that the observed interaction with NIK was therefore indirect. To investigate this further, we carried out pulldown assays using recombinant proteins which allowed us to detect direct interactions. Using recombinant His-tagged DDX3 purified from *E-coli* and GST-tagged IKKα in this assay, we confirmed a direct interaction between the two proteins (**Figure *9***).

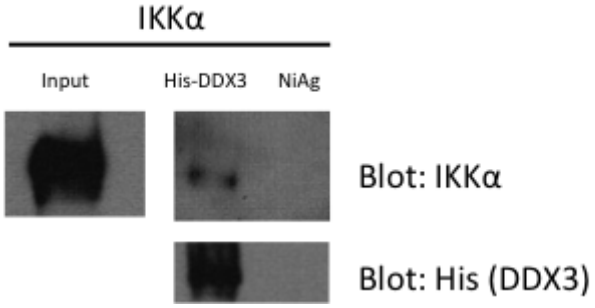

Figure 9: DDX3 directly interacts with IKKα.

Purified recombinant full-length His-DDX3 was incubated with recombinant GST-IKKα. Following pulldown with nickel agarose (Ni-Ag), interacting proteins were subjected to SDS-PAGE and WB analysis with the indicated antibodies (Shown is a representative experiment of 3 independent experiments).

As we had confirmed a direct interaction between DDX3 and IKKα, we next sought to characterise this interaction further. To this end we used a series of DDX3 truncation mutants to map the interaction sites between DDX3 and IKKα. Co-immunoprecipitations were carried out using Flag-tagged IKKα and Ha-tagged DDX3 mutants consisting of DDX3 full length (aa 1-662), DDX3 (aa 1-408), and DDX3 (aa 409-662). DDX3 (aa 1-408) and DDX3 (aa 409-662) represent the two

'halves' of DDX3, with the DDX3 protein split at the flexible linker region between the two RecA-like globular domains. IKKα successfully co-immunoprecipitated with full length DDX3 and with its N-Terminal region (aa 1-408) but not with the C-terminal region (aa 409-662) (**Figure *10***).

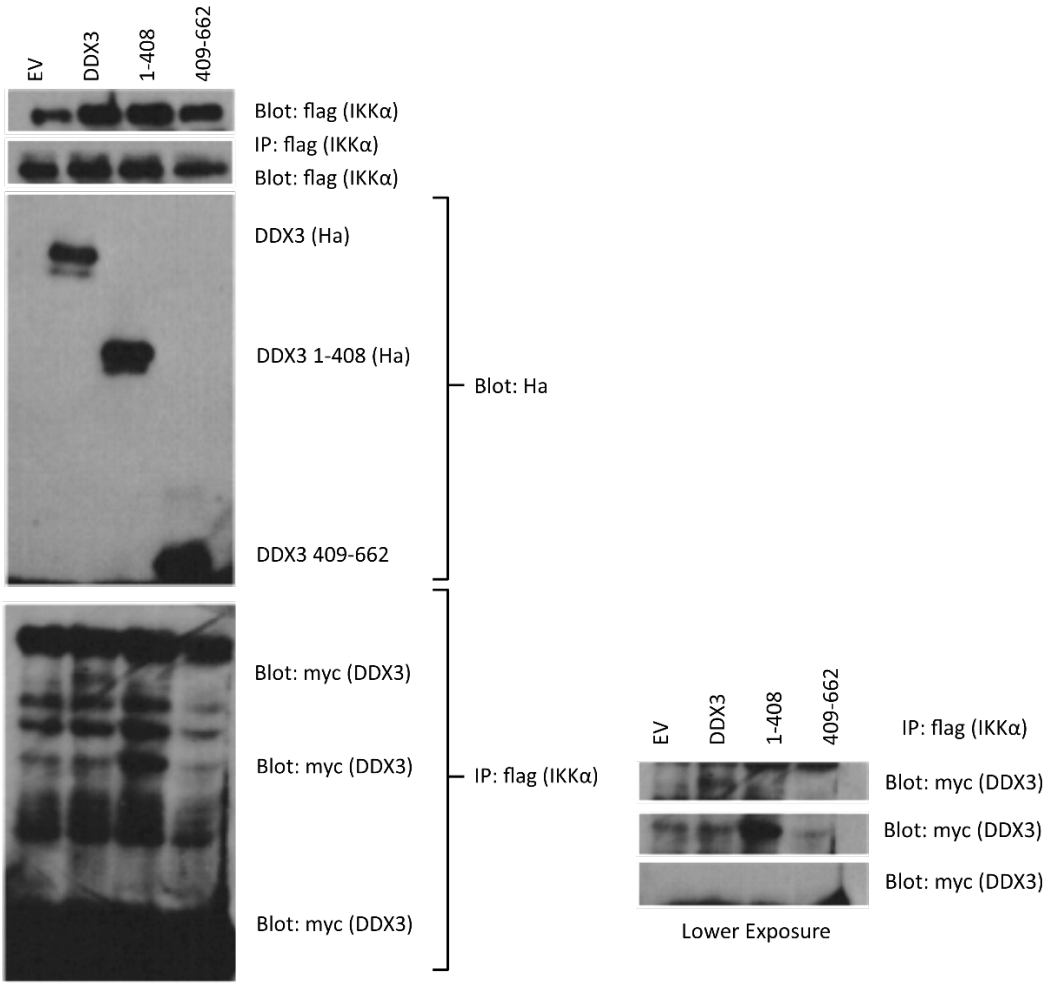

Figure 10: IKKα interacts with the N-terminal region of DDX3.

HEK293T cells were transfected with constructs for Flag-IKKα and one of Ha-tagged DDX3 full length (aa 1-662), DDX3 (aa 1-408), or DDX3 (aa 409-662). Cell lysates were subjected to immunoprecipitation (IP) with an anti-Flag antibody, followed by SDS-PAGE and WB analysis with the indicated antibodies (Shown is a representative experiment of 3 independent experiments).

In addition, pulldown assays, carried out by Dr. Lili Gu in our Host-Pathogen Interaction Lab, using recombinant His-tagged DDX3 mutants (DDX3 (aa 1-408), DDX3 (aa 139-408), DDX3 (aa 172-408) and DDX3 (aa 409-662)), to pull down flag-IKKα from cell lysates, corroborated these findings and further narrowed the binding site for IKKα on DDX3 (**Figure *11***). In this experiment IKKα interacted with the 1-408 and the 139-408 aa regions of DDX3, but not with the 172-408 and 409-662 aa regions (**Figure *11***). This suggested that IKKα interacts somewhere between aa 139 and aa 172 of DDX3, although it does not exclude the possibility of additional binding sites within the N-terminus of DDX3.

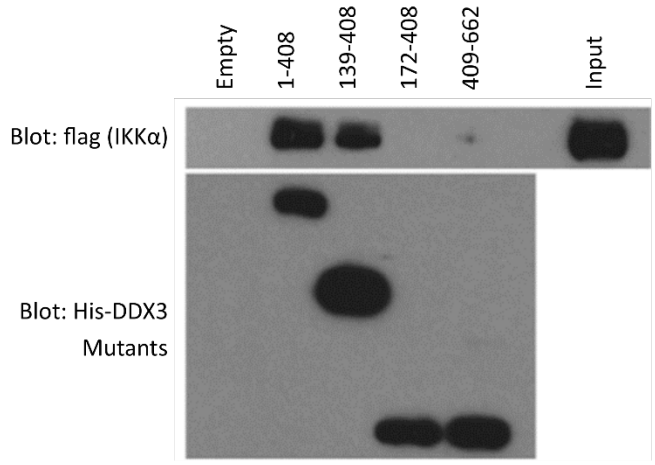

Figure 11: IKKα interacts with the region between aa 139 to 172 of DDX3.

His-tagged full-length DDX3 (aa 1-408), DDX3 (aa 138-408), DDX3 (aa 172-408), or DDX3 (aa 409-662) purified recombinant proteins were incubated with cell lysates from Flag-IKKα expressing HEK293T cells. Following pulldown with nickel agarose, interacting proteins were subjected to SDS-PAGE and WB analysis with the indicated antibodies (Shown is a representative experiment of 3 independent experiments). Figure prepared by Lili Gu – host pathogen interaction lab, NUI Maynooth.

The interaction between IKKα and DDX3 was also detectable at an endogenous level. We carried out immunoprecipitations using an endogenous DDX3 antibody or a related isotype control antibody, following a time course of CLO75 stimulation in HEK293-TLR7 cells. (**Figure *12***). Endogenous IKKα co-immunoprecipitated with DDX3 45 minutes after CLO75 stimulation, which confirmed that DDX3 is involved in TLR7/8 signalling via an inducible and transient association with IKKα.

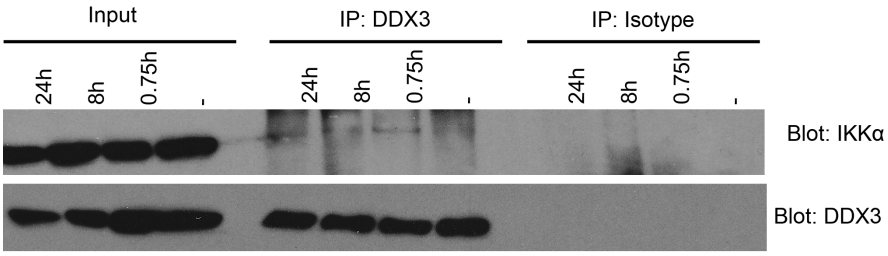

Figure 12: Endogenous DDX3 and IKKα interaction induced by the TLR7/8 ligand CLO75.

HEK293-TLR7 cells were stimulated for the indicated times with 1μg/ml CLO75. Cell lysates were subjected to immunoprecipitation (IP) with an anti-DDX3 antibody or the corresponding isotype control antibody, followed by SDS-PAGE and WB analysis with the indicated antibodies (Shown is a representative experiment of 3 independent experiments).

3.1.1 Summary

In this section we have shown that DDX3 can interact with both IKKα and NIK. We have demonstrated that at least IKKα and DDX3 interact directly and that the site of interaction/s is in the N-terminus of DDX3. Finally we have also shown that the interaction between IKKα and DDX3 can be shown at an endogenous level following stimulation with the TLR7/8 ligand CLO75.

3.2 DDX3 enhances IKKα activation

Since we have shown a clear interaction between IKKα and DDX3, we next endeavoured to investigate what effect, if any, DDX3 has on IKKα activity. In previous studies, we have shown that DDX3 enhances IKKε auto-phosphorylation and activation (Gu et al. 2013), therefore we hypothesised that DDX3 may perform a similar role in the case of IKKα. We carried out both radioactive and non-radioactive kinase assays using recombinant DDX3 (aa 1-408), (the region interacting with IKKα) and recombinant kinase proteins. Enhanced IKKα auto-phosphorylation was observed in samples with DDX3 (aa 1-408) present compared to IKKα alone (**Figure *13*a**). In addition, the non-radioactive kinase assays using a phospho-IKKα ser176/180 specific antibody confirmed that this enhanced phosphorylation is due at least in part to enhanced phosphorylation on the serines 176/180 present in the activation loop of IKKα (**Figure *13*b**).

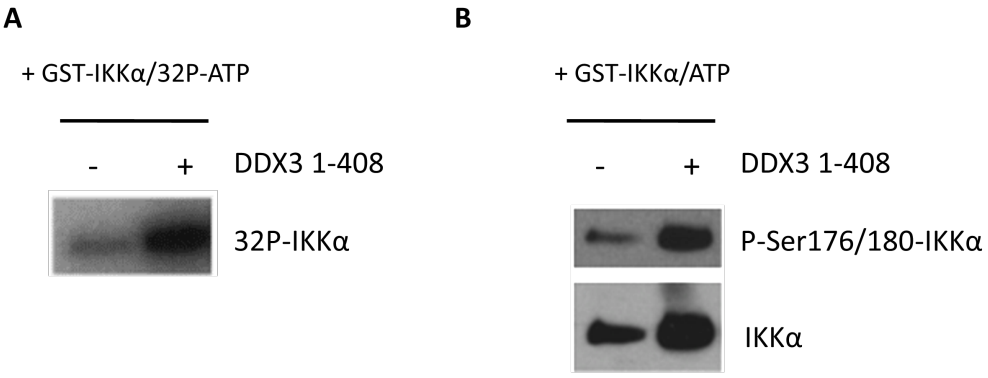

Figure 13: DDX3 enhances IKKα auto-phosphorylation in its activation loop.

(A) Recombinant GST-IKKα was incubated with recombinant His-DDX3 1-408 in the presence of [γ-32P]ATP. Samples were then subjected to SDS-PAGE and autoradiograph analysis showing incorporation of [γ-32P]ATP.

(B) Recombinant GST-IKKα was incubated with recombinant His-DDX3 1-408 in the presence of ATP. Samples were then subjected to SDS-PAGE and WB analysis with the indicated antibodies (Shown is a representative experiment of 3 independent experiments).

To confirm this effect was relevant in cells, we overexpressed Flag-tagged IKKα along with Ha-tagged DDX3 or with Ha-tagged K7, a vaccinia virus antagonist of DDX3 (Schröder et al. 2008). Subsequent probing with the phospho-specific (Ser176/180) IKKα antibody, showed that DDX3 enhanced IKKα auto-phosphorylation compared to IKKα alone, while K7, presumably targeting the endogenous DDX3 present in the cells, reduced this (**Figure *14***).

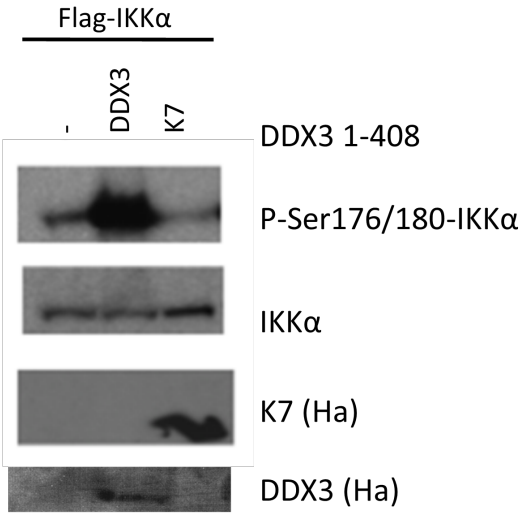

Figure 14: DDX3 enhances IKKα phosphorylation in its activation loop.

HEK293T cells were transfected with a plasmid vector for Flag-IKKα and either: Ha-DDX3, Ha-K7 or an empty vector. 24h after transfection samples were subjected to SDS-PAGE and WB analysis with the indicated antibodies (Shown is a representative experiment of 3 independent experiments).

To confirm a role for endogenous DDX3 in IKKα activation, we used a system n which DDX3 knockdown was inducible by the addition of doxycycline to HEK293-TLR7 cells stably expressing either pTRIPZ shDDX3 or the corresponding non silencing control (NSC) vector. This system allowed us to compare IKKα activation between cells with normal and reduced levels of DDX3. Following stimulation with CLO75 for 24 hours, the non-silencing control cells showed a slight increase in IKKα phosphorylation upon stimulation (**Figure 15**). However, IKKα phosphorylation, both in the presence and absence of CLO75 stimulation, was severely reduced in cells with reduced DDX3 (**Figure 15**).

Experiments using shorter time-points of stimulation showed that CLO75 increased IKKα phosphorylation, which peaked at approximately one hour after stimulation (**Figure 15**). In DDX3 knockdown cells both background levels and the induced IKKα phosphorylation were reduced. However, some phosphorylation did occur in a delayed manner compared to control cells, with some phosphorylation being observed at four hours after stimulation (**Figure 15**).

A

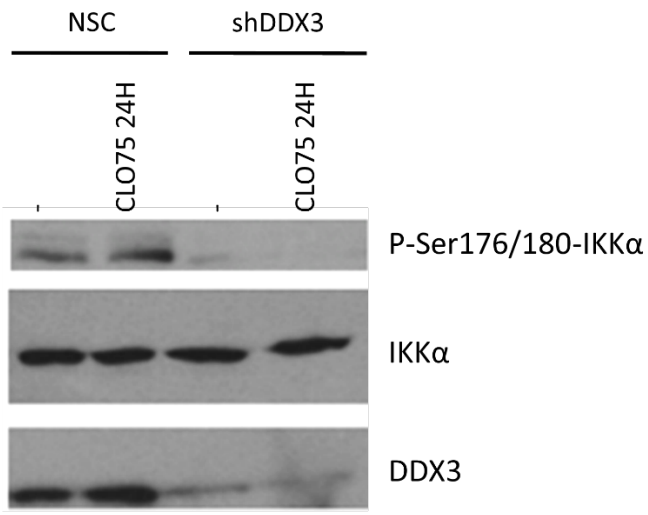
NSC
shDDX3
CLO75 24H
CLO75 24H
P-Ser176/180-IKKα
IKKα
DDX3

B

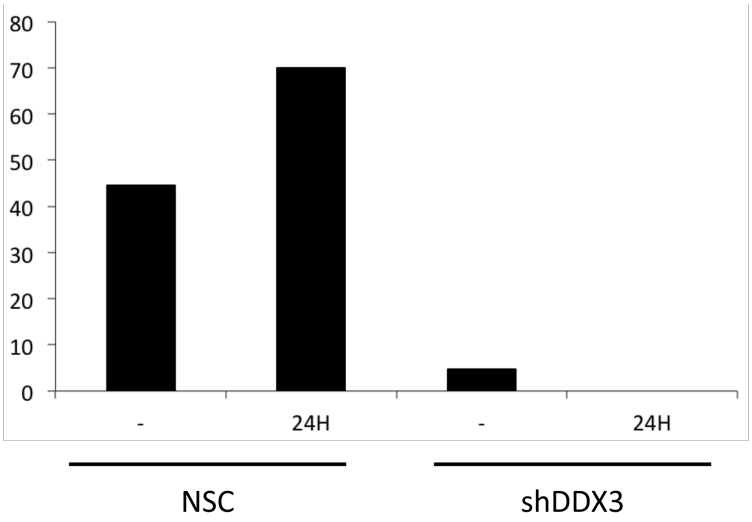
80
70
60
50
40
30
20
10
0
-
24H
-
24H
NSC
shDDX3

C

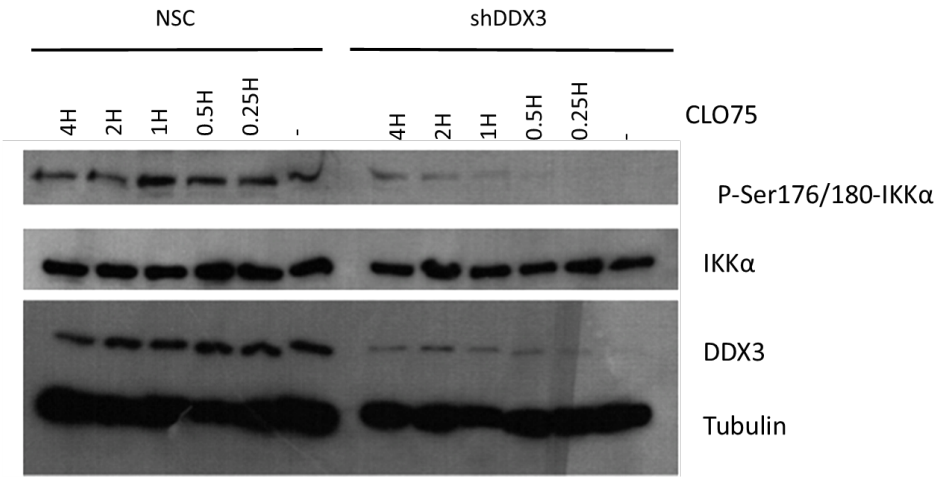

D

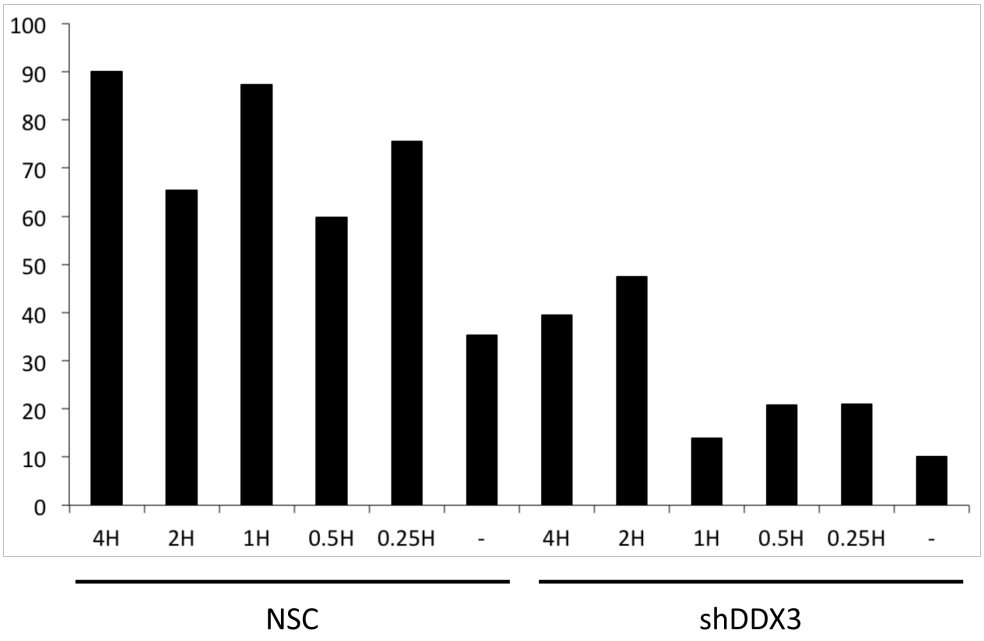

Figure 15: Knockdown of DDX3 both reduces and delays IKKα activation.

DDX3 knockdown was induced by the addition of 0.5 µg/ml doxycycline for 24 hrs to HEK293-TLR7 cells stably expressing either pTRIPZ shDDX3 or the corresponding non-silencing control (NSC). Cells were then stimulated with CLO75 for the indicated time periods followed by SDS-PAGE and WB analysis with the indicated antibodies (Shown is a representative experiment of 3 independent experiments) (A, C). Densitometry was carried out on IKKα and P-IKKα bands. Shown are P-IKKα band intensities shown as a percentage of total IKKα band intensity (B,D).

3.2.1 Summary

In this section we have investigated possible effects of the interaction between IKKα and DDX3. We have shown that DDX3 can enhance auto-phosphorylation of IKKα in its activation loop and that the DDX3 antagonist K7 can reduce this phosphorylation. We have also shown that knockdown of endogenous DDX3 can reduce and delay the activation-phosphorylation of IKKα following CLO75 stimulation. Our results clearly show that DDX3 has a direct role in enhancing IKKα auto-phosphorylation in its activation loop, therefore we next investigated signalling pathways that involve IKKα to determine whether there was any functional consequence of this interaction.

3.3 The effects of DDX3 on the alternative NF-κB pathway

3.3.1 DDX3 enhances processing of p100

To investigate a possible role of DDX3 in the alternative NF-κB pathway, we first set up a read-out system to test the effects on this pathway. A characteristic feature of this pathway is the processing of the p100 precursor NF-κB subunit to the smaller p52 subunit. The size difference between the two allowed us to visualise p100 processing simply by western blotting with an antibody that recognises both p100 and p52, and thus estimate the extent of induction of the pathway. Processing of p100 was inducible by a number of immune-relevant stimuli, including TNFα, CLO75, and Sendai Virus (SeV) (**Figure *16***).

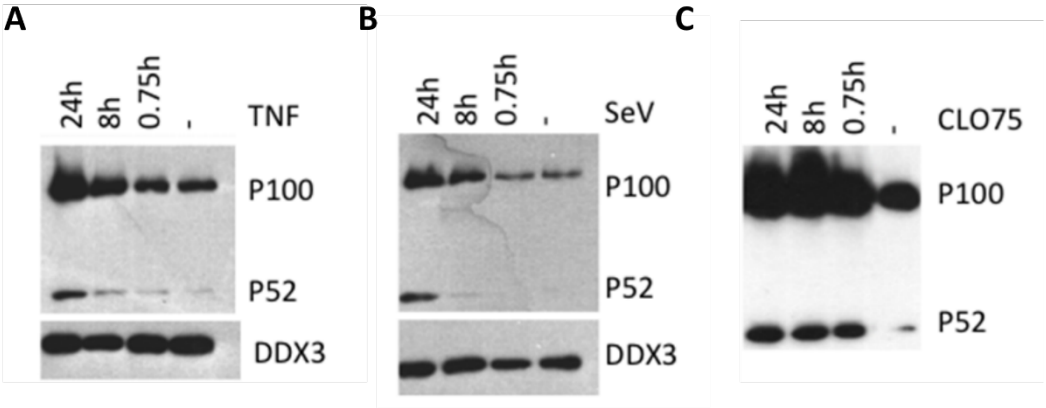

Figure 16: The alternative NF-κB pathway can be induced by CLO75, SeV and TNFα.

HEK293T cells were stimulated for the indicated time periods with TNFα (A) or SeV (B). HEK293-TLR7 cells were stimulated for the indicated times with CLO75 (C). Cell lysates were then subjected to SDS-PAGE and WB analysis with the indicated antibodies (Shown is a representative experiment of 3 independent experiments).

We showed that in addition to TNFα, p100 processing was inducible by both Sev and CLO75 demonstrating that it occurs downstream of RIG-I and TLR7 (**Figure 16**).

Using this setup as a readout for induction of the alternative NF-κB pathway, we then investigated the possible role of DDX3. Initially, we overexpressed Ha-tagged DDX3 or an empty vector control in HEK293T cells. Western-blot analysis showed that in the samples with DDX3, there was an increased smear in the band for p100 along with increased levels of p52 (**Figure *17***). A key step in the processing of p100 is K48-linked ubiquitination, which tags it for processing to p52 by the proteasome (Xiao et al. 2004). The smear we observed may well be indicative of this ubiquitination. This result was a first indication that DDX3 might play a role in the activation of this pathway, and therefore further investigation was warranted.

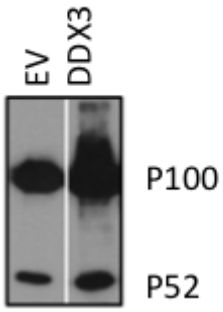

Figure 17: DDX3 induces a smear in p100 and increases levels of p52.

HEK293T cells were transfected with a plasmid vector for Ha-DDX3 or an empty vector (EV). 24h after transfection cells were subjected to SDS-PAGE and WB analysis with the indicated antibodies (Shown is a representative experiment of 3 independent experiments).

To investigate if DDX3 could affect p100 processing, we expressed a low and a high amount of Myc-tagged DDX3 or the Ha-tagged DDX3 antagonist K7 and subsequently stimulated HEK-293T cells with Sev for 24h. Increasing amounts of exogenous DDX3 led to a dose dependent enhancement of SeV-induced p100 processing, while the DDX3 antagonist K7 seemed to reduce this, demonstrating that DDX3 is a positive enhancer of p100 processing (**Figure *18***).

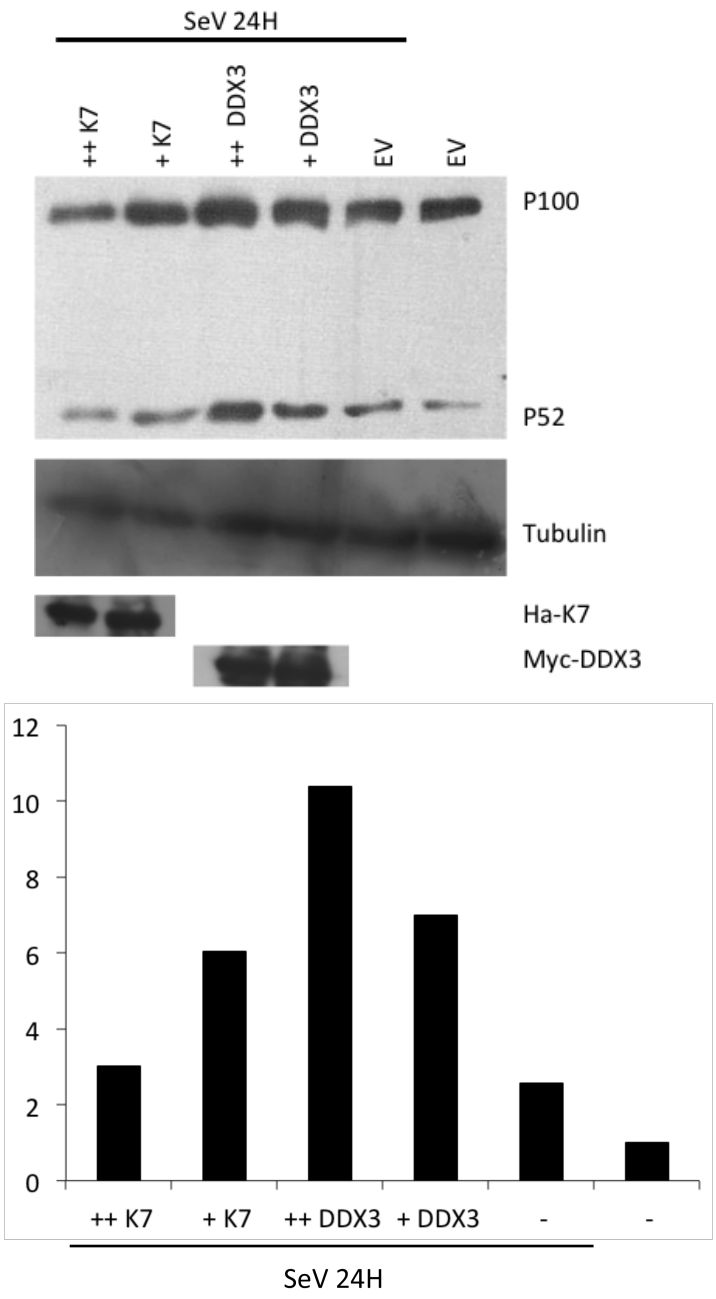

Figure 18: DDX3 enhances p100 processing.

HEK293T cells in 6 well plates were transfected with a plasmid vector for Ha-K7, Myc-DDX3 or an empty vector (++ 4µg plasmid DNA, + 2µg plasmid DNA). 24h after transfection cells were stimulated with SeV for 24h, samples were then subjected to SDS-PAGE and WB analysis with the indicated antibodies (Shown is a representative experiment of 3 independent experiments). Upper Panel) Densitometry was carried out on P52 and Tubulin bands. Shown are P52 band intensities normalised using Tubulin band intensities (Lower panel).

We next used our inducible DDX3 shRNA knockdown system in HEK293T cells and investigated the effect of reduced DDX3 levels on p100 processing induced by NIK and IKKα. We induced processing by expressing Flag-tagged NIK and IKKα in both control and knockdown cells and observed that p100 phosphorylation on serines 866/870 was somewhat reduced in cells with lowered DDX3 levels. These two serines are required for induction of p100 processing by facilitating the binding of IKKα to p100 (Xiao et al. 2004). As expected, this reduction in p100 phosphorylation corresponded to a matching reduction in p100 processing and therefore p52 levels (**Figure *19***).

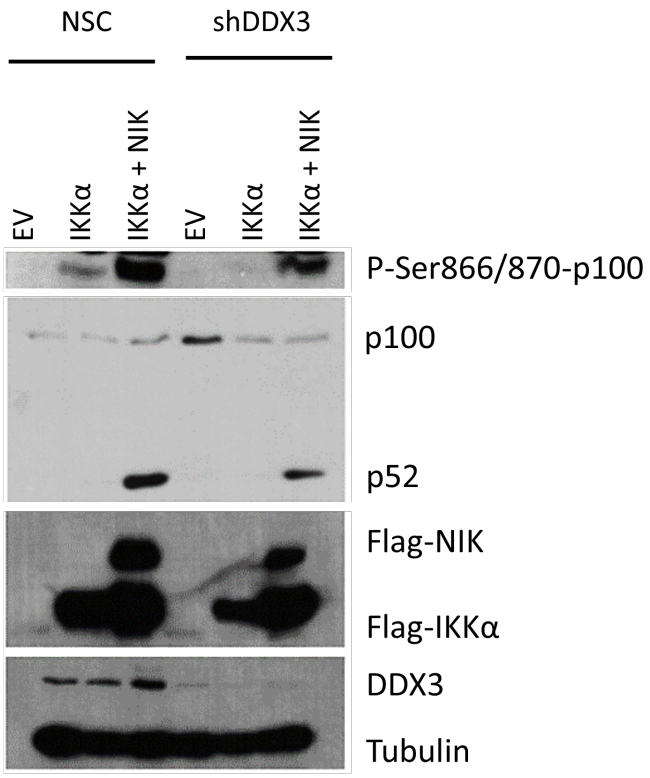

Figure 19: DDX3 knockdown reduces NIK-IKKα induced phosphorylation and processing of p100.

DDX3 knockdown was induced by the addition of 0.5 µg/ml doxycycline for 24 hrs to HEK293T cells stably expressing either pTRIPZ shDDX3 or the corresponding non-silencing control (NSC). Cells were then transfected with a plasmid vector for Flag-IKKα and Flag-NIK or an empty vector. 24h after transfection cells were then subjected to SDS-PAGE and WB analysis with the indicated antibodies (Shown is a representative experiment of 3 independent experiments).

In a similar experiment, using inducible DDX3 knockdown in HEK293-TLR7 cells, p100 phosphorylation was also reduced following CLO75 stimulation in DDX3 knockdown cells compared to control cells (**Figure *20***). In the same experiment IKKα phosphorylation was also delayed which could explain the reduced phosphorylation of p100. In addition, p100 processing to p52 was somewhat reduced in DDX3 knockdown cells.

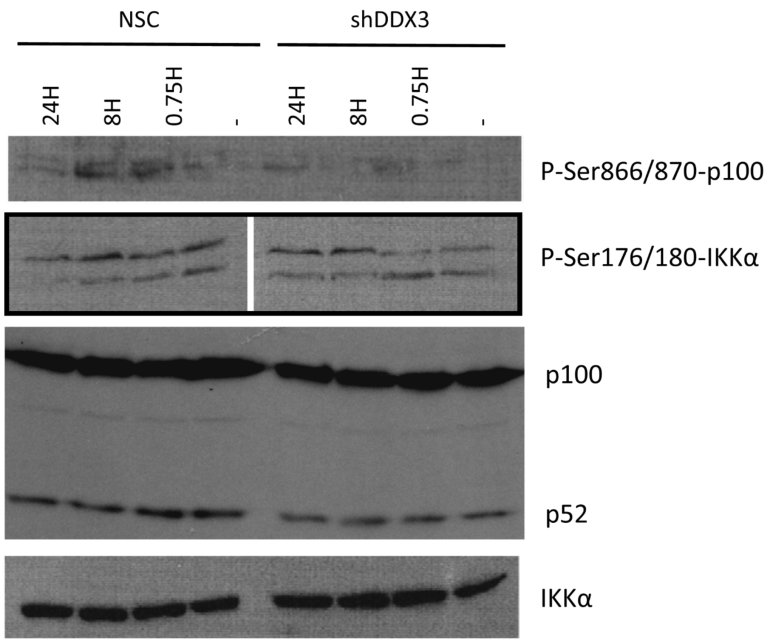

Figure 20: Knockdown of DDX3 reduces CLO75 induced p100 phosphorylation.

DDX3 knockdown was induced by the addition of 0.5 µg/ml doxycycline for 24 hrs to HEK293-TLR7 cells stably expressing either pTRIPZ shDDX3 or the corresponding non-silencing control (NSC). Cells were then stimulated with CLO75 for the indicated time periods and subjected to SDS-PAGE and WB analysis with the indicated antibodies (Shown is a representative experiment of 3 independent experiments).

3.3.2 DDX3 interacts with NF-κB subunits

With DDX3 and IKKα being in complex with each other, we next questioned whether downstream proteins could also form a complex with DDX3. In the case of the alternative NF-κB pathway we carried out co-immunoprecipitations with Myc-Tagged DDX3 and Ha-tagged p52 or p65. DDX3 clearly co-immunoprecipitated with both of these NF-κB subunits in this setup (**Figure *21***).

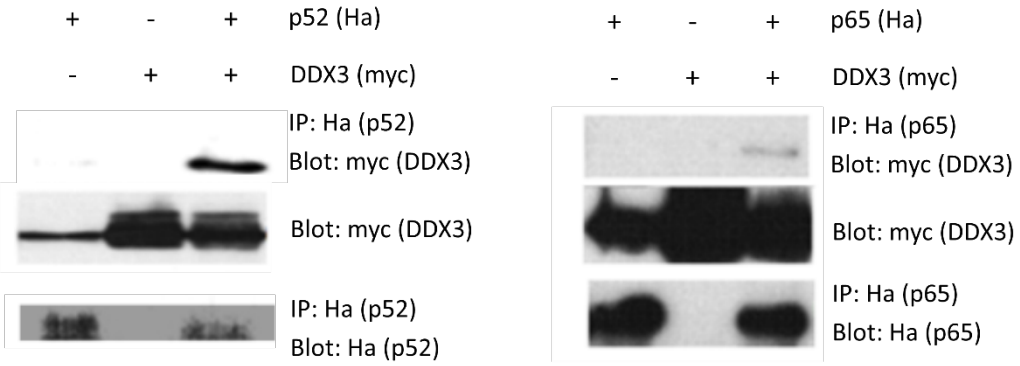

Figure 21: DDX3 interacts with p52 and p65.

HEK293T cells were transfected with constructs for Ha-P52 of Ha-p65and/or Myc-DDX3. Cell lysates were subjected to immunoprecipitation (IP) with an anti-Ha antibody, followed by SDS-PAGE and WB analysis with the indicated antibodies (Shown is a representative experiment of 3 independent experiments).

While p52 is a typical component of the alternative NF-κB pathway, p65 is a component of the classical NF-κB pathway. It can however be involved in the "hybrid pathway", in which p52 can dimerise with a subunit of the classical NF-κB pathway like p65 (Wietek et al. 2006). We next carried out endogenous co-immunoprecipitations of DDX3. DDX3 interacted with endogenous p100 and p65 constitutively (**Figure *22***). However, while stimulation of cells with CLO75 did not

affect the interaction with p100, the interaction with p65 was lost and only reappeared at the 24h time-point (**Figure *22***). Unfortunately we were unable to visualise p52 in these experiments as the size of p52 and the heavy chain of the IP antibody are a very similar size. With the IP and WB probing antibodies both produced in mouse the heavy chain of the IP antibody was bound by the mouse secondary antibody and obscured any p52 bands.

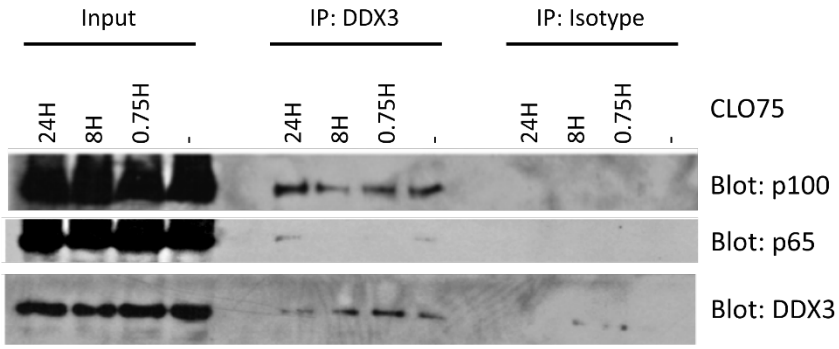

Figure 22: DDX3 constitutively interacts with p100 and p65.

HEK293-TLR7 cells were stimulated for the indicated time periods with 1µg/ml CLO75. Cell lysates were subjected to immunoprecipitation (IP) with an anti-DDX3 antibody or the corresponding isotype control antibody, followed by SDS-PAGE and WB analysis with the indicated antibodies (Shown is a representative experiment of 3 independent experiments).

3.3.3 Summary

In this section we investigated effects of DDX3 on one of the pathways that IKKα is involved in – the alternative NF-κB pathway. We showed that this pathway is activated following TLR7 and RIG-I stimulation. We have shown that in addition to DDX3 enhancing p100 processing its antagonist K7 can also inhibit this effect. We have demonstrated that knockdown of endogenous DDX3 reduces both phosphorylation of p100 at Ser866/870 and p100 processing downstream of NIK and IKKα, and following CLO75 stimulation. In an effort to investigate the role of DDX3 in this pathway further, we have also shown that DDX3 interacts with a number of NF-κB subunits, namely p52, p100, and p65.

3.4 Effects of DDX3 on TLR7 signalling

3.4.1 DDX3 is involved in IFN induction downstream of TLR7

While investigating the alternative NF-κB pathway, one of the ligands we used was CLO75, which stimulates TLR7/8. The TLR7 pathway is more commonly associated with the induction of large amounts of type 1 IFN following receptor engagement. As the pathway to IFN induction is in this case also mediated by NIK and IKKα, we considered a possible role of DDX3 in this pathway. Initial investigations were carried out by performing luciferase reporter gene assays, measuring induction of type 1 IFN promoters. Activation of the *ifnb* and *ifna4* promoters was induced by overexpressing both NIK and IKKα; and the involvement of DDX3 was assessed by co-expressing DDX3, its antagonist K7 or a dominant negative form of DDX3 (aa 1-139) (Schröder et al. 2008). Although a role for DDX3 in IFNβ induction had been shown previously, this was in the context of pathways mediated by the kinases IKKε/TBK1 (Schröder et al. 2008; Soulat et al. 2008). We demonstrated that our experimental setup was independent of these two kinases by using dominant negative forms of IKKε and TBK1 or the IKKε/TBK1 inhibitor BX795. Neither co-expression of the two dominant negative constructs nor the IKKε/TBK1 inhibitor had any effect on *ifnb* or *ifna4* promoter induction by NIK and IKKα (**Figure 23 A+B**). However DDX3 enhanced, while K7 and the dominant negative DDX3 (aa 1-139) inhibited both *ifnb* and *ifna4* induction (**Figure 23 A+B**).

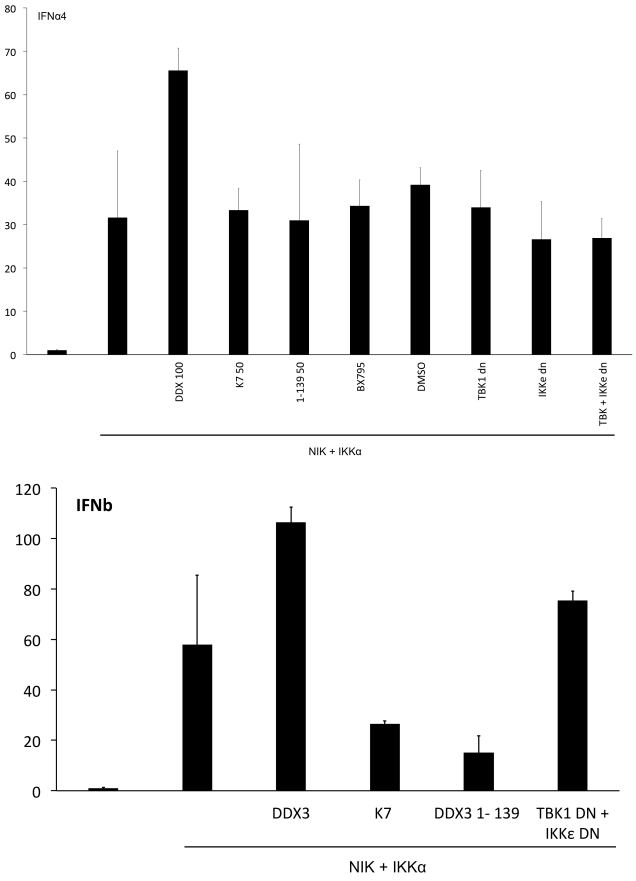

Figure 23: DDX3 mediates induction of IFNα4 and IFNβ by NIK/IKKα.

HEK293 cells were transfected with an ifnα4 (A) or ifnb (B) promoter reporter gene construct and expression constructs for Flag-IKKα/Flag-NIK and HA-DDX3, Ha-K7, HA-DDX3 1-139 or the dominant negative of TBK1/IKKε. Where indicated the inhibitor BX795 (50 ng/ml) was added 24h later and left for an additional 24h. Data for reporter gene assays are expressed as mean fold induction relative to control levels, +/- standard deviations. Shown are results of one representative experiment out of four, performed in triplicate.

In addition to inducing the pathway by overexpressing NIK and IKKα, we also carried out similar assays using CLO75. As HEK293-TLR7 cells naturally possess very low levels of the transcription factor IRF7, which is needed to activate the IFNα4 promoter, we co-transfected a small amount of IRF7. Transfection of a DDX3 construct resulted in a dose dependent increase in the induction of both *ifnb* and *ifna4* promoters (**Figure *24***).

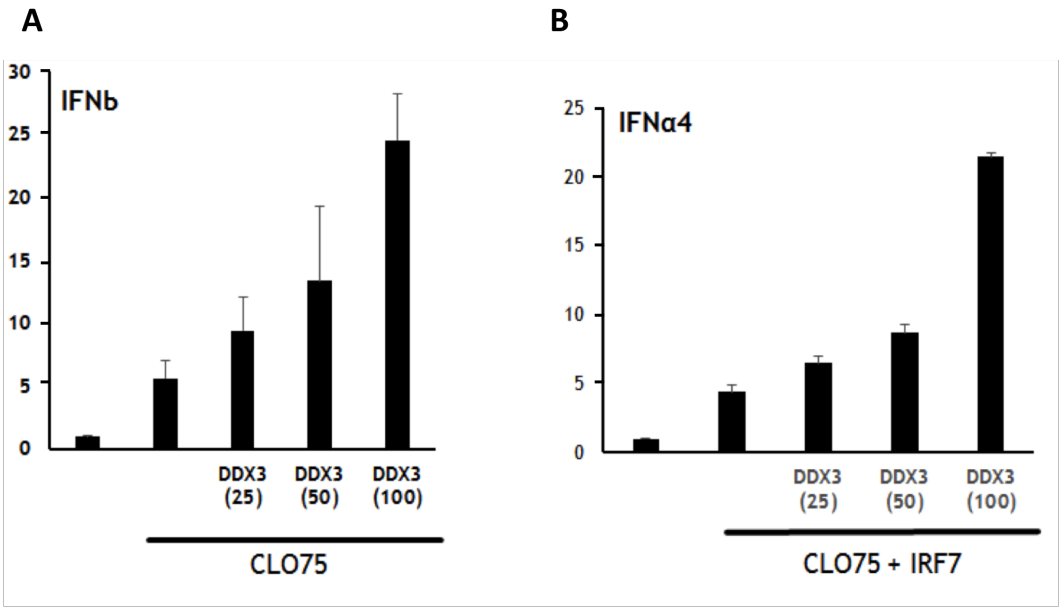

Figure 24: DDX3 enhances IFNα4 and IFNβ induction following CLO75 stimulation.

HEK293-TLR7 cells were transfected with an ifnα4 (A) or ifnb (B) promoter reporter gene construct and expression constructs for HA-DDX3 and Flag-IRF7. 24h after transfection cells were stimulated for the indicated times with 5µg/ml CLO75 for an additional 24h. Data for reporter gene assays are expressed as mean fold induction relative to control levels +/- standard deviations. Shown are results of one representative experiment out of four, performed in triplicate.

Similar luciferase reporter gene assays were carried out using DDX3 knockdown cells, both using the inducible shRNA system mentioned previously, and also by using unrelated siRNA oligos targeting DDX3. While these experiments did not result in statistically significant results, there did appear to be a trend of reduced induction in cells with decreased DDX3 levels (**Figure *25***).

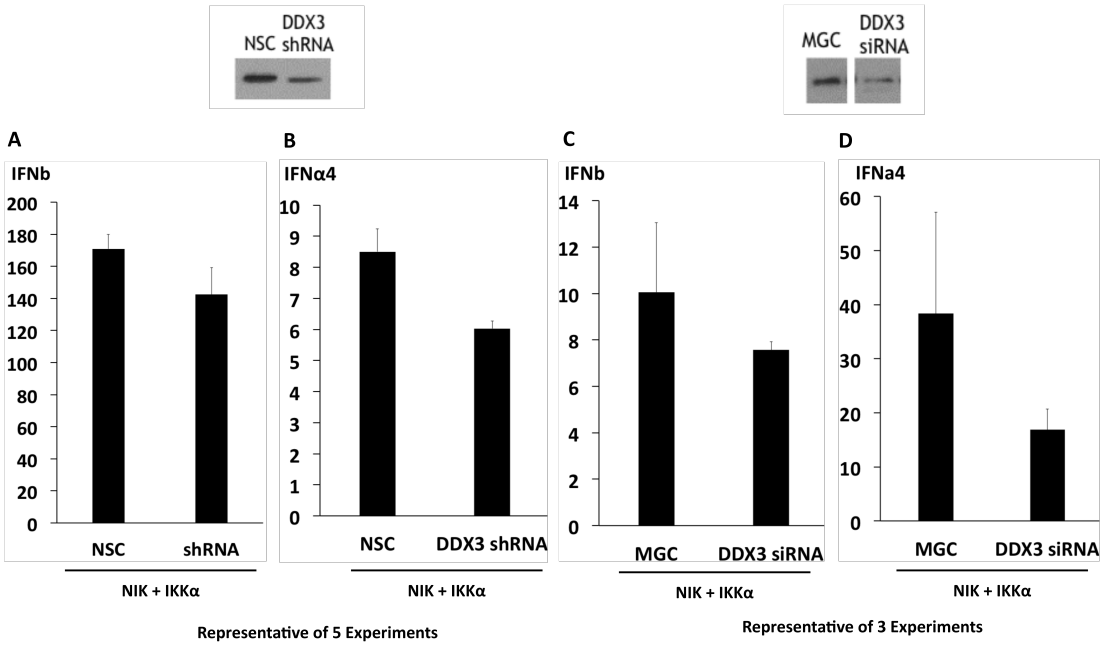

Figure 25: Knockdown of DDX3 may decrease induction of IFNα4 and IFNβ.

DDX3 knockdown was induced by the addition of 0.5 µg/ml doxycycline for 24 hrs to HEK293T cells stably expressing either pTRIPZ shDDX3 or the corresponding non-silencing control (NSC) (A,B) or by using an established siRNA oligo (Gu et al. 2013; Schröder et al. 2008) (C,D). The cells were then transfected with an ifna4 or ifnb promoter reporter gene construct and expression constructs for Flag-IKKα/NIK. 24h after transfection cells were harvested and measured. Data for reporter gene assays are expressed as mean fold induction relative to control levels with a representative experiment from 5 (A,B) or 3 (C,D) independent experiments shown, with each experiment performed in triplicate.

3.4.2 DDX3 enhances IRF7 activation

An important transcription factor for IFNβ induction and an essential one in the case of IFNα4 induction is IRF7. Therefore the effects that DDX3 has on IFNα4 (and IFNβ) induction are possibly mediated by this key transcription factor. As we have previously shown effects of DDX3 on IRF3 (Gu et al. 2013), we therefore investigated whether DDX3 can affect the activation of IRF7.

We first carried out radioactive kinase assays using GST-IKKα, GST-IRF7 (aa 468-503) and His-DDX3 recombinant proteins. With no other proteins present except IKKα and IRF7, the addition of DDX3 enhanced IKKα mediated phosphorylation of IRF7 (**Figure *26***).

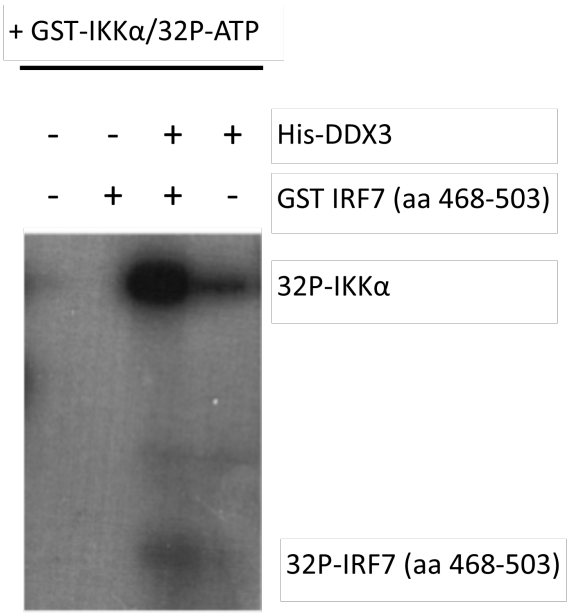

Figure 26: DDX3 enhances phosphorylation of IRF7 by IKKα.

Recombinant His-DDX3 and/or recombinant His-IRF7 (aa 468-503) were incubated with GST-IKKα and [γ-32P]ATP as indicated. Samples were then subjected to SDS-PAGE and autoradiograph analysis, showing incorporation of [γ-32P]ATP (Shown is a representative experiment of 3 independent experiments).

We then continued our investigations in HEK293T cells using an IRF7 antibody specific for phosphorylated serine 471/472 residues, which have been linked with IRF7 activation (Marié et al. 1998; Ning et al. 2003). We induced IRF7 activation by over-expressing small amounts of NIK and IKKα and determined the effect of DDX3 by co-expressing DDX3 or its viral antagonist K7. DDX3 enhanced phosphorylation of IRF7 on serines 471/472 (**Figure *27***), while K7 inhibited this phosphorylation (not shown)

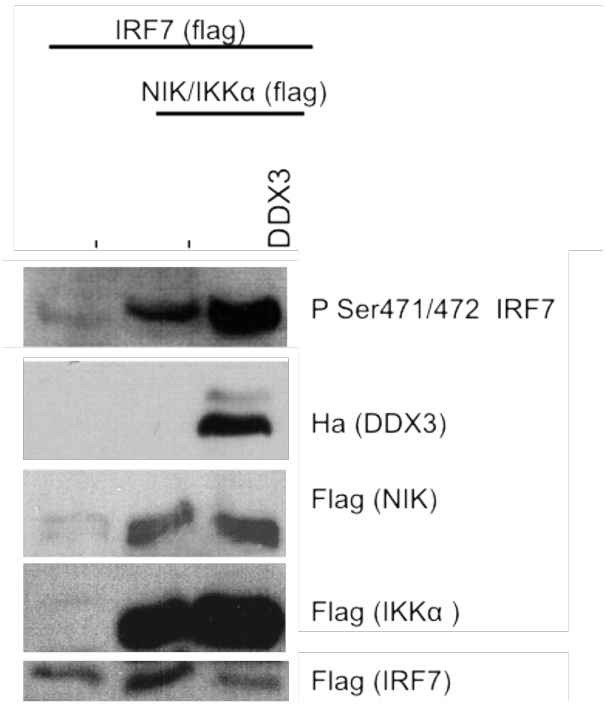

Figure 27: DDX3 enhances IRF7 Ser471/472 phosphorylation induced by NIK/IKKα.

HEK293T cells were transfected with a plasmid vector for Flag-IKKα and Flag-NIK or an empty vector along with Ha-tagged DDX3 or K7. 24h after transfection, cell lysates were subjected to SDS-PAGE and WB analysis with the indicated antibodies (Shown is a representative experiment of 3 independent experiments).

Using our inducible DDX3 knockdown system in HEK293-TLR7 cells, induction of IRF7 activation by NIK and IKKα was reduced in HEK293T cells with reduced DDX3 levels compared to the corresponding control cells (**Figure *28***).

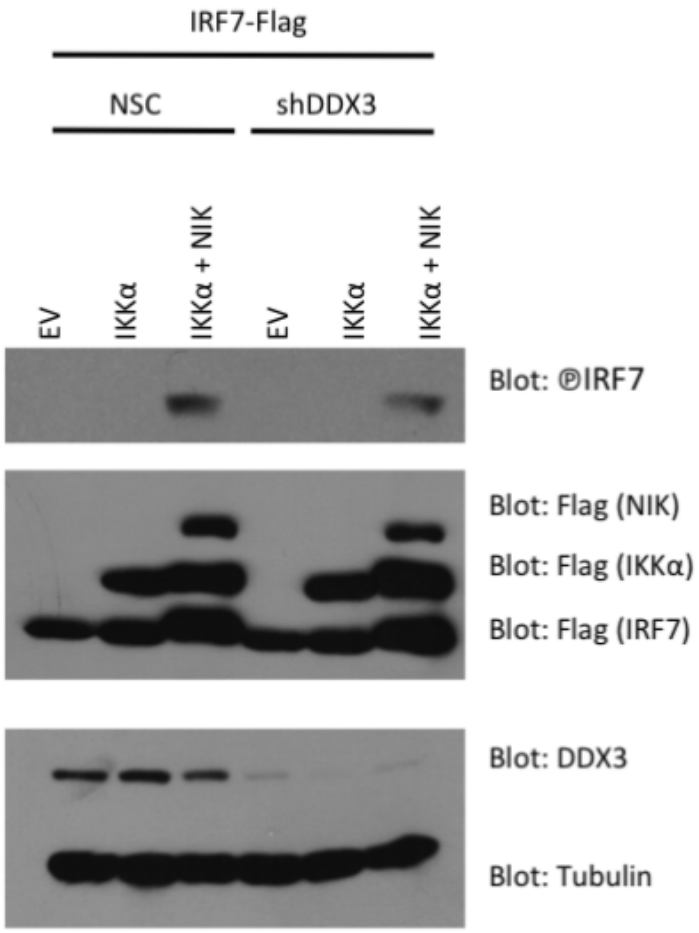

Figure 28: DDX3 knockdown reduces IRF7 phosphorylation induced by NIK/IKKα.

DDX3 knockdown was induced by the addition of 0.5 µg/ml doxycycline for 24 hrs to HEK293T cells stably expressing either pTRIPZ shDDX3 or the corresponding non silencing control (NSC). Cells were then transfected with Flag-IRF7 and one of the indicated Flag-tagged kinases or an empty vector control. 24h after transfection cell lysates were subjected to SDS-PAGE and WB analysis with the indicated antibodies (Shown is a representative experiment of 3 independent experiments).

Next, we induced IRF7 activation by stimulating HEK293-TLR7 cells with CLO75 in the DDX3 knockdown system. A time course of stimulation was carried out in both control and DDX3 knockdown cells. Cells with reduced DDX3 levels demonstrated markedly less IRF7 phosphorylation compared to control cells (**Figure *29***). Even though there does not appear to be much increase in phosphorylation upon stimulation in the control cells, there does appear to be less overall IRF7 phosphorylation in DDX3 knockdown cells even at background levels.

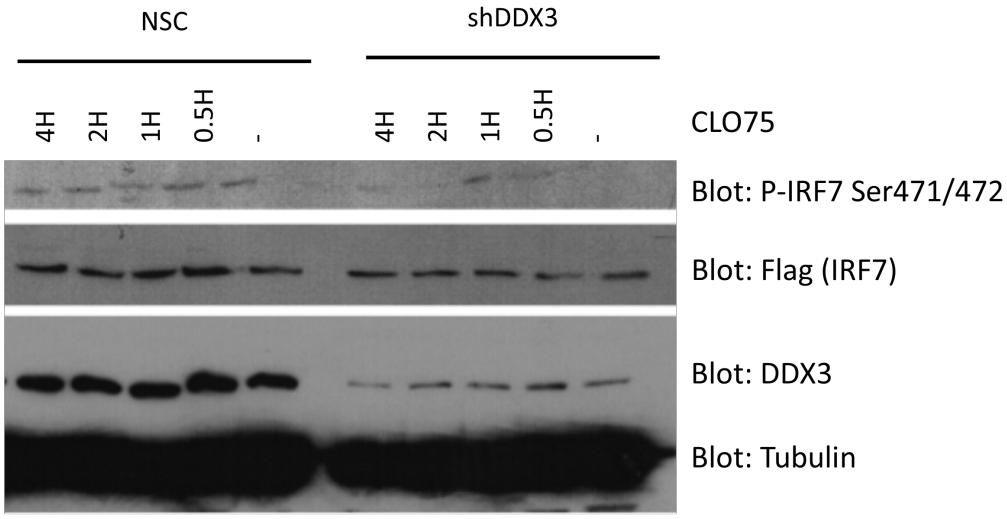

Figure 29: Knockdown of DDX3 reduces IRF7 phosphorylation induced by CLO75.

DDX3 knockdown was induced by the addition of 0.5 µg/ml doxycycline for 24 hrs to HEK293-TLR7 cells stably expressing either pTRIPZ shDDX3 or the corresponding non-silencing control (NSC). Cells were then transfected with Flag-IRF7 and 24h later were stimulated with CLO75 for the indicated time periods and cell lysates were subjected to SDS-PAGE and WB analysis with the indicated antibodies (Shown is a representative experiment of 3 independent experiments).

With DDX3 affecting IRF7 activation, we next investigated whether DDX3 was in complex with IRF7 in cells. We carried out immunoprecipitation assays by co-overexpressing Myc-tagged DDX3 and flag-tagged IRF7 in HEK-293T cells and using an anti-Flag antibody to immunoprecipitate IRF7. DDX3 showed a clear co-immunoprecipitation with IRF7 (**Figure *30***).

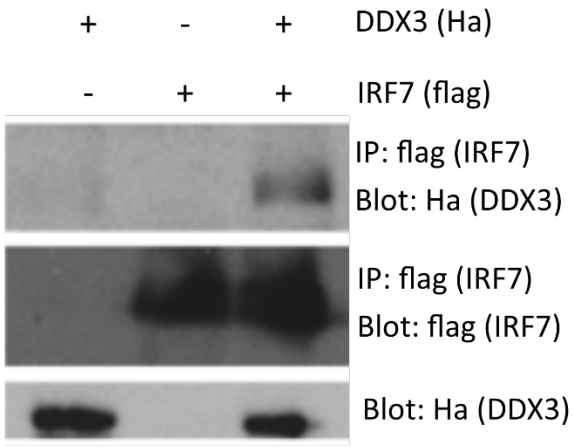

Figure 30: DDX3 co-immunoprecipitates with IRF7.

HEK293T cells were transfected with constructs for Ha-DDX3 and/or Flag-IRF7. Cell lysates were subjected to immunoprecipitation (IP) with an anti-Flag antibody, followed by SDS-PAGE and WB analysis with the indicated antibodies (Shown is a representative experiment of 3 independent experiments).

3.4.3 Summary

In this section we have investigated a second pathway that IKKα is involved in – the TLR7 pathway to type 1 IFN induction. We have shown that overexpression of DDX3 can enhance IFNα4 and IFNβ induction downstream of NIK/IKKα and following CLO75 stimulation. In addition, knockdown of endogenous DDX3 showed a trend of reduced IFN induction. Investigating the role of DDX3 in this pathway further revealed that DDX3 enhances the phosphorylation and activation of IRF7, with overexpression enhancing and knockdown of DDX3 reducing the phosphorylation. Finally we have shown that DDX3 can interact with IRF7.

3.5 DDX3 enhances the IKKα interaction with NIK and IRF7

So far, we have shown that DDX3 can enhance auto-phosphorylation and activity of IKKα and that this resulted in increased induction of the pathways IKKα is involved in. We next investigated in more detail how DDX3 exerted this effect on IKKα. We examined whether protein interactions with IKKα were affected. Co-immunoprecipitations were carried out examining the interaction between IKKα and NIK. In both the alternative NF-κB activation and TLR7/8 pathway to IFN induction, a key step in initial induction is NIK-mediated activation of IKKα. We have shown the NIK-IKKα interaction previously in **Figure *8***, and now tested whether disruption of DDX3 had any effect on this interaction. We carried out an immunoprecipitation using Flag-NIK and endogenous IKKα. IKKα clearly immunoprecipitated with Flag-NIK, however in the presence of the DDX3 antagonist K7 this interaction was reduced (**Figure *31***).

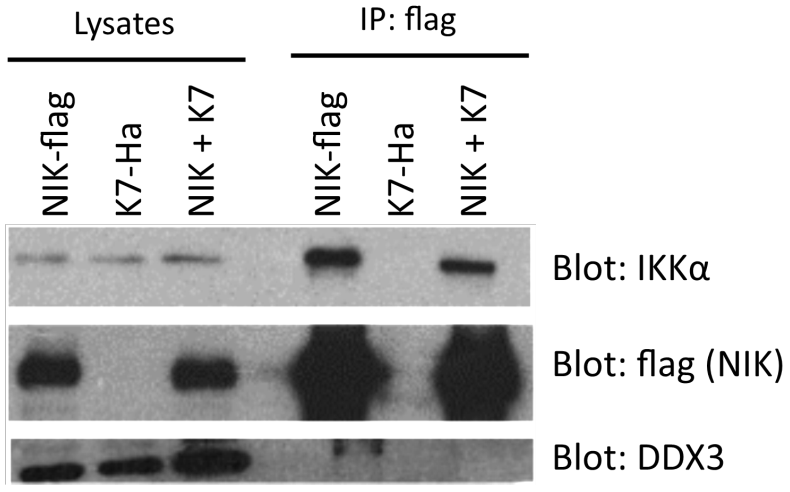

Figure 31: K7 reduces the interaction between NIK and IKKα.

HEK293T cells were transfected with constructs for Flag-NIK and/or Ha-K7. Cell lysates were subjected to immunoprecipitation (IP) with an anti-Flag antibody, followed by SDS-PAGE and WB analysis with the indicated antibodies (Shown is a representative experiment of 3 independent experiments).

A similar experiment was then carried out using DDX3 knockdown cells. This showed that in cells with reduced DDX3, the interaction between NIK and IKKα was also reduced (**Figure *32***).

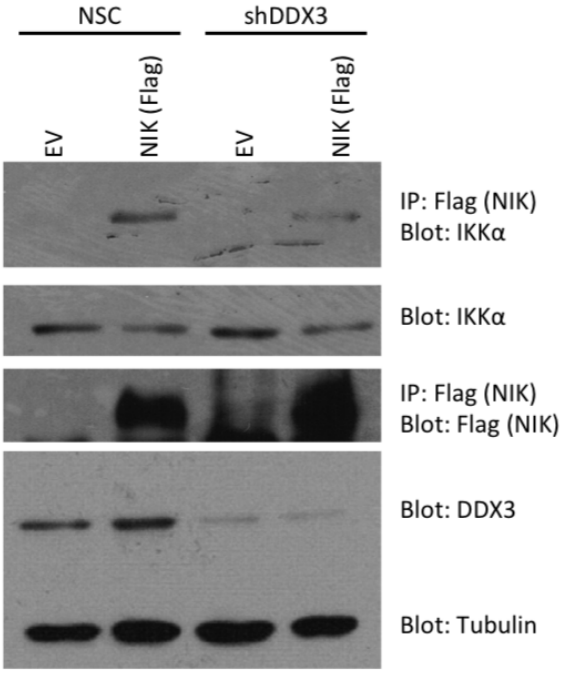

Figure 32: Knockdown of DDX3 reduces the interaction between NIK and IKKα.

DDX3 knockdown was induced by the addition of 0.5 μg/ml doxycycline for 24 hrs to HEK293-TLR7 cells stably expressing either pTRIPZ shDDX3 or the corresponding non silencing control (NSC). Cells were then transfected with constructs for Flag-NIK or an empty vector control. Cell lysates were subjected to immunoprecipitation (IP) with an anti-Flag antibody, followed by SDS-PAGE and WB analysis with the indicated antibodies (Shown is a representative experiment of 3 independent experiments).

As DDX3 affected the interaction between NIK and IKKα and presumably the activation of IKKα by NIK, we also tested whether this affected the downstream interactors of IKKα. We carried out experiments to examine the interaction between IRF7 and IKKα, in which Flag-tagged IRF7 was expressed with or without Ha-tagged K7 and immunoprecipitation was carried out using a Flag antibody. K7 reduced the interaction between IRF7 and IKKα (**Figure *33***). This suggests that

disrupting the NIK-IKKα interaction has further downstream effects, or that DDX3 may separately mediate IKKα interactions with a number of proteins, including NIK and IRF7.

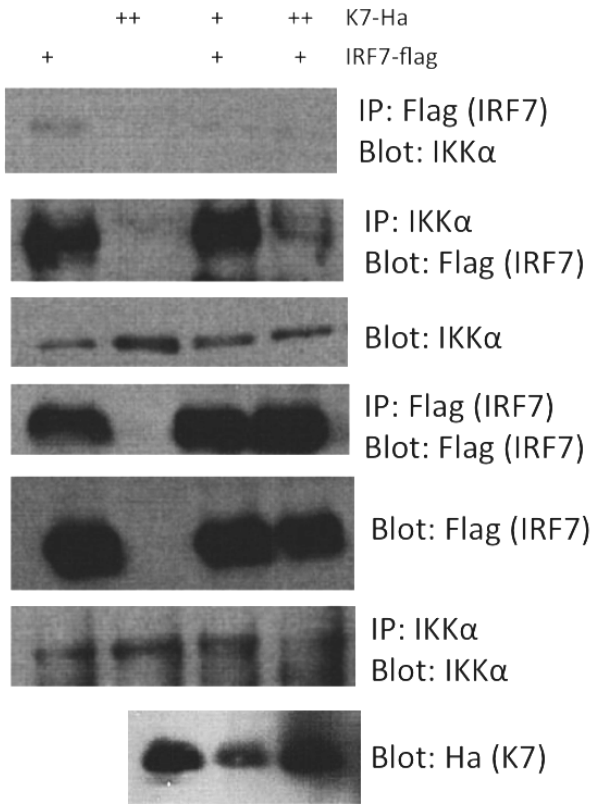

Figure 33: K7 reduces the interaction between IKKα and IRF7.

HEK293T cells were transfected with constructs for Flag-IRF7 and/or Ha-K7 as indicated. Cell lysates were subjected to immunoprecipitation (IP) with an anti-Flag antibody, followed by SDS-PAGE and WB analysis with the indicated antibodies (Shown is a representative experiment of 3 independent experiments).

3.5.1 Summary

Here we have attempted to elucidate the mechanism by which DDX3 exerts its effects on the IKKα mediated signalling pathways we investigated. We showed that K7 can disrupt the interactions between IKKα and NIK or IRF7. Additionally, we have shown that knockdown of endogenous DDX3 reduced the interaction between IKKα and NIK. This suggests that DDX3 may act as a bridging protein to bring IKKα in close proximity to other proteins.

3.6 DDX3 phosphorylation by the IKKs and IKK related kinases

When both IKKα and DDX3 were expressed together, we observed a marked shift in the band for DDX3 (**Figure *7***). As DDX3 has already been shown to be phosphorylated by the IKK related kinases IKKε and TBK1 (Soulat et al. 2008; Gu et al. 2013) we first compared the effects of the IKKs with the effects of IKK-related kinases on DDX3 phosphorylation by expressing Myc-DDX3 along with either IKKα, IKKβ, TBK1, IKKε or NIK (**Figure *34***).

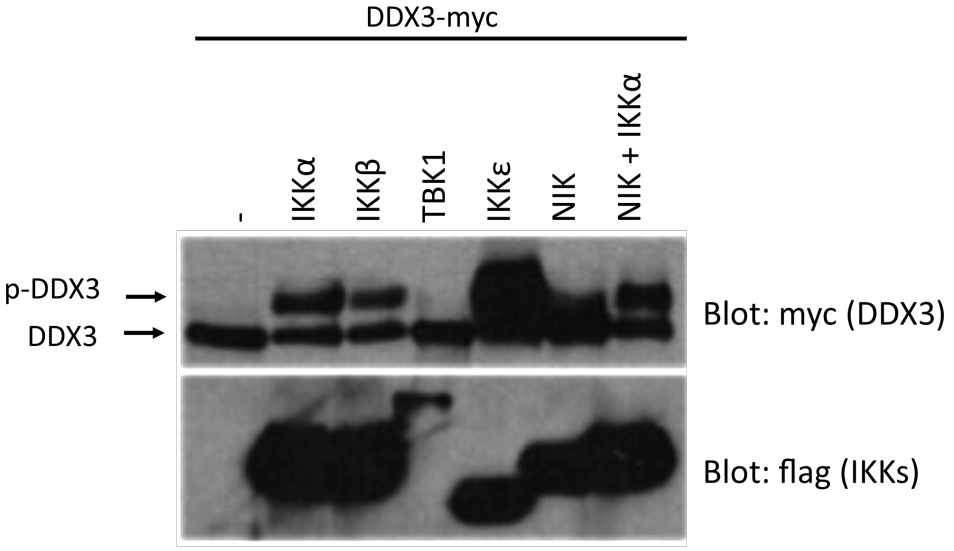

Figure 34: Higher molecular weight forms of DDX3 are observed in the presence of the IKKs and IKK related kinases.

HEK293T cells were transfected with a plasmid vector for Myc-DDX3 and one of the indicated Flag-tagged kinases. 24h after transfection cell lysates were prepared and subjected to SDS-PAGE and WB analysis with the indicated antibodies (Shown is a representative experiment of 10 independent experiments).

Interestingly the pattern of these higher molecular weight forms of DDX3 was different with each kinase. A shift was observed with IKKα, IKKβ and IKKε, while no strong shift was observed in the presence of NIK or TBK1 (**Figure *34***). While the shift induced with IKKε appeared as a smear, the shift induced by IKKα/β was a

clearer defined band suggesting the phosphorylation pattern of these kinases were different.

We next carried out radioactive kinases assays using recombinant His-DDX3 and recombinant GST-kinases to confirm that the observed modification was indeed phosphorylation. The truncation mutant DDX3 (aa 1-408) was used, as we had previously shown that IKKα and IKKε interact with this region of DDX3 (**Figure *10***) (Gu et al. 2013). DDX3 (aa 5-175) was also used as this had been shown to be strongly phosphorylated by IKKε (Gu et al. 2013).

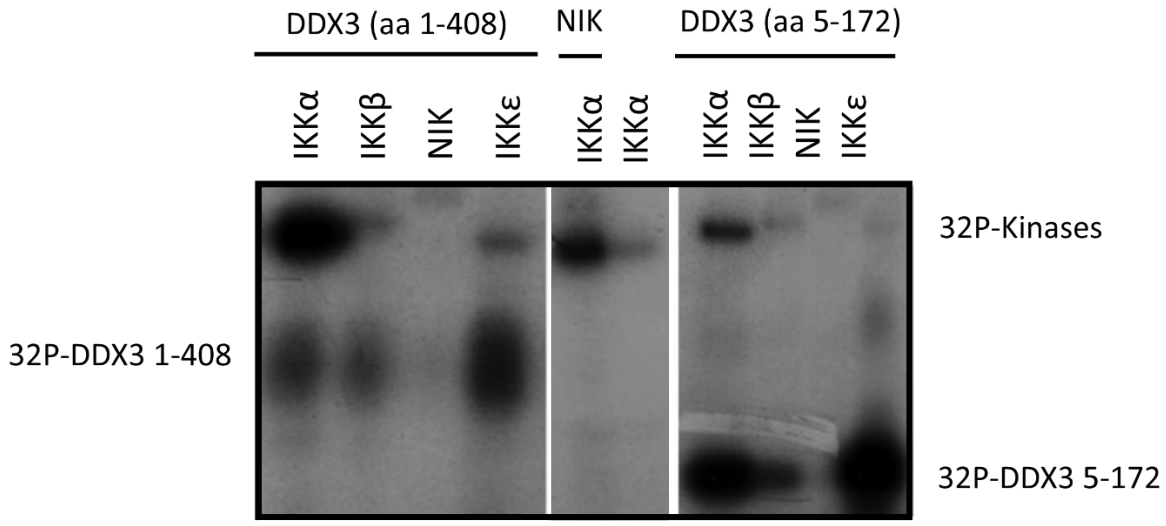

Figure 35: DDX3 is phosphorylated by IKKα, IKKβ and IKKε but not NIK.

Recombinant His-DDX3 (either 1-408 or 5-172) was incubated with recombinant GST-kinases as indicated in the presence of [γ-32P]ATP (left and right panels). GST-NIK was also incubated with its substrate IKKα in the presence of [γ-32P]ATP (middle panel). Samples were then subjected to SDS-PAGE and autoradiograph analysis, showing incorporation of [γ-32P]ATP (Shown is a representative experiment of 5 independent experiments).

IKKε phosphorylated DDX3 1-408 and 5-172 strongly as expected, but so too did IKKα and IKKβ albeit at a slightly lower level (**Figure *35***). NIK however, did not induce any phosphorylation of DDX3 (**Figure *35***). We therefore confirmed that the

NIK protein was active, by carrying out an assay with its substrate IKKα, showing that NIK could phosphorylate IKKα in the same experiment (middle panel).

We also carried out similar kinase assays to determine whether the DDX3 antagonist K7 could affect this phosphorylation of DDX by IKKα. In this assay we used GST-IKKα and DDX3 (aa 1-408) with and without the addition of K7 or an unrelated control protein Rab14. We showed that K7 could reduce the phosphorylation of DDX3 by IKKα, while the addition of the Rab14 control protein had no effect on IKKα mediated phosphorylation of DDX3 (**Figure *36***).

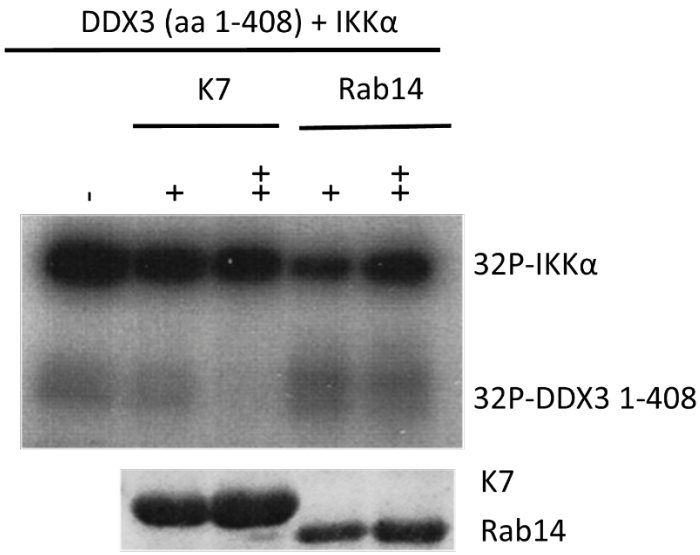

Figure 36: K7 inhibits the phosphorylation of DDX3 by IKKα.

Recombinant GST-IKKα was incubated with recombinant His-DDX3 (1-408) in the presence of [γ-32P]ATP and recombinant His-K7 or the unrelated control protein His-Rab14. Samples were then subjected to SDS-PAGE and autoradiograph analysis showing incorporation of [γ-32P]ATP. Total amounts of recombinant proteins were visualized by Coomassie staining (Shown is a representative experiment of 3 independent experiments).

As we observed differing patterns of shifts and levels of phosphorylation induced by the different kinases (**Figure *34***, **Figure *35***), this suggested that the residues being phosphorylated were not the same for each kinase. Phospho-proteomics work on the phosphorylation of DDX3 by IKKε indicated a number of residues that were phosphorylated by IKKε (Gu et al. 2013). As part of this screen, Dr. Lili Gu in our

lab produced a number of DDX3 serine to alanine mutants. Single alanine mutants were produced for S71, S102, and S152, a double mutant for S82 and S83 (2A mutant), a triple mutant for S82, S83 and S102 (3A mutant), and a quadruple mutant for S82, S83, S102 and S71 (4A mutant). We carried out radioactive kinase assays using these mutants to compare how DDX3 phosphorylation by IKKα or IKKε is impacted by these mutations (**Figure *37***).

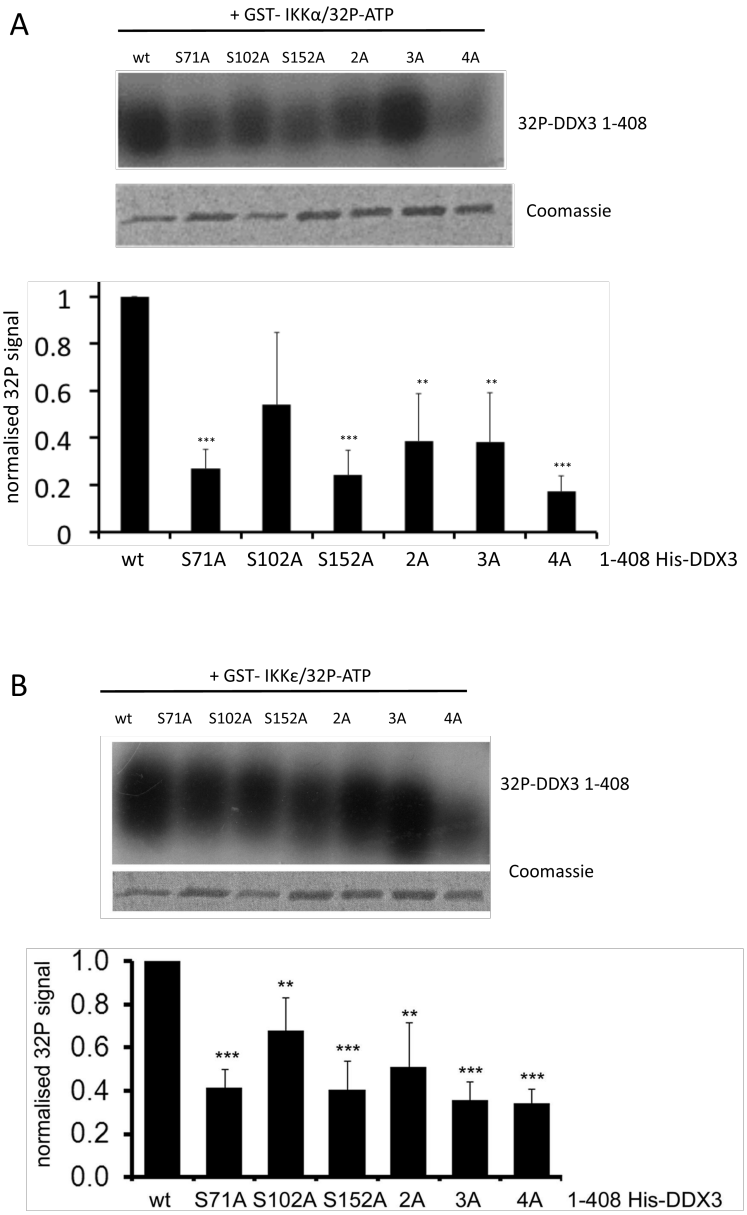

Figure 37: IKKα phosphorylates DDX3 on multiple sites.

Recombinant GST-IKKα (A) or GST-IKKε (B) were incubated with recombinant wild-type (wt) His-DDX3 (1–408) or the indicated DDX3(1–408) alanine mutants in the presence of [γ-32P]ATP. Samples were then subjected to SDS-PAGE and autoradiograph analysis. Total amounts of His-DDX3 mutants were visualized by Coomassie staining. The top panel in both A and B shows results of one representative experiment out of four. For each repeat experiment, the intensity of autoradiograph and Coomassie-stained bands was quantified using ImageJ software. Values for autoradiograph bands were normalized to the intensity of the corresponding Coomassie-stained bands to account for differences in protein loading. The normalized signal for DDX 3(1–408) was set to 1 in each case. Data in the lower panel in both A and B are presented as means +/- standard deviations from four independent experiments. *, $P < 0.05$; **, $P < 0.01$; ***, $P < 0.001$ [all compared to wt DDX3(1–408)] by an unpaired Student's t test.

In Dr. Gu's work, phosphorylation of serine 102 of DDX3 was shown to be essential for IKKε mediated IFNβ induction (Gu et al. 2013). In radioactive kinase assays, mutation of S102 to alanine does not impact IKKα phosphorylation as much as IKKε phosphorylation (**Figure *37***). The S71 and S152 mutants both show approximately a 75% reduction in phosphorylation by IKKα when compared to wt DDX3, however the S102 mutant did not show a significant difference (**Figure *37***). The 2A mutant showed approximately a 60% reduction in phosphorylation, the addition of the S102 mutation in the 3A mutant did not change this reduction, while addition of the S71 mutation in the 4A mutant reduced the phosphorylation further (**Figure *37***). For IKKε all the mutations showed a significant difference compared to wt DDX3 (**Figure *37***).

To confirm the difference between IKKα and IKKε with respect to the S102 residue, individual kinase assays were carried out using the DDX (aa 80-408) truncation mutant and an 80-408 S102A mutant, in an effort to isolate effects from other phosphorylated residues (**Figure *38***).

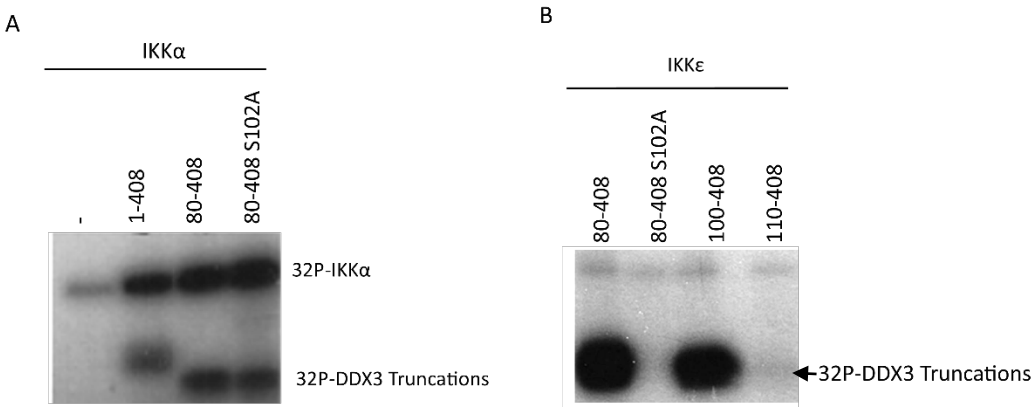

Figure 38: IKK*α* still strongly phosphorylates the S102A DDX3 alanine mutant.

Recombinant GST-IKKα or GST-IKKε were incubated with recombinant wild-type (wt) His-DDX3(1–408), His-DDX3(100–408), His-DDX3(80–408), or the DDX3(80–408) S102A alanine mutants in the presence of [γ-32P]ATP. Samples were then subjected to SDS-PAGE and autoradiograph analysis with the indicated antibodies (Shown is a representative experiment of 3 independent experiments). Right panel produced by Lili Gu – host pathogen interaction lab (Gu et al. 2013).

While the DDX3 (aa 80-408) S102A mutant failed to be phosphorylated strongly by IKKε (**Figure *38*b**) (Gu et al. 2013), this mutation did not appear to affect phosphorylation by IKKα (**Figure *38*a**).

As the S71A mutant seemed to have significantly reduced phosphorylation levels compared to wt DDX3 in the case of both IKKε and IKKα, and there was an S71-phospho-DDX3 antibody available (kindly donated by Sir Philip Cohen, MRC phosphorylation Unit, University of Dundee), experiments were carried out to study DDX3 S71 phosphorylation in HEK293T cells. Flag-tagged IKKα, IKKβ, IKKε or TBK1 were expressed along with DDX3 (aa 1-408) or DDX3 (aa 1-408)-S71A and samples were probed using the phospho-S71 specific DDX3 antibody (**Figure *39***).

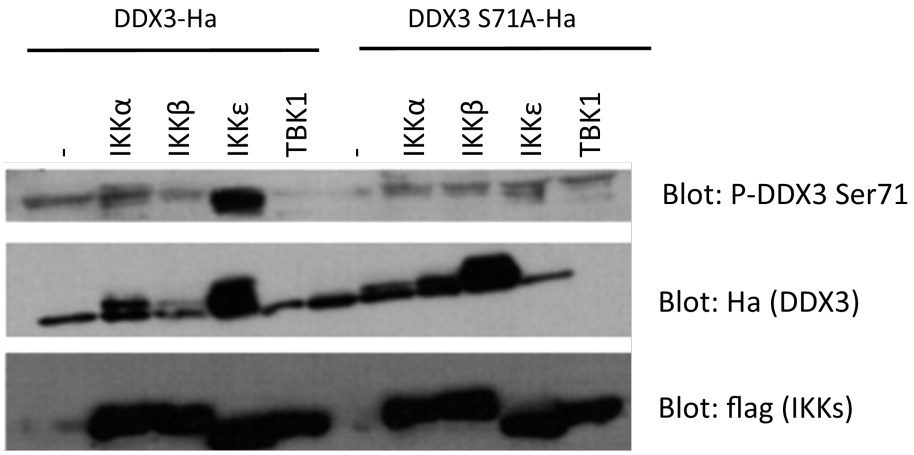

Figure 39: Both IKKα and IKKε phosphorylate DDX3 on serine 71.

HEK293T cells were transfected with a plasmid vector for wt Ha-DDX3 or the mutated S71A DDX3 and one of the indicated Flag-tagged kinases. 24h after transfection, cell lysates were prepared and subjected to SDS-PAGE and WB analysis with the indicated antibodies (Shown is a representative experiment of 3 independent experiments).

While both IKKα and IKKε did phosphorylate serine 71 of DDX3, the phosphorylation by IKKε was a lot stronger, while IKKα only induced a moderate increase in the band intensity for S71 (**Figure *39***).

In the course of these investigations we also carried out luciferase assays using the same serine to alanine DDX3 constructs we used in Figure 37. As the phosphorylation of DDX3 by IKKα was clearly affected upon mutation of these residues, we sought to clarify if this had any functional consequences on IFNα4 and IFNβ promoter induction. However, no significant differences in IFNα4 or IFNβ induction was apparent downstream of NIK/IKKα or CLO75 stimulation (**Figure 40**, **Figure 41**, **Figure 42**, **Figure 43**). In the case of IFNβ induction downstream of NIK/IKKα there did seem to be a trend of reduced IFNβ induction with a number of the DDX3 serine to alanine mutants compared to wt DDX3 (**Figure 40**) but they did not reach significance.

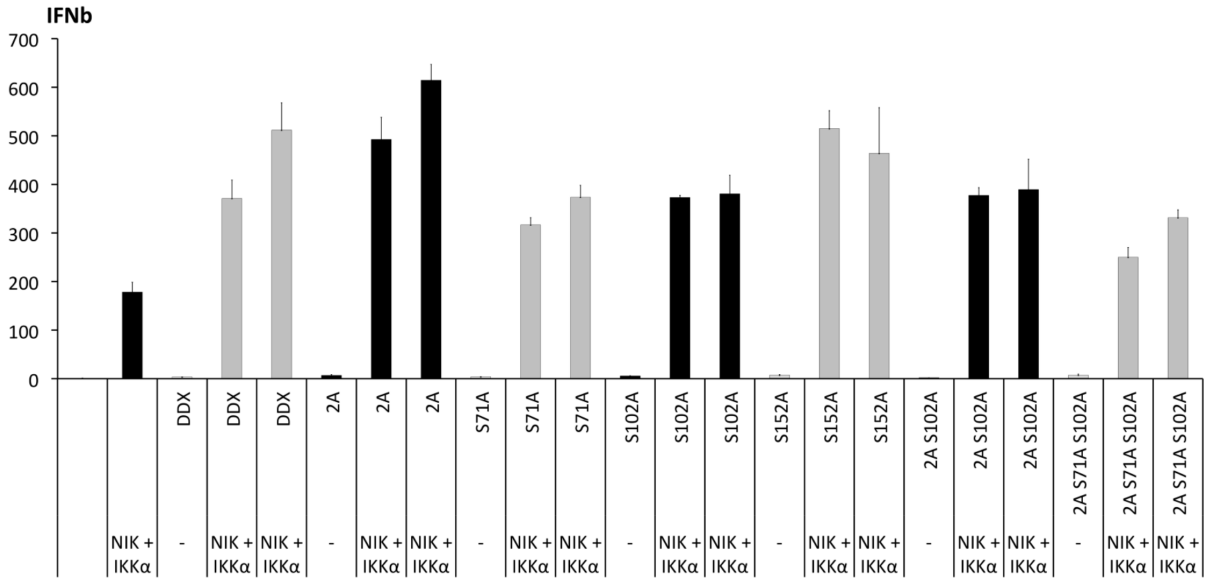

Figure 40: Mutation of serines on DDX3 does not affect IFNβ induction downstream of NIK/IKKα.

HEK293R1 cells were transfected with an *ifnb* promoter reporter gene construct and expression constructs for Flag-IKKα and Flag-NIK or empty vector controls along with the indicated DDX3 alanine mutants 24h after transfection cells were harvested and measured. Data for reporter gene assays are expressed as mean fold induction relative to control levels. A representative experiment from 6 independent experiments is shown, with each experiment performed in triplicate. Data are presented as means +/- standard deviations.

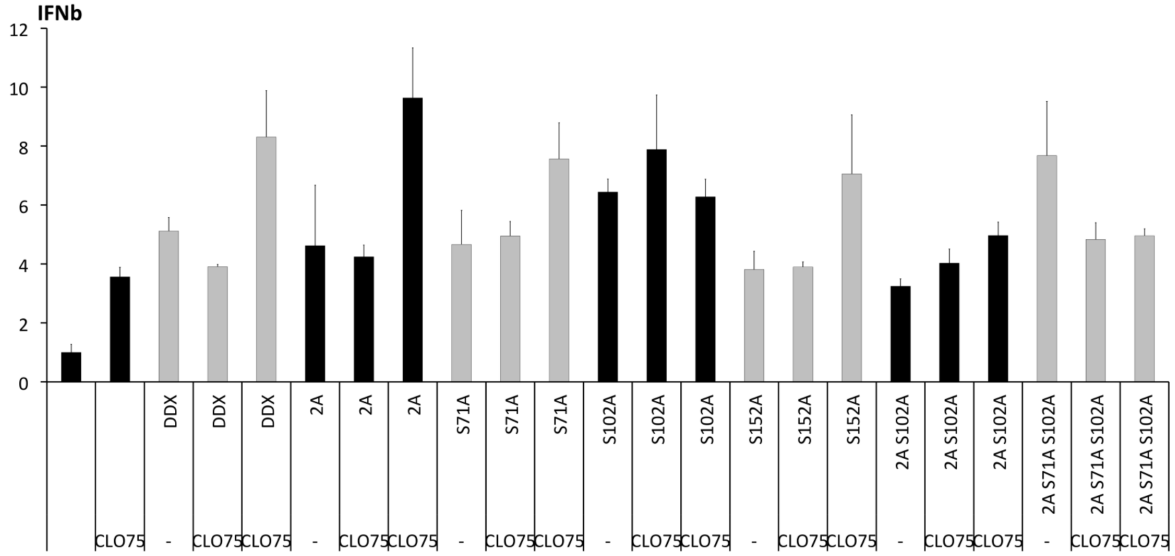

Figure 41: Mutation of serines on DDX3 does not affect IFNβ induction downstream of CLO75 stimulation.

HEK293-TLR7 cells were transfected with an *ifnb* promoter reporter gene construct and expression constructs for the indicated DDX3 alanine mutants or empty vector control. 24h after transfection cells were stimulated with CLO75 as indicated for 24h. Cells were then harvested and luciferase activity was measured. Data for reporter gene assays are expressed as mean fold induction relative to control levels. A representative experiment from 6 independent experiments is shown, with each experiment performed in triplicate. Data are presented as means +/- standard deviations.

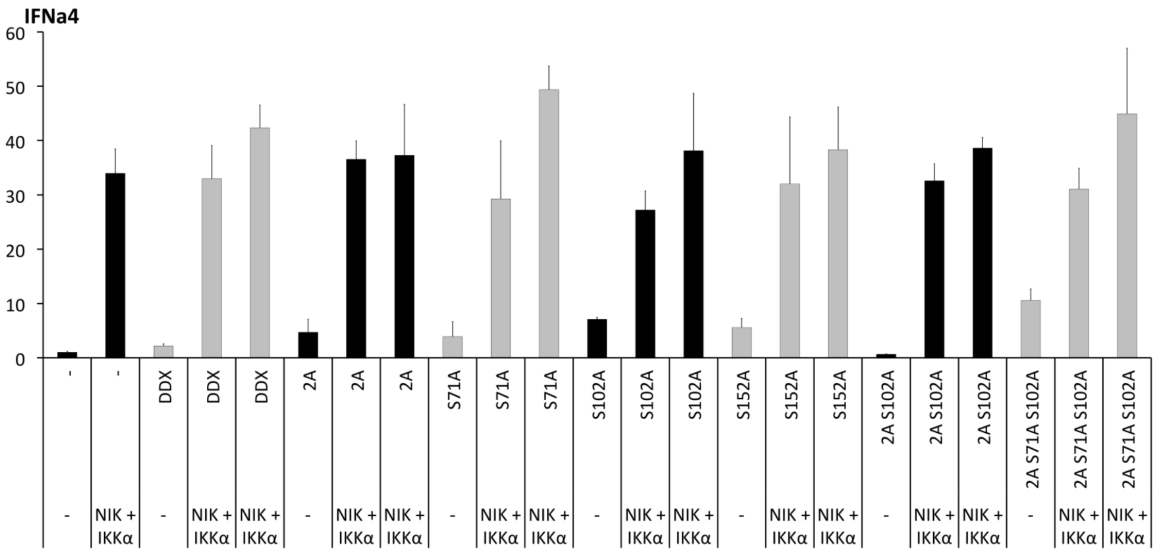

Figure 42: Mutation of serines on DDX3 does not affect IFNα4 induction downstream of NIK/IKKα.

HEK293R1 cells were transfected with an *ifna4* promoter reporter gene construct and expression constructs for Flag-IKKα/NIK or empty vector controls along with the indicated DDX3 alanine mutants 24h after transfection cells were harvested and measured. Data for reporter gene assays are expressed as mean fold induction relative to control levels. A representative experiment from 6 independent experiments is shown, with each experiment performed in triplicate. Data are presented as means +/- standard deviations.

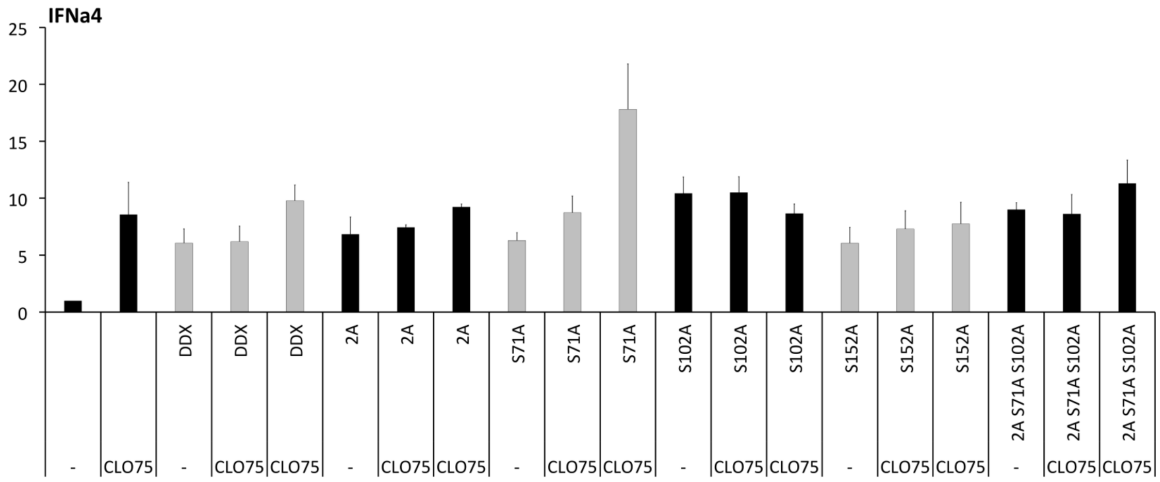

Figure 43: Mutation of serines on DDX3 does not affect IFNα4 induction downstream of CLO75 stimulation.

HEK293-TLR7 cells were transfected with an *ifna4* promoter reporter gene construct and expression constructs for the indicated DDX3 alanine mutants or empty vector control. 24h after transfection cells were stimulated with CLO75 as indicated for 24H. Cells were then harvested and luciferase activity was measured. Data for reporter gene assays are expressed as mean fold induction relative to control levels. A representative experiment from 6 independent experiments is shown, with each experiment performed in triplicate. Data are presented as means +/- standard deviations.

Due to the above results, we next aimed to determine whether IKKα phosphorylates different serine residues in DDX3. Thus, we carried out phosphoproteomics analysis to determine the specific residues that are phosphorylated by IKKα. We carried out phosphorylation site mapping by mass spectrometry. For this analysis, we used DDX3 (1–408) that had been phosphorylated *in vitro* using recombinant IKKα. We separated the phosphorylated protein by SDS-PAGE and carried out a tryptic digest of the protein band, followed by analysis of the tryptic peptides by ion trap mass spectrometry (IT-MS). This analysis showed that phosphorylated residues were present at position S2, S23, S71, S86 and S152 (**Table *5***).

Phosphorylated residues	Peptide sequence	IKKα	Peptide Sequence	IKKε
S2 or S23	MSHVAVENALGLD QQFAGLDLNSSDNQ SGGSTASK	?		
S23 or 24	MSHVAVENALGLDQ QFAGLDLNSSDNQS GGSTASK	?		
S70 or S71 or S74	DKDAYSSFGsR	?	K.DKDAYSSF GSR.S	?
S82 or S83 or S86			R.GKSSFFSDR. G	?
S86	SSFFSDR	?		
S102 or S109			R.GRSDYDGIG SR.G	?
S152	LEQELFSGGNTGINF EK	?	R.LEQELFSGG NTGINFEK.Y	?

Table 5: DDX3 is phosphorylated by IKKα on distinct residues from IKKε.

Showing phosphopeptides identified in IT-MSMS analysis of recombinant DDX3 (aa 1-408) phosphorylated by either IKKα (this study) or IKKε (Gu et al. 2013).

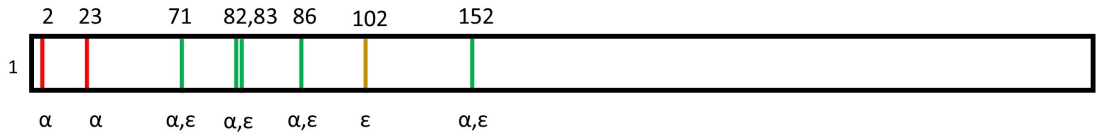

Figure 44: Cartoon representation of phosphorylation sites in the N-terminal region of DDX3

Showing IKKα phosphorylation sites in red, IKKε sites in yellow and sites that are phosphorylated by both kinases in green.

While the residues S152 and S71 were also detected in the IKKε screen, the other three residues S2, S23 and S86 were unique to IKKα (**Figure 44**). Therefore serine to alanine substitution mutants for each of these residues were generated along with a double mutant of S71A, S152A, a triple mutant of S71A, S152A and S23A, and a quadruple mutant of S71A, S152A, S23A and S2A. These substitution mutants were used in luciferase reporter assays to determine if there was a functional defect in DDX3 with these mutated serines (**Figure 45**, **Figure 46**, **Figure 47**, **Figure 48**). While single mutations of DDX3 showed no significant differences in IFNβ or IFNα4 promoter induction downstream of NIK/IKKα or CLO75 stimulation (not shown), there was a marked difference in IFN induction with some of the combination serine to alanine mutants. Although only preliminary results, it appeared that a triple mutant of S71A, S152A and S23A resulted in a slightly decreased enhancement of IFNβ and IFNα4 promoter induction compared to wt DDX3 (**Figure 45**, **Figure 46**, **Figure 47**, **Figure 48**). However the addition of the S2A mutation to this triple mutant appeared to negate this effect and actually enhanced the induction of IFN far above that of wt DDX3 (**Figure 46**, **Figure 47**, **Figure 48**), except in the case of IFNβ induction downstream of NIK/IKKα where it did the opposite and appeared to inhibit induction of IFNβ (**Figure 45**).

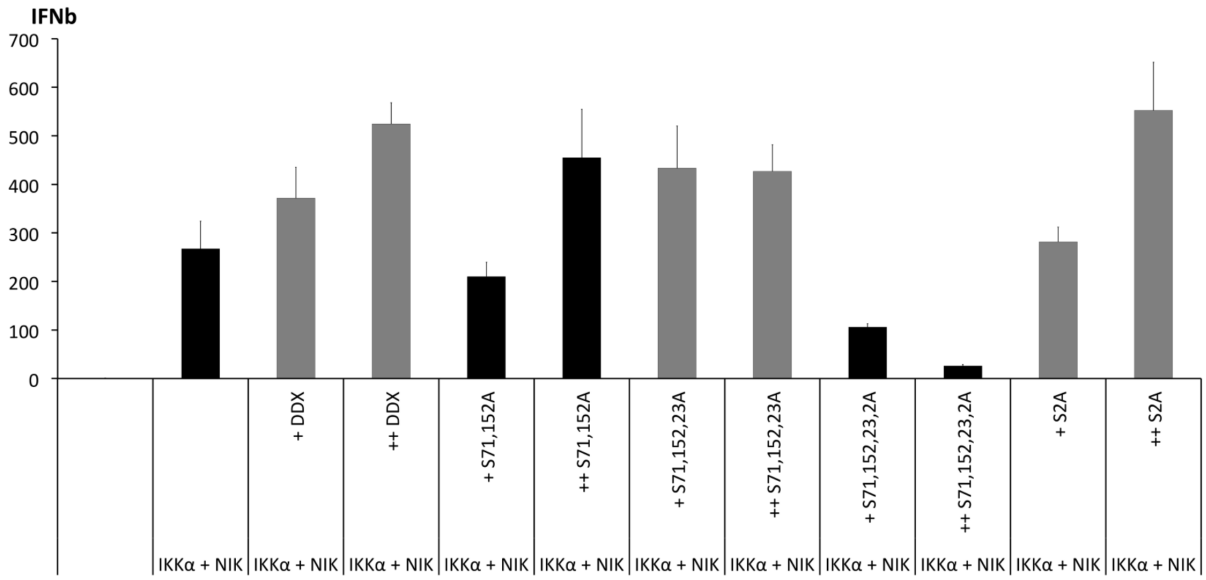

Figure 45: Mutation of serines on DDX3 affects IFNβ induction downstream of NIK/IKKα.

HEK293R1 cells were transfected with an ifnb promoter reporter gene construct and expression constructs for Flag-IKKα/NIK or empty vector controls along with the indicated DDX3 alanine mutants 24h after transfection cells were harvested and measured. Data for reporter gene assays are expressed as mean fold induction relative to control levels with the values averaged from 2 independent experiments, with each experiment performed in triplicate.

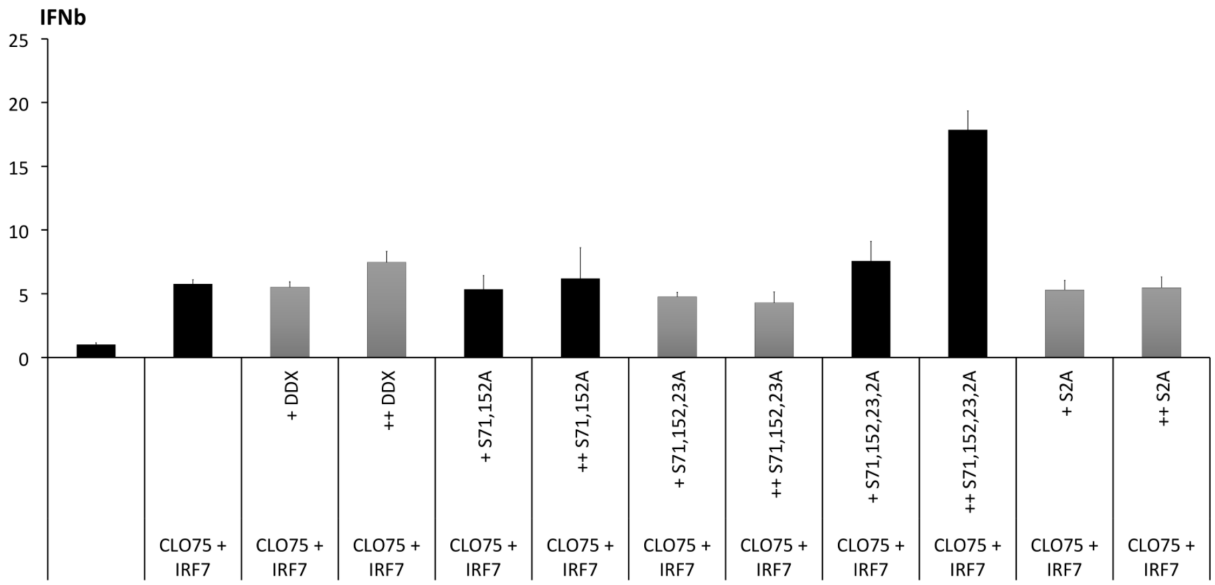

Figure 46: Mutation of serines on DDX3 affects IFNb induction downstream of CLO75 stimulation.

HEK293-TLR7 cells were transfected with an ifnb promoter reporter gene construct and expression constructs for the indicated DDX3 alanine mutants or empty vector control. 24h after transfection cells were stimulated with CLO75 as indicated for 24H. Cells were then harvested and luciferase activity was measured. Data for reporter gene assays are expressed as mean fold induction relative to control levels with the values averaged from 3 independent experiments, with each experiment performed in triplicate.

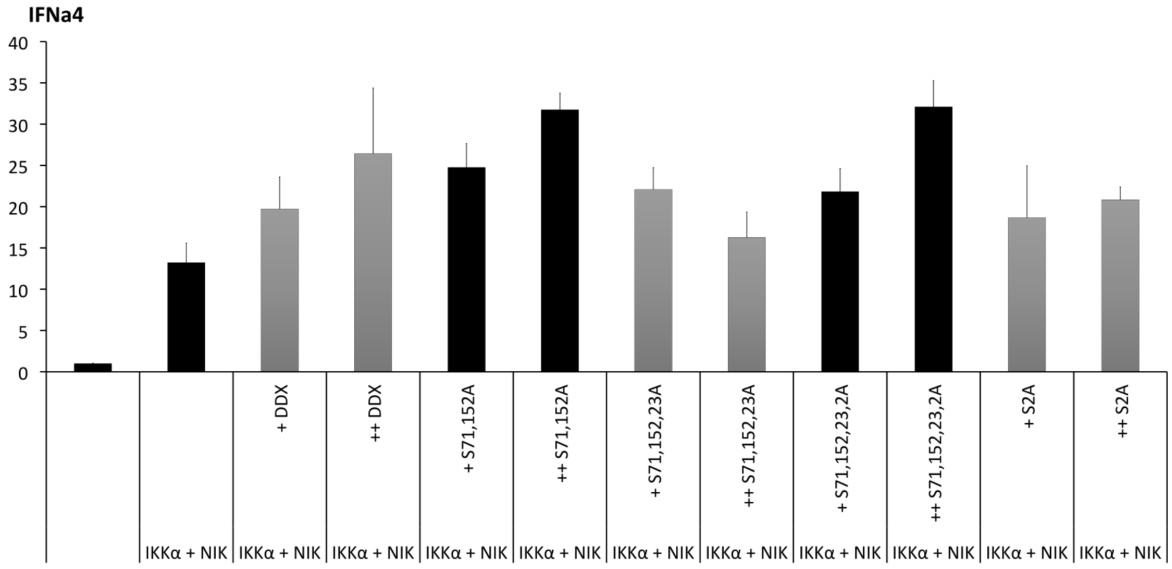

Figure 47: Mutation of serines on DDX3 affects IFNα4 induction downstream of NIK/IKKα.

HEK293R1 cells were transfected with an ifna4 promoter reporter gene construct and expression constructs for Flag-IKKα/NIK or empty vector controls along with the indicated DDX3 alanine mutants 24h after transfection cells were harvested and measured. Data for reporter gene assays are expressed as mean fold induction relative to control levels with the values averaged from 2independent experiments, with each experiment performed in triplicate.

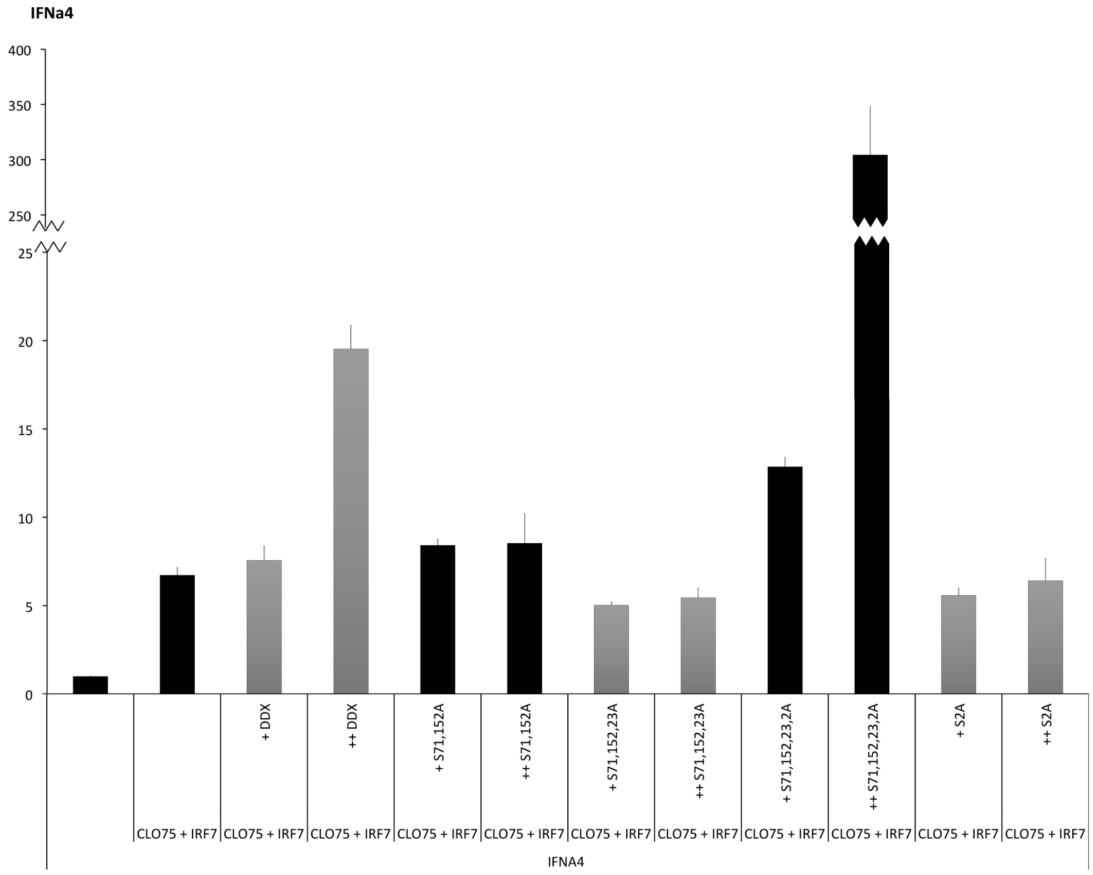

Figure 48: Mutation of serines on DDX3 affects IFNa4 induction downstream of CLO75 stimulation.

HEK293-TLR7 cells were transfected with an ifna4 promoter reporter gene construct and expression constructs for the indicated DDX3 alanine mutants or empty vector control. 24h after transfection cells were stimulated with CLO75 as indicated for 24H. Cells were then harvested and luciferase activity was measured. Data for reporter gene assays are expressed as mean fold induction relative to control levels with the values averaged from 3 independent experiments, with each experiment performed in triplicate.

3.6.1 Summary

In addition to investigating the effects DDX3 has on IKKα, we have investigated the effects IKKα has on DDX3. We initially observed a shift of DDX3 in western blots when co-expressed with IKKα in a pattern that was dissimilar to that of IKKε. We showed here that DDX3 is phosphorylated by IKKα. We have also demonstrated that while IKKα and IKKε share some target serine residues on DDX3, there are residues that are unique to each kinase. Phosphorylation of Ser102 appears to be unique to IKKε, while the Ser2 and S23 residues appear unique to IKKα, and Ser71, S86, S152 being common to both. We have also begun to investigate the functional effects of IKKα phosphorylation but have yet to obtain conclusive results.

3.7 Using Blue-Native PAGE for the isolation of Multi-Protein complexes

3.7.1 Introduction

This section, in addition to providing results from Blue Native PAGE experiments (sections 3.7.3 and 3.7.4.2) also explains the theory, methods, and considerations used in carrying out this work (sections 3.7.1.1, 3.7.1.2, 3.7.1.3, and 3.7.2).

3.7.1.1 Multi-Protein Complexes

Multi-protein complexes (MPCs) are an essential part of signalling pathways within the cell. The regulation and propagation of a signal requires protein-protein interactions, forming complexes ranging from simple pair-wise interactions to multi-protein complexes containing many different proteins. The composition of these complexes can affect protein function and signalling pathways, subtly changing the type of response that is brought about by changes in the cell environment.

Investigating MPCs is no trivial undertaking as their composition and stability can rapidly change due to a number of factors, for example, its location within the cell or the activation state of the cell, an example being the Myddosome that is formed upon TLR-ligand binding (Lin et al. 2010) (Section: 1.2.1.1.2). Composition of complexes can change within minutes of a receptor being engaged by its cognate stimulus. In addition, most proteins are involved in multiple distinct protein complexes and some might exist in both monomer and multimer form.

3.7.1.2 Investigating Multi-protein complexes - Blue Native-PAGE

Blue-Native Polyacrylamide Gel Electrophoresis is a method to identify and analyse multi-protein complexes. Numerous methods have been developed to investigate protein-protein interactions, from simple co-immunoprecipitations, to wide scale screens of interactions such as Yeast 2-Hybrid screens or tandem affinity purification. However, for investigations of proteins in their native state there are fewer methods available. Native isoelectric focusing is one such method that separates proteins according to their isoelectric point, but some proteins are not soluble at their isoelectric point. Gel filtration is another commonly used method that can separate complexes according to their size, however BN-PAGE provides a much higher resolution.

BN-PAGE can be used for a wide range of investigations. It was originally developed to isolate protein complexes from cell membranes (Schägger & von Jagow 1991) but has since been expanded to be used to investigate intracellular protein complex composition, complex sizes, and for other applications that require proteins to be separated in their native form (Swamy, Siegers, et al. 2006). The technique has also been further developed to incorporate a second dimension where the separated native complexes can be run in a reducing gel to separate out their constituent components, further expanding its usefulness (Wittig et al. 2006).

There are a number of advantages to using BN-PAGE for our investigations. It permits us to look at a wide range of complexes ranging in size from 10kD to 10MD. It allows us to determine the approximate size, subunit composition and relative abundance of the complexes. Additionally, it can allow us to determine the presence of monomeric forms of a protein, e.g. whether a protein of interest is present in

multiple complexes simultaneously or whether the composition of the complexes changes upon stimulation. A further advantage is that it is possible to distinguish between interactions that are direct or bridged by another protein e.g. between A-B, A-C, B-C, and A-B-C complexes. The BN-PAGE method can be expanded upon for different types of investigations, for example the NAMOS assay which is a "Native Antibody-based Mobility Shift technique", is used taking advantage of the native nature of the BN-PAGE gels to determine the stoichiometry of protein complexes (Swamy et al. 2007). As with all techniques however there are disadvantages: the MPCs being studied must be in abundance – those that are present in small amounts can be difficult to visualise. The method is quite sensitive, great care must be taken to avoid any SDS contamination at every step so as to not disrupt the complexes of interest. It is important to determine the optimum detergent/lysis conditions for every new investigation as the stabilities of complexes can vary greatly.

3.7.1.3 Principle of BN-PAGE

In normal SDS-PAGE, denatured proteins are coated in SDS so that the proteins are given a charge in relation to its size. Without this, the proteins' charge is mostly dependent on its amino acid composition and not directly proportional to its size. When running native gels the same problem arises, but instead of SDS the anionic dye Coomassie Blue G-250 is used. It performs a similar role to the SDS in that it binds non-specifically to all proteins and coats it in a negative charge, allowing it to migrate towards the anode when running the gel, even at a neutral pH of 7.5. The Coomassie Blue G-250 does not act as a detergent and preserves the structure of the complexes. It also reduces the risk of denaturation and protein aggregation, as the negatively charged complexes will repel each other. It is hydrophobic enough that it

can bind to membrane proteins but is also sufficiently soluble in water (Schägger et al. 1994).

While the first dimension Blue-Native gel separates the intact protein complexes according to their size, a second dimension denaturing gel can separate out the components of these complexes. The separated complexes in the native gel are placed in a reducing sample buffer, allowing the complexes to be separated out into their individual protein components in a standard SDS-PAGE gel. This can show, for example, the composition of particular complexes (**Figure *49***).

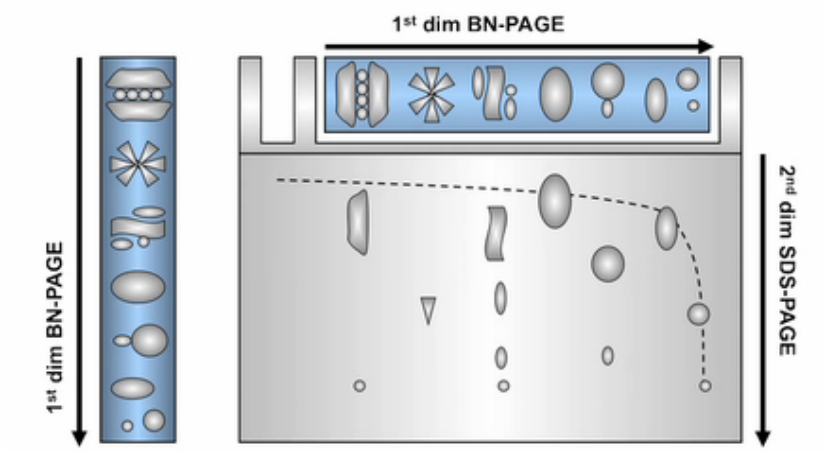

Figure 49: Principle of first and second dimension BN-PAGE

The first dimension BN-PAGE separates whole complexes according to their relative sizes, the second dimension is a denaturing SDS-PAGE gel which separates out the components of the individual complexes. Figure from (Fiala et al. 2011).

3.7.2 Establishing conditions for BN-PAGE experiments

3.7.2.1 Co-Immunoprecipitations

In carrying out our previous co-immunoprecipitations we obtained two key points of information for our BN-PAGE experiments. The first is that the complexes are abundant enough to be detected and secondly it provided a starting point for the buffer conditions under which the complexes of interest may be stable. In previous experiments, DDX3 was successfully co-immunoprecipitated with another protein of interest using Triton X-100 as the detergent. This implied that at least some of the complexes in which DDX3 is involved are abundant enough to be detected by BN-PAGE. Also as Triton X-100 did not disrupt the interaction in normal co-immunoprecipitations, this was the first buffer used in carrying out BN-PAGE with DDX.

3.7.2.2 Choice of detergent

One of the most important things we had to consider in carrying out BN-PAGE is the choice of detergent to be used in the lysis buffer. A balance must be struck with it being strong enough to lyse the cells and solubilise the protein complexes effectively, while not disrupting the complex of interest. A non-ionic detergent must be chosen and samples must have a low ionic strength, as any cations present in the samples will react with the Coomassie in the running buffer, resulting in the precipitation of both the Coomassie and the protein in the sample, leading to impaired entry into the gel [**Figure *50***] (Camacho-Carvajal et al. 2004). For example, 50mM is the maximum tolerated concentration of sodium ions in the samples to allow them to successfully enter the gel (Swamy, Siegers, et al. 2006). When the ionic strength of a sample is too high it starts to precipitate out of solution

and does not enter the gel correctly (**Figure 50**) lanes (A,B). This can be counteracted by running a smaller amount of sample (**Figure 50**) lane (C).

Figure 50: The effect of running a sample with a high ionic strength

Lanes A and B show precipitation of samples in gel wells as the ionic strength was too high resulting in impaired entry into the gel. Lane C shows that this can be counteracted by running a smaller amount of sample. HEK293T cells were lysed in a 0.1% Triton X-100 lysis buffer, dialysed for 6 hours and run on a 4-10% gradient BN-PAGE Gel A -40µl, B – 20µl, C- 10µl.

Common detergents used for BN-PAGE include: digitonin 0.5-1% - one of the mildest detergents, dodecylmaltoside 0.1-0.5% -also a mild detergent but slightly stronger, disrupting some of the weaker hydrophobic interactions, Brij 96 0.1-0.5%, and Triton X-100 0.1-0.5% - under higher concentrations Triton X-100 can solubilise membrane proteins.

A number of things can be done to reduce the ion concentration, including dialysis and immunoprecipitation followed by native elution from the beads (which has the added benefit of concentrating the complex of interest). The second aspect to take into consideration is the concentration of protein in the sample. This is tied with the ionic concentration of the sample and detergent choice. If the concentration of protein is too high it is more likely to precipitate out while running the gel. The

protein samples start to precipitate out of the gel as it reaches the lower parts of the gel with a smaller pore size (**Figure 51**), but if the protein concentration is too low it may be below the detection limit.

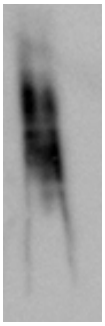

Figure 51: The effect of having protein and/or detergent concentration that is too high.

HEK293T cells were lysed in a 0.5% Triton X-100 lysis buffer, dialysed overnight and run on a 4-10% gradient BN-PAGE Gel, subsequent western blotting and probing with DDX3 antibody [Santa Cruz] was carried out.

Initial experiments were carried out to test several different detergents at various concentrations along with varying cell numbers. The best detergent was determined to be Triton X-100 at a concentration of 0.1% and the ideal cell number was determined to be between 500,000 and 800,000. The combination of these two conditions gave the best detectability of DDX3 from cell lysates and did not result in the precipitation of samples as they ran through the gel (**Figure 52**). It can be seen that a 0.5% Triton X-100 lysis buffer resulted in the sample precipitating out near the bottom of the gel (**Figure *52***).

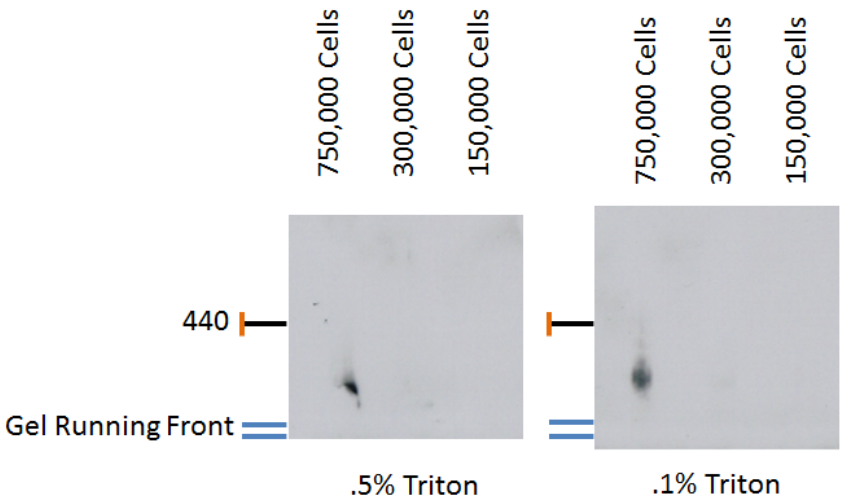

Figure 52: Showing the best conditions for BN-PAGE for DDX3

HEK293T cells were lysed in either a 0.5% or a 0.1% Triton X-100 lysis buffer, dialysed overnight and run on a 4-10% gradient BN-PAGE Gel, subsequent western blotting and probing with DDX3 antibody [Santa Cruz] was carried out.

3.7.3 Aim

We wanted to explore BN-PAGE in order to investigate the multi-protein complexes that DDX3 might be involved in within the cell and to determine whether these complexes change with stimulation. It should also allow us to investigate whether DDX3 exist as a monomer or if higher order complexes exist.

Previous work showed that stimulation-induced complexes could not be resolved (Swamy, Kulathu, et al. 2006). However, we tried to optimise the technique and attempted to see if the complexes that DDX3 is part of change with Sendai Virus (SeV) stimulation. We chose Sendai Virus stimulation, as the role of DDX3 in RIG-I signalling is well established and SeV strongly triggers this pathway. This therefore gives us the best chance at detecting possible changes in DDX3-containing complexes.

3.7.4 Results

3.7.4.1 Stimulation induced changes in DDX3 complexes.

After establishing the conditions necessary to investigate DDX3-containing complexes, we next carried out a comparison of stimulated and unstimulated samples. 24h of SeV stimulation resulted in an increase in the number of bands of DDX3 in the native gels. In unstimulated cells, DDX3 was mostly in one lower size band with some higher bands barely detectable. In the stimulated sample DDX3 seemed to shift from this lower sized band and redistributed to the higher bands (**Figure *53***).

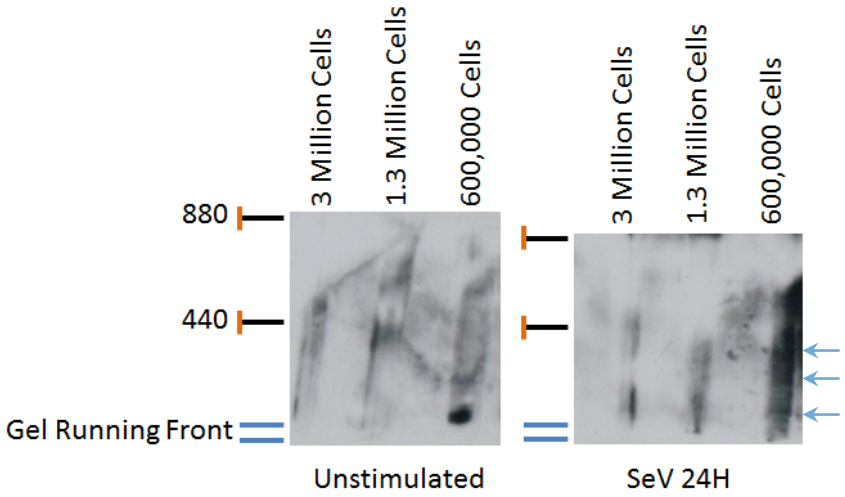

Figure 53: DDX3 redistributes into higher molecular weight bands upon Sendai virus stimulation.

Unstimulated and SeV stimulated (24h) HEK293T cells were lysed in a 0.1% Triton X-100 lysis buffer, dialysed for 6 hours and run on a 4-10% gradient BN-PAGE Gel. Subsequent western blotting and probing with DDX3 antibody [Santa Cruz] was carried out. Arrows show the redistribution of DDX3 in the stimulated sample (Shown is a representative experiment of 3 independent experiments).

To further confirm that the observed bands indeed contained DDX3, we carried out a second dimension SDS-page gel in addition to a first dimension BN-PAGE gel. As some sample is lost upon carrying out the second dimension, we used both a sample using 0.5 million cells (sample D) and one with a higher number cells (2 million) (Sample A). Sample A resulted in a streak in the second dimension which is a result of having a protein concentration that is too high, while in sample D the 2 bands that were apparent in unstimulated cells also gave 2 bands at a molecular weight of 72 in the second dimension denaturing gel, confirming the fact that this was indeed DDX3 (**Figure 54**).

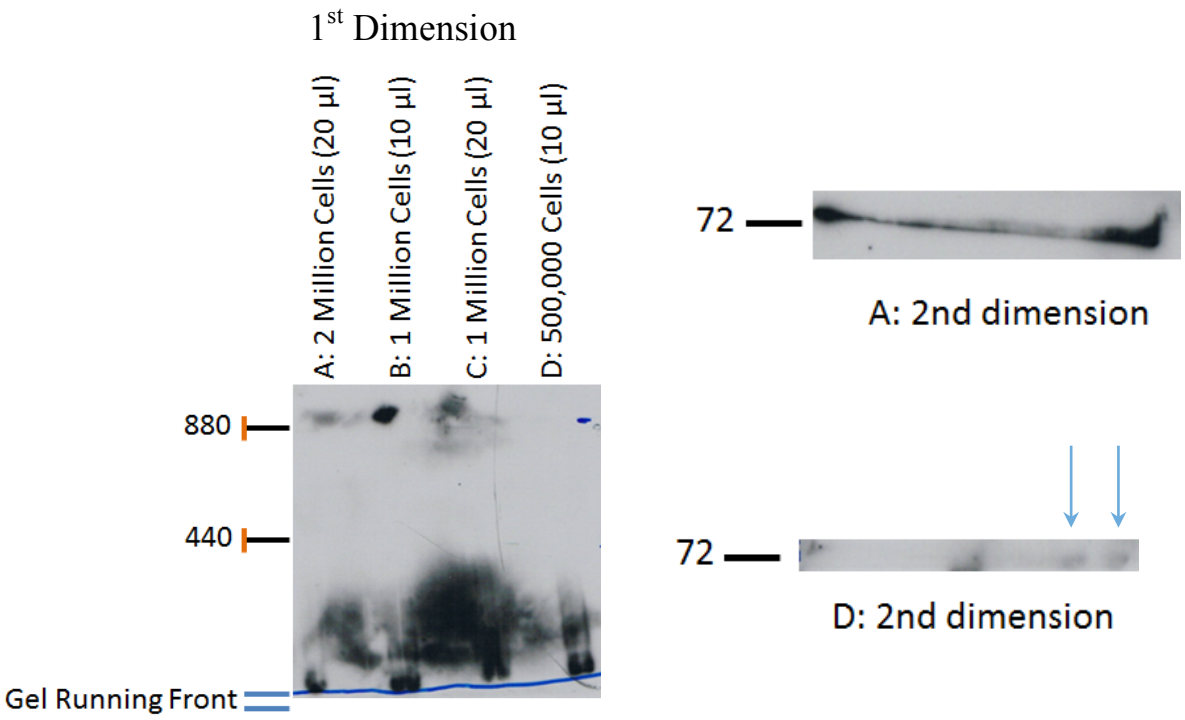

Figure 54: DDX3 appears as two distinct bands in unstimulated cells.

Unstimulated HEK293T cells were lysed in a 0.1% Triton X-100 lysis buffer, dialysed overnight and run on a 4-10% gradient BN-PAGE Gel, subsequent western blotting and probing with DDX3 antibody [Santa Cruz] was carried out [Left Panel] (Shown is a representative experiment of 3 independent experiments). In addition a second dimension SDS-PAGE gel was carried out on samples A and D [Right Panels].

To get a better picture of the changes in DDX3 containing complexes upon stimulation, we carried out experiments with shorter SeV stimulation times. It became apparent that while DDX3 appears as two bands in unstimulated samples this increases to 4 bands after 1 hour of SeV stimulation. These higher bands decrease in intensity at 2h and 4h (**Figure 55)**.

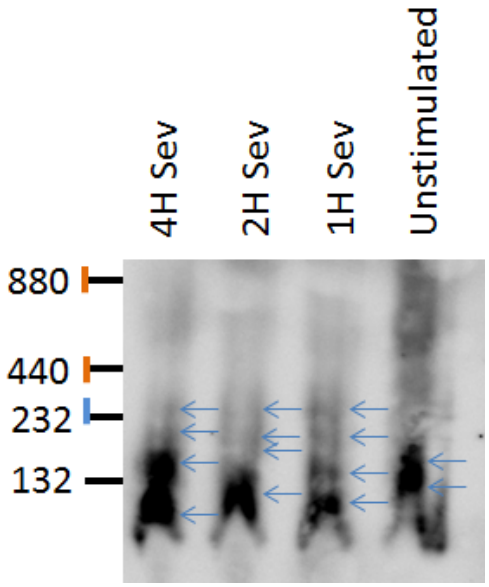

Figure 55: DDX3 changes its banding pattern upon short SeV stimulation.

Unstimulated and SeV stimulated HEK293T cells were lysed in a 0.1% Triton X-100 lysis buffer, dialysed overnight and run on a 4-10% gradient BN-PAGE Gel, subsequent western blotting and probing with DDX3 antibody [Santa Cruz] was carried out. Arrows show the redistribution of DDX3 in the stimulated samples (Shown is a representative experiment of 3 independent experiments).

To determine if the observed higher bands were indeed due to DDX3 being involved in multiple complexes, half of a sample was boiled in SDS and simultaneously run on a BN-PAGE gel along with the other non-boiled half. This was done to disrupt any complexes that were present. In the boiled samples only 2 bands remained, this suggests that the bottom two bands may represent the monomer of DDX3 and possibly a posttranslationally modified form of DDX3 (**Figure 56**) due to the SeV stimulation.

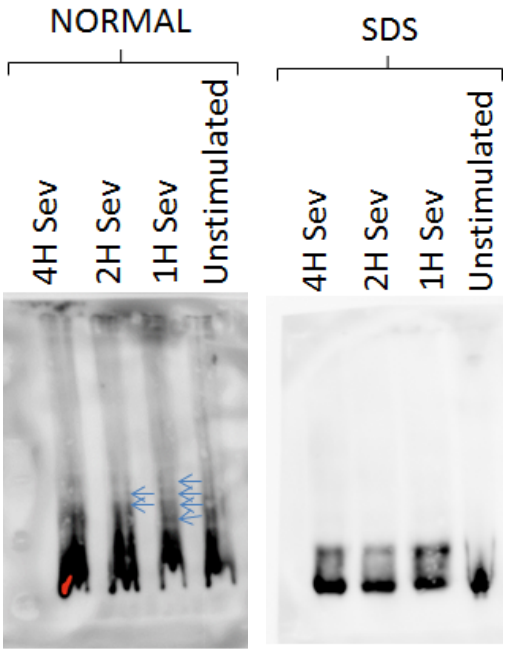

Figure 56: The higher sized bands containing DDX3 disappear upon boiling samples with SDS.

Unstimulated and SeV stimulated HEK293T cells were lysed in a 0.1% Triton X-100 lysis buffer, dialysed for 6 hours, half of each sample was taken and boiled in the presence of SDS and run alongside the non-boiled samples on a 4-10% gradient BN-PAGE Gel, subsequent western blotting and probing with DDX3 antibody [Santa Cruz] was carried out. Arrows show the redistribution of DDX3 in the stimulated un-boiled samples.

3.7.4.2 Investigation of DDX3 oligomers

In addition to our studies on native DDX3 containing complexes in response to SeV stimulation, we investigated the possibility that DDX3 exists as an oligomer. To achieve this we ran purified recombinant His-DDX3 on a BN-PAGE gel. Four bands that corresponded approximately to multiples of DDX3s size were observed (DDX3 MW=72kDa).

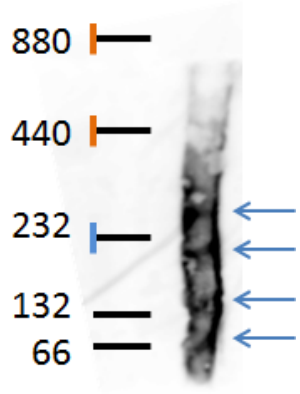

Figure 57: DDX3 may exist as monomer, dimer, trimer and tetramer species.

Purified recombinant His-DDX3 was dialysed overnight and run on a 4-10% gradient BN-PAGE Gel, subsequent western blotting and probing with DDX3 antibody [Santa Cruz] was carried out. Arrows show bands corresponding to multiples of the size of DDX3 (Shown is a representative experiment of 2 independent experiments).

3.7.5 Summary

Here we have used the BN-PAGE method to investigate DDX3 containing complexes. With DDX3 interacting with a number of different signalling mediators, we sought to investigate what complexes are formed and what proteins are involved. Ur results suggest that DDX3 is primarily in 2 main complexes in unstimulated cells [**Figure *54***]. Subsequent experiments involving boiling samples in SDS indicated that this may not in fact be complexes. It instead implied that the higher band was a post-translationally modified form of DDX3, with the majority being a free monomeric species [**Figure *56***]. The pair of bands was still present after denaturation in the stimulated samples, while only one band was present in the boiled unstimulated sample that corresponded to the size of DDX3 protein.

The pattern of banding did change upon SeV stimulation, the lower of the two main bands seen in the unstimulated sample appeared to redistribute to higher molecular weight bands. With increasing stimulation time however these higher bands seemed to reduce in intensity. This suggests that DDX is moving to different complexes upon stimulation and is dissociating from these complexes by the 2 hour time point and reverting back to its resting state. It cannot be excluded however that these higher molecular weight complexes are not simply multimers of DDX3 without further investigation, it would be interesting to further examine the stoichiometry of these DDX3 containing complexes, for example by using the NAMOs assay.

4 Discussion

4.1 The effect of DDX3 on IKKα activity

In this work we aimed to investigate a possible relationship between DDX3 and the kinase IKKα. As DDX3 had previously been shown to be an interaction partner of IKKε (Schröder et al. 2008) and TBK1 (Soulat et al. 2008), we decided to investigate potential interactions with proteins that are closely related to these kinases. IKKα drew our interest as it is involved in multiple important immune signalling pathways and is highly similar to IKKε, showing a 28% aa identity and 45% similarity. A possible interaction with NIK was also investigated as it is a kinase that is known to regulate IKKα in the signalling pathways we are interested in.

We have here established that DDX3 is a direct interaction partner of IKKα. However, while both IKKα and NIK successfully co-immunoprecipitated with DDX3 in overexpression experiments, this experimental set-up does not demonstrate a direct interaction, and the possibility that the interactions are bridged by another protein could not be excluded. In carrying out His-pulldown assays we were able to show that there was a direct interaction between IKKα and DDX3. We also narrowed down the region of DDX3 that IKKα interacts with, using DDX3 truncation mutants. In co-immunoprecipitation studies in cells, we showed that IKKα co-immunoprecipitates with the N-terminal region aa 1-408 region of DDX3. This was confirmed in work carried out by Dr. Lili Gu in our lab, that showed a direct interaction between IKKα and the region between aa 139 and 172 of DDX3. This is in contrast to data on the interaction between DDX3 and IKKε recently published by our lab (Gu et al. 2013). This data suggested that there were at least two sites of IKKε interaction on DDX3, one in the C-terminal region aa 409-662 of DDX3 and

one in the N-terminal aa 1-139 region, with no interaction demonstrated with the aa 139-408 truncation mutant. In the case of IKKα, our data shows that it does not interact with the C-terminal aa 409-662 region of DDX3 but can still interact with an aa 139-408 DDX3 truncation mutant. This suggests that there is at least one site of interaction for IKKα on the N-terminus of DDX3 and that there are functional differences in the interactions between IKKα-DDX3 and IKKε-DDX3.

We have also shown that this interaction can be detected at an endogenous level and can be induced following stimulation with the TLR7/8 ligand CLO75. Our work showing the DDX3 and IKKα interaction is backed up in a recent paper by Li *et al.* that showed an interaction between IKKα and DDX3 was induced by poly(I:C) transfection or HCV infection in Huh 7.5.1 cells (Li et al. 2013). These data confirm that the interaction is relevant in the context of immune signalling in the response to viral infection.

Following on from demonstrating this interaction we have shown that DDX3 can enhance the kinase activity of IKKα. We have previously shown that DDX3 facilitates the auto-phosphorylation and auto-activation of IKKε (Gu et al. 2013). Here we have shown that DDX3 has a similar effect on IKKα. DDX3 also enhances IKKα auto-phosphorylation, including phosphorylation of serines 176/180 located in its activation loop, which is known to activate IKKα in certain contexts (Mercurio 1997). IKKα phosphorylation on Ser176/180 was inducible by CLO75 stimulation and peaked after 1 hour of stimulation, this was clearly reduced in DDX3 knockdown cells. However IKKα phosphorylation was observable at the 4 hour stimulation timepoint suggesting that IKKα activation could still occur, albeit in a somewhat delayed manner. The fact that there were some residual levels of DDX3 in the knockdown cells may contribute to this observed IKKα phosphorylation, but

IKKα may simply be activated via an alternative means that is independent of DDX3 but is involved in a later phase of signalling.

The observations that DDX3 directly interacts with IKKα and enhances its phosphorylation, including phosphorylation in its activation loop, led us to investigate possible effects this interaction may have on pathways that are mediated by IKKα.

4.2 DDX3 enhances signalling downstream of IKKα

Two important immune signalling pathways mediated by IKKα are the TLR7 pathway to IFN induction and the alternative NF-κB pathway. We have shown that the increased activation of IKKα facilitated by DDX3 can result in augmented phosphorylation of its downstream targets, which results in amplified activation of these signalling pathways.

We have shown that DDX3 enhanced p100 processing in the alternative NF-κB pathway and that knockdown of DDX3 reduced both IKKα phosphorylation in its activation loop and p100 phosphorylation which is required for its processing. This, as expected, led to reduced p100 processing to p52 and therefore reduced signalling in this pathway overall. This enhancement of processing may simply be due to the enhancement of IKKα activity by DDX3, but it is also possible that DDX3 may strengthen the interaction between IKKα and p100, as we have shown that DDX3 is constitutively in complex with p100, while the interaction with IKKα is inducible. However, it is clear that DDX3 has a role as a positive regulator of p100 processing and therefore the alternative NF-κB pathway as a whole. As the genes regulated by the alternative NF-κB pathway include those involved in cell cycle progression like *skp2* (Schneider et al. 2006) and genes involved in development of lymphoid organs (Senftleben et al. 2001) this suggest that DDX3 may well play a role in development of lymphoid malignancies (Yu et al. 2012) and autoimmune disorders (Brown et al. 2008).

We have also implicated DDX3 as having a role in the TLR7-mediated pathway to IFN induction. Here, DDX3 also interacted with IRF7, which is a key transcription factor that leads to IFNα4 and IFNβ induction. Overexpression of DDX3 enhanced

induction of both of these IFNs downstream of NIK and IKKα and downstream of CLO75/TLR7 stimulation. We have shown that DDX3 can directly enhance phosphorylation of IRF7 by IKKα, which results in its activation, and leads to increased IFN induction. While we were not able to show significant differences in IFNα4 or IFNβ induction upon knockdown of DDX3, we did show that DDX3 knockdown does reduce the interaction between IKKα and IRF7. It is possible that a significant difference in IFN induction upon knockdown of DDX3 could be observed with improved knockdown of DDX3 and more experimental repeats, as a trend of reduced IFN induction was observed. As DDX3 is not completely knocked down there may still be enough DDX present to enable a certain amount of IRF7 signalling.

While we have shown that the interaction between IKKα and DDX3 has an effect on these two signalling pathways, the study by (Li *et al.* 2013) showed that the IKKα-DDX3 interaction results in an increased lipogenesis pathway induction also. The authors suggested that DDX3 acts to detect HCV 3'UTR RNA and recruits IKKα to induce IKKα mediated signalling. In this case IKKα activates CREB binding protein (CBP)/p300 which enhances SREBP-mediated lipogenesis and lipid droplet formation (Li et al. 2013). As HCV requires lipid droplets for its replication and assembly, this appears to enable viral infection. DDX3 has previously been shown to be required for HCV infection (Ariumi et al. 2007) and it is possible that this enhancement of IKKα activity may contribute to this effect.

With this data combined with our own, DDX3 has now been implicated in at least three pathways that are mediated by IKKα, the alternative NF-κB, the TLR7 and the lipogenesis pathways. However, IKKα is a particularly interesting member of the IKK family. In addition to these roles of IKKα, it has also been implicated in a

number of other important signalling pathways, strengthening its position as a key regulator in innate immunity. It is traditionally known for its involvement in the canonical NF-κB pathway but interestingly, a number of activities that are independent of its direct activity with NF-κB have also become apparent. IKKα has been shown to have roles in the nucleus, for example, it can indirectly enhance NF-κB activity through its phosphorylation of the SMRT co-repressor, resulting in the release of HDAC3 allowing NF-κB mediated transcription (Hoberg et al. 2004). It can also regulate chromatin remodelling, and therefore gene expression, by phosphorylating histone H3 serine 10 through its interaction with CBP (Yamamoto et al. 2003). It is also involved in crosstalk between NF-κB and the tumor suppressor protein p53, as IKKα phosphorylation of CBP switches its binding from p53 to NF-κB. This shifting of the preference of CBP results in increased expression of NF-κB induced genes but a concurrent decreased expression of genes induced by p53(Huang et al. 2007). IKKα is also involved in cell cycle regulation, for example through its phosphorylation of β-catenin (Lamberti et al. 2001), ERα (Park et al. 2005) and SRC3 (Wu et al. 2002), which promote cyclin D1 expression. IKKα can also phosphorylate cyclin D1 itself, which induces its degradation (Kwak et al. 2005) and thus possibly prevents it from being over-induced. As we have now shown that DDX3 plays a role in IKKα activation coupled with the fact that IKKα shows differing effects on a range of gene products it is clear that we are only yet scratching the surface of the varied effects IKKα may have and concurrently the role DDX3 might have also.

4.3 DDX3 acts as a scaffold protein?

There are now two reports suggesting that DDX3 acts as a PRR; Li *et al.* proposed that their observed interaction between DDX3 and IKKα occurs following direct recognition of HCV RNA by DDX3 (Li et al. 2013) and a paper by Oshiumi *et al.* (2010) suggested that DDX3 recognition of HCV RNA results in signalling via RIG-I/mda-5/MAVS to induce IFN induction. In both cases DDX3 appears to act as a PRR to induce downstream signalling. However our data here and our previous studies have shown a role for DDX3 as a downstream signalling adaptor (Gu et al. 2013). Several other studies in addition to our own have also shown a role for DDX3 downstream of IKKε/TBK1 (Soulat et al. 2008; Wang & Ryu 2010; Yu et al. 2010; DeFilippis et al. 2010). My work now places DDX3 as being a signalling adaptor at the level of IKKα. We propose that DDX3 acts as a scaffold that facilitates protein-protein interactions, for example, by bringing kinases in close proximity to their substrates. We have previously shown a role for DDX3 acting as a scaffold protein in IKKε-IRF3 signalling. IKKε interacts with and phosphorylates DDX3 Ser102 which allows IRF3 recruitment, bringing it in close proximity to IKKε acilitating its activation (Gu et al. 2013). In this work we present evidence that DDX3 may function in a similar manner in the enhancement of IKKα-mediated pathways.

We have seen some evidence in our BN-PAGE studies that DDX3 may form multimer species, as we have observed band sizes consistent with monomer, dimer, trimer and tetramer species of DDX3 in native gels. It is therefore conceivable that DDX3 could serve as a platform incorporating a number of different interactors. DDX3 acting as a scaffold could also be the mechanism whereby IKKα auto-activation is increased. Even though DDX3 may possess only one IKKα binding site,

a multimer of DDX3 could still act to bring together IKKα proteins allowing them to phosphorylate each other. The closely related kinase, IKKβ, has previously been shown to possess dimerization domains and the residues present in this domain are also highly conserved in IKKα (Xu et al. 2011), which makes sense as IKKα and IKKβ can form both homodimers and heterodimers with each other. However the authors noted that the structure of the dimers did not allow the kinase domains to be in close proximity to allow transautophosphorylation. They suggested that higher order oligomers may facilitate the activation, as a tetramer formation showed more favourable proximity of kinase domains. They also proposed that NEMO may act as a scaffold to allow this to occur (Xu et al. 2011). DDX3 may act in a similar manner to facilitate the stabilisation of IKKα homo-dimers to allow transautophosphorylation to occur.

While the functional relevance of the phosphorylation of DDX3 by IKKα is still unclear, it may also act in a similar way to the phosphorylation by IKKε, which facilitates the IRF3 interaction. Phosphorylation of DDX3 may change DDX3s potential interaction partners and therefore the substrates which are brought together with IKKα.

Our evidence for DDX3 acting as a scaffold protein comes from the fact that the DDX3 antagonist K7 can inhibit many of the activating effects that we have shown for DDX3. K7 has previously been shown to mask two key residues that are essential for DDX3's enhancement of IKKε induced IRF3 activation and *ifnβ* induction (Oda et al. 2009). The binding of K7 to DDX3 appears to block other interactions from occurring, as transfection of K7 reduced both IRF7-IKKα and NIK-IKKα interactions. We also have some preliminary data showing that NIK and DDX3 may also directly interact (not shown). This suggests that the observed co-

immunoprecipitation between IKKα and NIK may in fact be bridged by DDX3, with both DDX3 and IKKα being pulled down when NIK was immunoprecipitated. In addition we have shown that knockdown of DDX3 results in a decreased NIK-IKKα interaction. As NIK is a known regulator of IKKα activity this obviously has implications for all pathways that they are involved in. The effects of DDX3 on the alternative NF-κB pathway and TLR7 pathway to IFN induction are also consistent with DDX3 acting as a scaffold protein. We have seen that DDX3 can interact with numerous proteins that are in these pathways, such as p100, p52 and p65 in the alternative NF-κB pathway, IRF7 in TLR7 signalling, in addition to IKKα and NIK which activate both pathways. However, it has yet to be determined if the interactions with the transcription factors are direct or possibly bridged by IKKα. DDX3 could act in a similar manner to what we have shown for IRF3 activation bringing together kinases and their substrates (Gu et al. 2013). It is also possible that DDX3 may additionally function in the nucleus via its interaction with the transcription factors p52, p65, and IRF7 as it has been suggested to act directly on the IFNβ promoter where it could allow formation of complexes at the promoter region (Soulat et al. 2008).

A role for DDX3 acting as a scaffold protein has also been shown in a similar manner in work done by Cruciat *et al.* 2013. These authors showed that DDX3 can interact with an unrelated kinase to the IKKs, Casein Kinase 1 (CK1), which is involved in regulation of the Wnt pathway. DDX3 enhanced the activity of this kinase in a strikingly similar manner to what we have shown here for IKKα and previously shown for IKKε. DDX3 appeared to bridge the interaction between CK1 and its substrate, dishevelled, thereby facilitating its phosphorylation. However, in

the case of CK1 activation it was the C-terminus of DDX3 that was required for this, in contrast to the N-terminus for IKKα/ε-mediated pathways.

While the data demonstrating that DDX3 acts as a scaffold protein is quite clear, what has yet to be explained is the inducible nature of DDX3's enhancement of signalling pathways. We have shown that the interaction between IKKα and DDX3 is inducible upon CLO75 stimulation, but we do not yet know the link between stimulation of the TLR7 receptor and the induced interaction.

Another clue may come from our observation that DDX3 may form a tetramer upon stimulation. We do not know what might induce the formation of these higher order structures, but a possible theory may come from the two studies that suggest DDX3 acts as a PRR (Oshiumi, et al. 2010; Li et al. 2013). A common feature among PRRs is that upon recognition of their cognate ligand, oligomerisation takes place. A similar event may occur here also for DDX3. Upon binding of RNA a conformational change might arise in DDX3, (RNA binding by RNA helicases typically results in a change from an open to a closed conformation) resulting in formation of tetramers allowing a greater number of interactors to bind and thereby enhancing signalling. The fact that we did not introduce any exogenous viral RNA in our experimental set-ups may discount this theory. However, we cannot fully exclude the possibility that DDX3 could also recognise the TLR7/8 base analogue ligand, CLO75 which could induce a conformational change in DDX3.

Over-expression of DDX3 could also artificially induce formation of the tetramers, we have seen that recombinant DDX3 BN-PAGE experiments showed band sizes consistent with DDX3 tetramers. The phosphorylation of DDX3 could also theoretically induce oligomerisation. There is also a slight possibility that, with DDX3 interacting with the known PRRS like TLR7, which themselves can dimerise,

could bring DDX3 dimers together. DDX3 has previously been shown to interact with the RIG-I adaptor IPS1, and the fact that RIG-I also forms dimers upon recognition of its ligand (Cui et al. 2008) lends itself to the possibility that two dimers of DDX3 may be brought into close proximity to each other via interactions with other mediators and structural changes could be induced to allow the formation of a tetramer.

Undeniably there are a number of possibilities that have yet to be tested. DDX3 may indeed be a *bone fide* PRR and may recognise similar ligands to TLR7 and RIG-I. DDX3 could play a more passive role, and simply play a scaffolding role downstream of PRRs. In any case it is still unclear as to how DDX3 is activated to exert its effects on IKKα (or indeed IKKε). However, have clearly shown here that it can enhance IKKα activity and that this results in increased induction of the pathways that are mediated by IKKα.

4.4 The effect of IKKα on DDX3

The interaction between IKKα and DDX3 is not one-sided as we have also shown that DDX3 is affected by this interaction by being phosphorylated by IKKα. In our IKKε studies we had previously shown that DDX3 was phosphorylated by IKKε on a number of different serines. Following on from the observation that IKKα induces a shift when co-expressed with IKKα, we compared the phosphorylation of DDX3 by IKKα and IKKε. When one of these two kinases and DDX3 were co-expressed they each resulted in a different shift pattern in DDX3 blots. As IKKα and IKKε seemed to bind DDX3 on different sites, it suggested that they may also phosphorylate different residues, and indeed this was the case. When we tested IKKα phosphorylation of DDX3 with serine to alanine mutations that were found to be phosphorylated by IKKε in a phospho-proteomics screen, several differences were found in DDX3 phosphorylation. This work showed that both IKKα and IKKε share some phosphorylation sites in DDX3, however mutation of these residues did not lead to differences in IFN induction in pathways regulated by IKKα. In reporter assays no significant difference was found in either CLO75 of NIK/IKKα induced IFNβ or IFNα4 induction. It is possible that these residues play minor role in these pathways and effects were undetectable using this system. In any case it is apparent that phosphorylation of these residues by IKKα does not have an essential role in these pathways. It was also interesting to note that there was no significant difference in DDX3 phosphorylation by IKKα when serine 102 was mutated to alanine. We have shown previously that serine 102 phosphorylation by IKKε is essential for *IFNβ* promoter induction in IKKε mediated pathways (Gu et al. 2013). In this case S102 phosphorylation allowed DDX to interact with IRF3, acting as a scaffold to facilitate IRF3 activation by IKKε.

The serine 102 site also appears to be unique to IKKε. We therefore looked for possible sites that may be unique to IKKα. It has been shown previously that IKKα and IKKε can have overlapping and distinct phosphorylation sites on other substrates, for example p65 is phosphorylated on serine 536 by both IKKα and IKKε but on serine 468 by IKKε only (Mattioli et al. 2006). Our phosphoproteomics screen identified serines on DDX3 which are phosphorylated by both kinases (serines 71 and 152), but we also found serines 2, 23 and 86 which appear to be uniquely phosphorylated by IKKα. We produced serine to alanine site mutant constructs to investigate these phosphorylation sites. The preliminary data obtained from luciferase reporter gene assays with these mutants is not yet clear. While the triple serine to alanine mutation of serines 23, 71, and 152 appeared to reduce the enhancement of IFNβ and IFNα4 by DDX3 (**Figure 45 Figure 46 Figure 47 Figure 48**), the addition of an additional mutation of S2A provided results that were harder to explain. The triple mutant of DDX3 points to a possible mechanism that may be similar to what we have shown with IKKε/IRF3 (Gu et al. 2013), that phosphorylation on these sites by IKKα may allow other interactions to occur. We cannot yet however explain the outcome with the quadruple DDX3 mutant, the addition of this mutation appeared to enhance the induction compared to wt DDX3. This could be explained by Ser2 being a site for an inhibitory/regulatory phosphorylation, except for the fact that the S2A mutant alone does not appear to alter the enhancement of IFN induction and the fact that the quadruple mutant has the opposite effect in the case of IFNβ induction induced by NIK/IKKα (**Figure 45**). We cannot yet say anything conclusive as further work needs to be done to characterise these mutants. However the apparent opposing effects of the triple and quadruple serine to alanine mutants of DDX3 may prove to be quite interesting.

Further work must be carried out to confirm these preliminary results, and to test if these serine mutants have altered binding affinity for some of the interactors we have shown here, such as IRF7 and the NF-κB subunits, and to determine whether phosphorylation of DDX3 actually required for interactions. It would also be interesting to investigate if phosphorylation of DDX3 affects its other functions/activities other than its role in IFNβ and IFNα4 induction

4.5 Relevance of the IKKα-DDX3 interaction in disease

This new role for DDX3 in regulating IKKα activity that has been demonstrated here along with its previously described role in regulating IKKε activity, demonstrates that DDX3 is likely a key mediator in innate immune signalling. This is significant in the context of understanding the interplay between pathogens and the immune system. Its importance is greatly increased when we look at the role that these signalling pathways have in a number of diseases, including, for example cancer and auto-immune disorders. With the involvement of DDX3 in IKKα mediated pathways now clear, DDX3 may likely play a role in IKKα-mediated pathways that have been associated with disease.

IKKα is known to have numerous roles in several important signalling pathways, it is not surprising then that alterations in IKKα expression and activity have been detected in various diseases, including a number of cancers (Liu et al. 2012; Nottingham et al. 2013; Margalef et al. 2012). The exact mechanisms of IKKα involvement in tumorgenesis are still unclear, but it appears that the nuclear roles of IKKα might be significant in this respect. A truncated nuclear form of IKKα has been identified to be associated with colorectal cancer and has been suggested as a possible drug target that might leave the other functions of full length IKKα intact (Margalef et al. 2012). In addition, aberrant signalling of the alternative NF-κB pathway has also been linked with various cancer including, multiple myeloma (Busino et al. 2012) and pancreatic cancer (Storz 2013).

Additionally, while the anti-viral TLRs play a key role in recognising foreign nucleic acids, it has become apparent that some are also involved in auto-immune disorders,

where they recognise endogenous nucleic acids. TLR7 and 9 have been heavily implicated as playing a part in the development of systemic lupus erythematosus (SLE) (Celhar et al. 2012); in addition type 1 IFN is used as a biomarker for SLE (Elkon & Wiedeman 2012). For example TLR9 has been shown to be activated in response to SLE-immune complexes, containing DNA and autoantibodies (Means et al. 2005). The autoantibodies bind both the SLE DNA and CD32 receptors, which internalises the autoantibody-DNA immune complex into lysosomes where TLR9 can be activated by the DNA (Means et al. 2005). Similarly, TLR7/8 have been shown to recognise small nuclear ribonucleoprotein particles contained in internalised SLE immune complexes (Vollmer et al. 2005). In addition an IRF5 SNP has been shown to be a risk factor for SLE (Graham et al. 2006) and IRAK1 has a crucial role in SLE (Jacob et al. 2009), further showing that the IFN-induction pathway downstream of TLR7/9 plays a role in this disease. In the case of TLR7/9, it has been suggested that these may be useful targets in the treatment of SLE, which might improve the efficacy of current treatments like glucocorticoids (Guiducci et al. 2010). The fact that DDX3 is now implicated in TLR7 signalling is particularly interesting. As DDX3X is located on the X-chromosome and escapes X-inactivation (Werler et al. 2011), women have higher levels of DDX3 protein than men (unpublished results, Dr. Yvette Höhn, Host-Pathogen interaction Lab). Coupled with the fact that autoimmune diseases, such as SLE, have a far greater prevalence in women than men (Eaton et al. 2007), this makes DDX3 an inviting topic of research in this regard.

TLR7 has been shown to be involved in a number of diseases in addition to SLE, for example it has been suggested as a possible target for asthma treatment as it appears to aid in bronchodilation via induction of nitric oxide upon agonist binding (Drake et

al. 2013). It has also been shown to mediate the early response to malaria infection (Baccarella et al. 2013). TLR inhibitors are an area that may prove to be interesting for the treatment of particular diseases with a number of TLR signalling modulators already in clinical trials, for example the TLR2 antibody OPN-305 is showing some promise in reducing tissue injury following ischemia/reperfusion (Arslan et al. 2012). TLR7 and 9 agonists and antagonists are being developed for a range of treatments (Kandimalla et al. 2013) including cancer (Holldack 2013), sepsis (Boyd 2012), psoriasis (Jiang et al. 2013). DDX3 could also be a potential drug target in the treatment of these diseases due to its role in TLR signalling and modulation of its function could possibly be used in a number of disease cases.

4.6 Conclusion

In this work we have demonstrated a role for the DEAD-box helicase DDX3 in the activation of the kinase IKKα and subsequently two pathways in which IKKα is a key mediator – the alternative NF-κB and the TLR7 pathway to type 1 IFN induction. We have proposed that DDX3 acts as a scaffolding protein to bring IKKα in close proximity to other signalling proteins. It is likely that DDX3 binds both IKKα and NIK which may allow NIK to more easily activate IKKα in some contexts. We have also shown that DDX3 can directly enhance auto-activation of IKKα, possibly by bringing two IKKα proteins together allowing them to phosphorylate each other. The fact that we have shown that DDX3 can interact with so many important mediators in these signalling pathways, including transcription factors, lends itself to the hypothesis that it functions as a scaffold to bring substrates in close proximity to IKKα. Further work must be done to determine if the DDX3 interactions with these IKKα-substrates are direct, if DDX3 function with transcription factors in the nucleus, and if phosphorylation of DDX3 is required for some interactions. With DDX3 being involved in a number of important signalling pathways and a possible link to diseases such as auto-immune disorders, DDX3 may yet prove to be an interesting drug target in the future.

5 References

Alexopoulou, L. et al., 2001. Recognition of double-stranded RNA and activation of NF-kappaB by Toll-like receptor 3. *Nature*, 413(6857), pp.732–8.

Alter, M.J., 2007. Epidemiology of hepatitis C virus infection. *World journal of gastroenterology : WJG*, 13(17), pp.2436–41.

An, H. et al., 2008. Phosphatase SHP-1 promotes TLR- and RIG-I-activated production of type I interferon by inhibiting the kinase IRAK1. *Nature immunology*, 9(5), pp.542–50.

Anderson, K. V, Jürgens, G. & Nüsslein-Volhard, C., 1985. Establishment of dorsal-ventral polarity in the Drosophila embryo: genetic studies on the role of the Toll gene product. *Cell*, 42(3), pp.779–89.

Angus, A.G.N. et al., 2010. Requirement of cellular DDX3 for hepatitis C virus replication is unrelated to its interaction with the viral core protein. *The Journal of general virology*, 91(Pt 1), pp.122–32.

Ariumi, Y. et al., 2007. DDX3 DEAD-box RNA helicase is required for hepatitis C virus RNA replication. *Journal of virology*, 81(24), pp.13922–6.

Arslan, F. et al., 2012. Treatment with OPN-305, a humanized anti-Toll-Like receptor-2 antibody, reduces myocardial ischemia/reperfusion injury in pigs. *Circulation. Cardiovascular interventions*, 5(2), pp.279–87.

Baccarella, A. et al., 2013. Toll-like receptor 7 mediates early innate immune responses to malaria. *Infection and immunity*.

Barnes, B.J. et al., 2004. Global and distinct targets of IRF-5 and IRF-7 during innate response to viral infection. *The Journal of biological chemistry*, 279(43), pp.45194–207.

Barnes, B.J., Field, A.E. & Pitha-Rowe, P.M., 2003. Virus-induced heterodimer formation between IRF-5 and IRF-7 modulates assembly of the IFNA enhanceosome in vivo and transcriptional activity of IFNA genes. *The Journal of biological chemistry*, 278(19), pp.16630–41.

Beg, A.A. & Baldwin, A.S., 1993. The I kappa B proteins: multifunctional regulators of Rel/NF-kappa B transcription factors. *Genes & development*, 7(11), pp.2064–70.

Bernard, N.J. & O'Neill, L.A., 2013. Mal, more than a bridge to MyD88. *IUBMB life*, 65(9), pp.777–86.

Binder, M. et al., 2011. Molecular mechanism of signal perception and integration by the innate immune sensor retinoic acid-inducible gene-I (RIG-I). *The Journal of biological chemistry*, 286(31), pp.27278–87.

Bonizzi, G. & Karin, M., 2004. The two NF-kappaB activation pathways and their role in innate and adaptive immunity. *Trends in immunology*, 25(6), pp.280–8.

Botlagunta, M. et al., 2011. Expression of DDX3 is directly modulated by hypoxia inducible factor-1 alpha in breast epithelial cells. *PloS one*, 6(3), p.e17563.

Botlagunta, M. et al., 2008. Oncogenic role of DDX3 in breast cancer biogenesis. *Oncogene*, 27(28), pp.3912–22.

Boyd, J.H., 2012. Toll-like receptors and opportunities for new sepsis therapeutics. *Current infectious disease reports*, 14(5), pp.455–61.

Van den Broek, M.F. et al., 1995. Antiviral defense in mice lacking both alpha/beta and gamma interferon receptors. *Journal of virology*, 69(8), pp.4792–6.

Brown, K.D., Claudio, E. & Siebenlist, U., 2008. The roles of the classical and alternative nuclear factor-kappaB pathways: potential implications for autoimmunity and rheumatoid arthritis. *Arthritis research & therapy*, 10(4), p.212.

Broz, P. & Monack, D.M., 2013. Newly described pattern recognition receptors team up against intracellular pathogens. *Nature reviews. Immunology*, 13(8), pp.551–65.

Bruni, D. et al., 2013. A novel IRAK1-IKKε signaling axis limits the activation of TAK1-IKKβ downstream of TLR3. *Journal of immunology (Baltimore, Md. : 1950)*, 190(6), pp.2844–56.

Busino, L., Millman, S.E. & Pagano, M., 2012. SCF-mediated degradation of p100 (NF-κB2): mechanisms and relevance in multiple myeloma. *Science signaling*, 5(253), p.pt14.

Camacho-Carvajal, M.M. et al., 2004. Two-dimensional Blue native/SDS gel electrophoresis of multi-protein complexes from whole cellular lysates: a proteomics approach. *Molecular & cellular proteomics : MCP*, 3(2), pp.176–82.

Carty, M. et al., 2006. The human adaptor SARM negatively regulates adaptor protein TRIF-dependent Toll-like receptor signaling. *Nature immunology*, 7(10), pp.1074–81.

Caruthers, J.M. & McKay, D.B., 2002. Helicase structure and mechanism. *Current opinion in structural biology*, 12(1), pp.123–33.

Celhar, T., Magalhães, R. & Fairhurst, A.-M., 2012. TLR7 and TLR9 in SLE: when sensing self goes wrong. *Immunologic research*, 53(1-3), pp.58–77.

Chahar, H.S., Chen, S. & Manjunath, N., 2013. P-body components LSM1, GW182, DDX3, DDX6 and XRN1 are recruited to WNV replication sites and positively regulate viral replication. *Virology*, 436(1), pp.1–7.

Chang, P.-C. et al., 2006. DDX3, a DEAD box RNA helicase, is deregulated in hepatitis virus-associated hepatocellular carcinoma and is involved in cell growth control. *Oncogene*, 25(14), pp.1991–2003.

Chang, Z.L., 2010. Important aspects of Toll-like receptors, ligands and their signaling pathways. *Inflammation research : official journal of the European Histamine Research Society ... [et al.]*, 59(10), pp.791–808.

Chao, C.-H. et al., 2006. DDX3, a DEAD box RNA helicase with tumor growth-suppressive property and transcriptional regulation activity of the p21waf1/cip1 promoter, is a candidate tumor suppressor. *Cancer research*, 66(13), pp.6579–88.

Chatzigeorgiou, A. et al., CD40/CD40L signaling and its implication in health and disease. *BioFactors (Oxford, England)*, 35(6), pp.474–83.

Chelbi-Alix, M. et al., 2007. The IRF family, revisited. *Biochimie*, 89(6), pp.744–753.

Chen, W. & Royer, W.E., 2010. Structural insights into interferon regulatory factor activation. *Cellular signalling*, 22(6), pp.883–7.

Cherfils-Vicini, J. et al., 2010. Triggering of TLR7 and TLR8 expressed by human lung cancer cells induces cell survival and chemoresistance. *The Journal of clinical investigation*, 120(4), pp.1285–97.

Chiu, Y.-H., Macmillan, J.B. & Chen, Z.J., 2009. RNA polymerase III detects cytosolic DNA and induces type I interferons through the RIG-I pathway. *Cell*, 138(3), pp.576–91.

Choi, Y.-J. & Lee, S.-G., 2012. The DEAD-box RNA helicase DDX3 interacts with DDX5, co-localizes with it in the cytoplasm during the G2/M phase of the cycle, and affects its shuttling during mRNP export. *Journal of cellular biochemistry*, 113(3), pp.985–96.

Clark, K. et al., 2011. Novel cross-talk within the IKK family controls innate immunity. *The Biochemical journal*, 434(1), pp.93–104.

Claudio, E. et al., 2002. BAFF-induced NEMO-independent processing of NF-kappa B2 in maturing B cells. *Nature immunology*, 3(10), pp.958–65.

Colonna, M., 2007. TLR pathways and IFN-regulatory factors: to each its own. *European journal of immunology*, 37(2), pp.306–9.

Cordin, O. et al., 2006. The DEAD-box protein family of RNA helicases. *Gene*, 367(null), pp.17–37.

Cruciat, C.-M. et al., 2013. RNA helicase DDX3 is a regulatory subunit of casein kinase 1 in Wnt-β-catenin signaling. *Science (New York, N.Y.)*, 339(6126), pp.1436–41.

Cui, S. et al., 2008. The C-terminal regulatory domain is the RNA 5'-triphosphate sensor of RIG-I. *Molecular Cell*, 29(2), pp.169–79.

DeFilippis, V.R. et al., 2010. Human cytomegalovirus induces the interferon response via the DNA sensor ZBP1. *Journal of virology*, 84(1), pp.585–98.

Der, S.D. et al., 1998. Identification of genes differentially regulated by interferon alpha, beta, or gamma using oligonucleotide arrays. *Proceedings of the National Academy of Sciences of the United States of America*, 95, pp.15623–15628.

Doyle, S.L. & O'Neill, L. a J., 2006. Toll-like receptors: from the discovery of NFkappaB to new insights into transcriptional regulations in innate immunity. *Biochemical pharmacology*, 72(9), pp.1102–13.

Drake, M.G. et al., 2013. Toll-like Receptor 7 Rapidly Relaxes Human Airways. *American journal of respiratory and critical care medicine*, 188(6), pp.664–72.

Eaton, W.W. et al., 2007. Epidemiology of autoimmune diseases in Denmark. *Journal of autoimmunity*, 29(1), pp.1–9.

Elkon, K.B. & Wiedeman, A., 2012. Type I IFN system in the development and manifestations of SLE. *Current opinion in rheumatology*, 24(5), pp.499–505.

Fairman-Williams, M.E., Guenther, U.-P. & Jankowsky, E., 2010. SF1 and SF2 helicases: family matters. *Current opinion in structural biology*, 20(3), pp.313–24.

Fiala, G.J., Schamel, W.W.A. & Blumenthal, B., 2011. Blue native polyacrylamide gel electrophoresis (BN-PAGE) for analysis of multiprotein complexes from cellular lysates. *Journal of visualized experiments : JoVE*, (48).

Fitzgerald, K.A., McWhirter, S.M., et al., 2003. IKKepsilon and TBK1 are essential components of the IRF3 signaling pathway. *Nature immunology*, 4(5), pp.491–6.

Fitzgerald, K.A., Rowe, D.C., et al., 2003. LPS-TLR4 signaling to IRF-3/7 and NF-kappaB involves the toll adapters TRAM and TRIF. *The Journal of experimental medicine*, 198(7), pp.1043–55.

Fitzgerald, K.A. et al., 2001. Mal (MyD88-adapter-like) is required for Toll-like receptor-4 signal transduction. *Nature*, 413(6851), pp.78–83.

Fullam, A. & Schröder, M., 2013. DExD/H-box RNA helicases as mediators of anti-viral innate immunity and essential host factors for viral replication. *Biochimica et biophysica acta*, 1829(8), pp.854–65.

Fuller-Pace, F. V, 2006. DExD/H box RNA helicases: multifunctional proteins with important roles in transcriptional regulation. *Nucleic acids research*, 34(15), pp.4206–15.

Fuller-Pace, F. V, 1994. RNA helicases: modulators of RNA structure. *Trends in cell biology*, 4(8), pp.271–4.

Fuller-Pace, F. V & Nicol, S.M., 2012. DEAD-box RNA helicases as transcription cofactors. *Methods in enzymology*, 511, pp.347–67.

Gay, N.J., Gangloff, M. & O'Neill, L.A.J., 2011. What the Myddosome structure tells us about the initiation of innate immunity. *Trends in immunology*, 32(3), pp.104–9.

Geissler, R., Golbik, R.P. & Behrens, S.-E., 2012. The DEAD-box helicase DDX3 supports the assembly of functional 80S ribosomes. *Nucleic acids research*, 40(11), pp.4998–5011.

Giardino Torchia, M.L., Conze, D.B. & Ashwell, J.D., 2013. c-IAP1 and c-IAP2 redundancy differs between T and B cells. *PloS one*, 8(6), p.e66161.

Gorbalenya, A.E. et al., 1989. Two related superfamilies of putative helicases involved in replication, recombination, repair and expression of DNA and RNA genomes. *Nucleic acids research*, 17(12), pp.4713–30.

Gorbalenya, A.E. & Koonin, E. V., 1993. Helicases: amino acid sequence comparisons and structure-function relationships. *Current Opinion in Structural Biology*, 3(3), pp.419–429.

Gorden, K.B. et al., 2005. Synthetic TLR agonists reveal functional differences between human TLR7 and TLR8. *Journal of immunology (Baltimore, Md. : 1950)*, 174(3), pp.1259–68.

Graham, R.R. et al., 2006. A common haplotype of interferon regulatory factor 5 (IRF5) regulates splicing and expression and is associated with increased risk of systemic lupus erythematosus. *Nature genetics*, 38(5), pp.550–5.

Gu, L. et al., 2013. The human DEAD-box helicase 3 couples IKK-epsilon to IRF3 activation. *Molecular and cellular biology*.

Guiducci, C. et al., 2010. TLR recognition of self nucleic acids hampers glucocorticoid activity in lupus. *Nature*, 465(7300), pp.937–41.

Guttridge, D.C. et al., 1999. NF-kappaB controls cell growth and differentiation through transcriptional regulation of cyclin D1. *Molecular and cellular biology*, 19(8), pp.5785–99.

Han, K.-J. et al., 2004. Mechanisms of the TRIF-induced interferon-stimulated response element and NF-kappaB activation and apoptosis pathways. *The Journal of biological chemistry*, 279(15), pp.15652–61.

Heil, F. et al., 2004. Species-specific recognition of single-stranded RNA via toll-like receptor 7 and 8. *Science (New York, N.Y.)*, 303(5663), pp.1526–9.

Hemmi, H. et al., 2000. A Toll-like receptor recognizes bacterial DNA. *Nature*, 408(6813), pp.740–5.

Hemmi, H. et al., 2002. Small anti-viral compounds activate immune cells via the TLR7 MyD88-dependent signaling pathway. *Nature immunology*, 3(2), pp.196–200.

Hemmi, H. et al., 2004. The roles of two IkappaB kinase-related kinases in lipopolysaccharide and double stranded RNA signaling and viral infection. *The Journal of experimental medicine*, 199(12), pp.1641–50.

Hickman, A.B. & Dyda, F., 2005. Binding and unwinding: SF3 viral helicases. *Current opinion in structural biology*, 15(1), pp.77–85.

Hoberg, J.E., Yeung, F. & Mayo, M.W., 2004. SMRT derepression by the IkappaB kinase alpha: a prerequisite to NF-kappaB transcription and survival. *Molecular cell*, 16(2), pp.245–55.

Holldack, J., 2013. Toll-like receptors as therapeutic targets for cancer. *Drug discovery today*.

Holmes, E.C., 2007. Viral evolution in the genomic age. *PLoS biology*, 5(10), p.e278.

Horng, T., Barton, G.M. & Medzhitov, R., 2001. TIRAP: an adapter molecule in the Toll signaling pathway. *Nature immunology*, 2(9), pp.835–41.

Hoshino, K. et al., 2006. IkappaB kinase-alpha is critical for interferon-alpha production induced by Toll-like receptors 7 and 9. *Nature*, 440(7086), pp.949–53.

Huang, W.-C. et al., 2007. Phosphorylation of CBP by IKKalpha promotes cell growth by switching the binding preference of CBP from p53 to NF-kappaB. *Molecular cell*, 26(1), pp.75–87.

Hultmark, D., 1994. Macrophage Differentiation Marker MyD88 Is a Member of the Toll/IL-1 Receptor Family. *Biochemical and Biophysical Research Communications*, 199(1), pp.144–146.

Ishaq, M. et al., 2008. Knockdown of cellular RNA helicase DDX3 by short hairpin RNAs suppresses HIV-1 viral replication without inducing apoptosis. *Molecular biotechnology*, 39(3), pp.231–8.

Ishii, K.J. et al., 2006. A Toll-like receptor-independent antiviral response induced by double-stranded B-form DNA. *Nature immunology*, 7(1), pp.40–8.

Ishikawa, H. & Barber, G.N., 2008. STING is an endoplasmic reticulum adaptor that facilitates innate immune signalling. *Nature*, 455(7213), pp.674–8.

Ito, T., 2002. Interferon-alpha and Interleukin-12 Are Induced Differentially by Toll-like Receptor 7 Ligands in Human Blood Dendritic Cell Subsets. *Journal of Experimental Medicine*, 195(11), pp.1507–1512.

Jacob, C.O. et al., 2009. Identification of IRAK1 as a risk gene with critical role in the pathogenesis of systemic lupus erythematosus. *Proceedings of the National Academy of Sciences of the United States of America*, 106(15), pp.6256–61.

Jacobs, B.L. & Langland, J.O., 1996. When Two Strands Are Better Than One: The Mediators and Modulators of the Cellular Responses to Double-Stranded RNA. *Virology*, 219(2), pp.339–349.

Jiang, W. et al., 2013. A Toll-like receptor 7, 8, and 9 antagonist inhibits Th1 and Th17 responses and inflammasome activation in a model of IL-23-induced psoriasis. *The Journal of investigative dermatology*, 133(7), pp.1777–84.

Johnson, E.R. & McKay, D.B., 1999. Crystallographic structure of the amino terminal domain of yeast initiation factor 4A, a representative DEAD-box RNA helicase. *RNA (New York, N.Y.)*, 5(12), pp.1526–34.

Jorba, N. et al., 2008. Analysis of the interaction of influenza virus polymerase complex with human cell factors. *Proteomics*, 8(10), pp.2077–88.

Kandimalla, E.R. et al., 2013. Design, synthesis and biological evaluation of novel antagonist compounds of Toll-like receptors 7, 8 and 9. *Nucleic acids research*, 41(6), pp.3947–61.

Kang, J.-I., Kwon, Y.-C. & Ahn, B.-Y., 2012. Modulation of the type I interferon pathways by culture-adaptive hepatitis C virus core mutants. *FEBS letters*, 586(9), pp.1272–8.

Katze, M.G., He, Y.P. & Gale, M., 2002. Viruses and interferon: A fight for supremacy. *Nature Reviews Immunology*, 2, pp.675–687.

Kawagoe, T. et al., 2008. Sequential control of Toll-like receptor-dependent responses by IRAK1 and IRAK2. *Nature immunology*, 9(6), pp.684–91.

Kawai, T. & Akira, S., 2010. The role of pattern-recognition receptors in innate immunity: update on Toll-like receptors. *Nature immunology*, 11(5), pp.373–84.

Kayagaki, N. et al., 2002. BAFF/BLyS receptor 3 binds the B cell survival factor BAFF ligand through a discrete surface loop and promotes processing of NF-kappaB2. *Immunity*, 17(4), pp.515–24.

Kim, T. et al., 2010. Aspartate-glutamate-alanine-histidine box motif (DEAH)/RNA helicase A helicases sense microbial DNA in human plasmacytoid dendritic

cells. *Proceedings of the National Academy of Sciences of the United States of America*, 107(34), pp.15181–6.

Kim, Y.S.S. et al., 2001. Gene structure of the human DDX3 and chromosome mapping of its related sequences. *Molecules and cells*, 12(2), pp.209–214.

Koonin, E. V, Senkevich, T.G. & Dolja, V. V, 2006. The ancient Virus World and evolution of cells. *Biology direct*, 1, p.29.

Kotenko, S. V et al., 2003. IFN-lambdas mediate antiviral protection through a distinct class II cytokine receptor complex. *Nature immunology*, 4(1), pp.69–77.

Krishnan, V. & Zeichner, S.L., 2004. Alterations in the expression of DEAD-box and other RNA binding proteins during HIV-1 replication. *Retrovirology*, 1, p.42.

Kwak, Y.-T. et al., 2005. IkappaB kinase alpha regulates subcellular distribution and turnover of cyclin D1 by phosphorylation. *The Journal of biological chemistry*, 280(40), pp.33945–52.

Kwong, A.D., Rao, B.G. & Jeang, K.-T., 2005. Viral and cellular RNA helicases as antiviral targets. *Nature reviews. Drug discovery*, 4(10), pp.845–53.

Lahn, B.T., 1997. Functional Coherence of the Human Y Chromosome. *Science*, 278(5338), pp.675–680.

Lamberti, C. et al., 2001. Regulation of beta-catenin function by the IkappaB kinases. *The Journal of biological chemistry*, 276(45), pp.42276–86.

Lee, H.K. et al., 2007. Autophagy-dependent viral recognition by plasmacytoid dendritic cells. *Science (New York, N.Y.)*, 315(5817), pp.1398–401.

Leipe, D.D. et al., 2002. Classification and evolution of P-loop GTPases and related ATPases. *Journal of molecular biology*, 317(1), pp.41–72.

Lemaitre, B. et al., 1996. The dorsoventral regulatory gene cassette spätzle/Toll/cactus controls the potent antifungal response in Drosophila adults. *Cell*, 86(6), pp.973–83.

Li, Q. et al., 2013. Hepatitis C virus infection activates an innate pathway involving IKK-α in lipogenesis and viral assembly. *Nature medicine*, 19(6), pp.722–9.

Li, S. et al., 2002. IRAK-4: a novel member of the IRAK family with the properties of an IRAK-kinase. *Proceedings of the National Academy of Sciences of the United States of America*, 99(8), pp.5567–72.

Liang, C., Zhang, M. & Sun, S.-C., 2006. beta-TrCP binding and processing of NF-kappaB2/p100 involve its phosphorylation at serines 866 and 870. *Cellular signalling*, 18(8), pp.1309–17.

Liao, G. et al., 2004. Regulation of the NF-kappaB-inducing kinase by tumor necrosis factor receptor-associated factor 3-induced degradation. *The Journal of biological chemistry*, 279(25), pp.26243–50.

Lin, R., Mamane, Y. & Hiscott, J., 2000. Multiple regulatory domains control IRF-7 activity in response to virus infection. *The Journal of biological chemistry*, 275(44), pp.34320–7.

Lin, S.-C., Lo, Y.-C. & Wu, H., 2010. Helical assembly in the MyD88-IRAK4-IRAK2 complex in TLR/IL-1R signalling. *Nature*, 465(7300), pp.885–90.

Linder, P. et al., 1989. Birth of the D-E-A-D box. *Nature*, 337(6203), pp.121–2.

Ling, L., Cao, Z. & Goeddel, D. V, 1998. NF-kappaB-inducing kinase activates IKK-alpha by phosphorylation of Ser-176. *Proceedings of the National Academy of Sciences of the United States of America*, 95(7), pp.3792–7.

Liu, H. et al., 2012. Screening of autoantibodies as potential biomarkers for hepatocellular carcinoma by using T7 phase display system. *Cancer epidemiology*, 36(1), pp.82–8.

Liu, S. et al., 2012. IκB kinase alpha and cancer. *Journal of interferon & cytokine research : the official journal of the International Society for Interferon and Cytokine Research*, 32(4), pp.152–8.

Lu, R., Moore, P.A. & Pitha, P.M., 2002. Stimulation of IRF-7 gene expression by tumor necrosis factor alpha: requirement for NFkappa B transcription factor and gene accessibility. *The Journal of biological chemistry*, 277(19), pp.16592–8.

Lund, J. et al., 2003. Toll-like receptor 9-mediated recognition of Herpes simplex virus-2 by plasmacytoid dendritic cells. *The Journal of experimental medicine*, 198(3), pp.513–20.

Maga, G. et al., 2008. Pharmacophore Modeling and Molecular Docking Led to the Discovery of Inhibitors of Human Immunodeficiency Virus-1 Replication Targeting the Human Cellular Acid-Alanine-Aspartic Acid Box Polypeptide 3. *Journal of Medicinal Chemistryournal of Medicinal Chemistry*, 51(21), pp.6635–6638.

Mamiya, N. & Worman, H.J., 1999. Hepatitis C virus core protein binds to a DEAD box RNA helicase. *The Journal of biological chemistry*, 274(22), pp.15751–6.

Mancino, A. et al., 2013. I kappa B kinase alpha (IKKα) activity is required for functional maturation of dendritic cells and acquired immunity to infection. *The EMBO journal*, 32(6), pp.816–28.

Margalef, P. et al., 2012. A truncated form of IKKα is responsible for specific nuclear IKK activity in colorectal cancer. *Cell reports*, 2(4), pp.840–54.

Marié, I., Durbin, J.E. & Levy, D.E., 1998. Differential viral induction of distinct interferon-alpha genes by positive feedback through interferon regulatory factor-7. *The EMBO journal*, 17(22), pp.6660–9.

Mattioli, I. et al., 2006. Inducible phosphorylation of NF-kappa B p65 at serine 468 by T cell costimulation is mediated by IKK epsilon. *The Journal of biological chemistry*, 281(10), pp.6175–83.

Means, T.K. et al., 2005. Human lupus autoantibody-DNA complexes activate DCs through cooperation of CD32 and TLR9. *The Journal of clinical investigation*, 115(2), pp.407–17.

Medzhitov, R., Preston-Hurlburt, P. & Janeway, C.A., 1997. A human homologue of the Drosophila Toll protein signals activation of adaptive immunity. *Nature*, 388(6640), pp.394–7.

Mercurio, F., 1997. IKK-1 and IKK-2: Cytokine-Activated IB Kinases Essential for NF-B Activation. *Science*, 278(5339), pp.860–866.

Merika, M. et al., 1998. Recruitment of CBP/p300 by the IFN beta enhanceosome is required for synergistic activation of transcription. *Molecular cell*, 1(2), pp.277–87.

Miyashita, M. et al., 2011. DDX60, a DEXD/H box helicase, is a novel antiviral factor promoting RIG-I-like receptor-mediated signaling. *Molecular and cellular biology*, 31(18), pp.3802–19.

Moon, E.-Y. & Park, H., 2007. B cell activating factor (BAFF) gene promoter activity depends upon co-activator, p300. *Immunobiology*, 212(8), pp.637–45.

Mori, N. & Prager, D., 1996. Transactivation of the interleukin-1alpha promoter by human T-cell leukemia virus type I and type II Tax proteins. *Blood*, 87(8), pp.3410–7.

Moriguchi, T. et al., 1996. A novel kinase cascade mediated by mitogen-activated protein kinase kinase 6 and MKK3. *The Journal of biological chemistry*, 271(23), pp.13675–9.

Moriuchi, H., Moriuchi, M. & Fauci, A.S., 1997. Nuclear factor-kappa B potently up-regulates the promoter activity of RANTES, a chemokine that blocks HIV infection. *Journal of immunology (Baltimore, Md. : 1950)*, 158(7), pp.3483–91.

Morrison, M.D. et al., 2005. An atypical tumor necrosis factor (TNF) receptor-associated factor-binding motif of B cell-activating factor belonging to the TNF family (BAFF) receptor mediates induction of the noncanonical NF-kappaB signaling pathway. *The Journal of biological chemistry*, 280(11), pp.10018–24.

Motshwene, P.G. et al., 2009. An oligomeric signaling platform formed by the Toll-like receptor signal transducers MyD88 and IRAK-4. *The Journal of biological chemistry*, 284(37), pp.25404–11.

Müller, J.R. & Siebenlist, U., 2003. Lymphotoxin beta receptor induces sequential activation of distinct NF-kappa B factors via separate signaling pathways. *The Journal of biological chemistry*, 278(14), pp.12006–12.

Muzio, M. et al., 1997. IRAK (Pelle) family member IRAK-2 and MyD88 as proximal mediators of IL-1 signaling. *Science (New York, N.Y.)*, 278(5343), pp.1612–5.

Nabel, G.J. & Verma, I.M., 1993. Proposed NF-kappa B/I kappa B family nomenclature. *Genes & development*, 7(11), p.2063.

Neumann, D. et al., 2008. Threonine 66 in the death domain of IRAK-1 is critical for interaction with signaling molecules but is not a target site for autophosphorylation. *Journal of leukocyte biology*, 84(3), pp.807–13.

Ning, S. et al., 2003. Interferon regulatory factor 7 regulates expression of Epstein-Barr virus latent membrane protein 1: a regulatory circuit. *Journal of virology*, 77(17), pp.9359–68.

Nishiya, T. & DeFranco, A.L., 2004. Ligand-regulated chimeric receptor approach reveals distinctive subcellular localization and signaling properties of the Toll-like receptors. *The Journal of biological chemistry*, 279(18), pp.19008–17.

Nottingham, L.K. et al., 2013. Aberrant IKKα and IKKβ cooperatively activate NF-κB and induce EGFR/AP1 signaling to promote survival and migration of head and neck cancer. *Oncogene*.

O'Neill, L.A.J. & Bowie, A.G., 2007. The family of five: TIR-domain-containing adaptors in Toll-like receptor signalling. *Nature reviews. Immunology*, 7(5), pp.353–64.

O'Neill, L.A.J., Fitzgerald, K.A. & Bowie, A.G., 2003. The Toll-IL-1 receptor adaptor family grows to five members. *Trends in immunology*, 24(6), pp.286–90.

Oda, S.-I., Schröder, M. & Khan, A.R., 2009. Structural basis for targeting of human RNA helicase DDX3 by poxvirus protein K7. *Structure (London, England : 1993)*, 17(11), pp.1528–37.

Oganesyan, G. et al., 2006. Critical role of TRAF3 in the Toll-like receptor-dependent and -independent antiviral response. *Nature*, 439(7073), pp.208–11.

Oshiumi, H., Sakai, K., et al., 2010. DEAD/H BOX 3 (DDX3) helicase binds the RIG-I adaptor IPS-1 to up-regulate IFN-beta-inducing potential. *European journal of immunology*, 40(4), pp.940–8.

Oshiumi, H., Ikeda, M., et al., 2010. Hepatitis C virus core protein abrogates the DDX3 function that enhances IPS-1-mediated IFN-beta induction. *PloS one*, 5(12), p.e14258.

Ota, T. et al., 2004. Complete sequencing and characterization of 21,243 full-length human cDNAs. *Nature genetics*, 36(1), pp.40–5.

Owsianka, a M. & Patel, a H., 1999. Hepatitis C virus core protein interacts with a human DEAD box protein DDX3. *Virology*, 257(2), pp.330–40.

Park, K.-J. et al., 2005. Formation of an IKKalpha-dependent transcription complex is required for estrogen receptor-mediated gene activation. *Molecular cell*, 18(1), pp.71–82.

Pauls, E. et al., 2012. Essential role for IKKβ in production of type 1 interferons by plasmacytoid dendritic cells. *The Journal of biological chemistry*, 287(23), pp.19216–28.

Perkins, N.D., 2007. Integrating cell-signalling pathways with NF-kappaB and IKK function. *Nature reviews. Molecular cell biology*, 8(1), pp.49–62.

Perkins, N.D. & Gilmore, T.D., 2006. Good cop, bad cop: the different faces of NF-kappaB. *Cell death and differentiation*, 13(5), pp.759–72.

Pichlmair, A. et al., 2009. Activation of MDA5 requires higher-order RNA structures generated during virus infection. *Journal of virology*, 83(20), pp.10761–9.

Pippig, D.A. et al., 2009. The regulatory domain of the RIG-I family ATPase LGP2 senses double-stranded RNA. *Nucleic acids research*, 37(6), pp.2014–25.

Prakash, A. & Levy, D.E., 2006. Regulation of IRF7 through cell type-specific protein stability. *Biochemical and biophysical research communications*, 342(1), pp.50–6.

Pyle, A.M., 2008. Translocation and unwinding mechanisms of RNA and DNA helicases. *Annual review of biophysics*, 37, pp.317–36.

Radi, M. et al., 2012. Discovery of the first small molecule inhibitor of human DDX3 specifically designed to target the RNA binding site: towards the next generation HIV-1 inhibitors. *Bioorganic & medicinal chemistry letters*, 22(5), pp.2094–8.

Raj, N.B., Au, W.C. & Pitha, P.M., 1991. Identification of a novel virus-responsive sequence in the promoter of murine interferon-alpha genes. *The Journal of biological chemistry*, 266(17), pp.11360–5.

Randall, G. et al., 2007. Cellular cofactors affecting hepatitis C virus infection and replication. *Proceedings of the National Academy of Sciences of the United States of America*, 104(31), pp.12884–9.

Rothenfusser, S. et al., 2005. The RNA helicase Lgp2 inhibits TLR-independent sensing of viral replication by retinoic acid-inducible gene-I. *The Journal of Immunology*, 175, pp.5260–5268.

Sakurai, H., 1999. Ikappa B Kinases Phosphorylate NF-kappa B p65 Subunit on Serine 536 in the Transactivation Domain. *Journal of Biological Chemistry*, 274(43), pp.30353–30356.

Sanjo, H. et al., 2010. Allosteric regulation of the ubiquitin:NIK and ubiquitin:TRAF3 E3 ligases by the lymphotoxin-beta receptor. *The Journal of biological chemistry*, 285(22), pp.17148–55.

Sato, M. et al., 2000. Distinct and Essential Roles of Transcription Factors IRF-3 and IRF-7 in Response to Viruses for IFN-α/β Gene Induction. *Immunity*, 13(4), pp.539–548.

Satoh, T. et al., 2010. LGP2 is a positive regulator of RIG-I- and MDA5-mediated antiviral responses. *Proceedings of the National Academy of Sciences of the United States of America*, 107, pp.1512–1517.

Sauer, J.-D. et al., 2011. The N-ethyl-N-nitrosourea-induced Goldenticket mouse mutant reveals an essential function of Sting in the in vivo interferon response to Listeria monocytogenes and cyclic dinucleotides. *Infection and immunity*, 79(2), pp.688–94.

Schägger, H., Cramer, W.A. & von Jagow, G., 1994. Analysis of molecular masses and oligomeric states of protein complexes by blue native electrophoresis and isolation of membrane protein complexes by two-dimensional native electrophoresis. *Analytical biochemistry*, 217(2), pp.220–30.

Schägger, H. & von Jagow, G., 1991. Blue native electrophoresis for isolation of membrane protein complexes in enzymatically active form. *Analytical biochemistry*, 199(2), pp.223–31.

Schlee, M. et al., 2009. Recognition of 5’ triphosphate by RIG-I helicase requires short blunt double-stranded RNA as contained in panhandle of negative-strand virus. *Immunity*, 31(1), pp.25–34.

Schmidt, A., Rothenfusser, S. & Hopfner, K.-P., 2012. Sensing of viral nucleic acids by RIG-I: from translocation to translation. *European journal of cell biology*, 91(1), pp.78–85.

Schneider, G. et al., 2006. IKKalpha controls p52/RelB at the skp2 gene promoter to regulate G1- to S-phase progression. *The EMBO journal*, 25(16), pp.3801–12.

Schoenemeyer, A. et al., 2005. The interferon regulatory factor, IRF5, is a central mediator of toll-like receptor 7 signaling. *The Journal of biological chemistry*, 280(17), pp.17005–12.

Schröder, M., 2010. Human DEAD-box protein 3 has multiple functions in gene regulation and cell cycle control and is a prime target for viral manipulation. *Biochemical pharmacology*, 79(3), pp.297–306.

Schröder, M., Baran, M. & Bowie, A.G., 2008. Viral targeting of DEAD box protein 3 reveals its role in TBK1/IKKepsilon-mediated IRF activation. *The EMBO journal*, 27(15), pp.2147–57.

Senftleben, U. et al., 2001. Activation by IKKalpha of a second, evolutionary conserved, NF-kappa B signaling pathway. *Science (New York, N.Y.)*, 293(5534), pp.1495–9.

Seo, Y. et al., 2012. Accumulation of p100, a precursor of NF-κB2, enhances osteoblastic differentiation in vitro and bone formation in vivo in aly/aly mice. *Molecular endocrinology (Baltimore, Md.)*, 26(3), pp.414–22.

Seth, R.B. et al., 2005. Identification and characterization of MAVS, a mitochondrial antiviral signaling protein that activates NF-kappaB and IRF 3. *Cell*, 122(5), pp.669–82.

Shah, S. et al., 2013. Cutting Edge: Mycobacterium tuberculosis but Not Nonvirulent Mycobacteria Inhibits IFN-β and AIM2 Inflammasome-Dependent IL-1β Production via Its ESX-1 Secretion System. *Journal of immunology (Baltimore, Md. : 1950)*, 191(7), pp.3514–8.

Shakhov, A.N. et al., 1990. Kappa B-type enhancers are involved in lipopolysaccharide-mediated transcriptional activation of the tumor necrosis factor alpha gene in primary macrophages. *The Journal of experimental medicine*, 171(1), pp.35–47.

Sharma, S. et al., 2003. Triggering the interferon antiviral response through an IKK-related pathway. *Science (New York, N.Y.)*, 300(5622), pp.1148–51.

Shen, F. et al., 2006. Identification of common transcriptional regulatory elements in interleukin-17 target genes. *The Journal of biological chemistry*, 281(34), pp.24138–48.

Singleton, M.R., Dillingham, M.S. & Wigley, D.B., 2007. Structure and mechanism of helicases and nucleic acid translocases. *Annual review of biochemistry*, 76, pp.23–50.

Son, Y.-H. et al., 2008. Roles of MAPK and NF-kappaB in interleukin-6 induction by lipopolysaccharide in vascular smooth muscle cells. *Journal of cardiovascular pharmacology*, 51(1), pp.71–7.

Soulat, D. et al., 2008. The DEAD-box helicase DDX3X is a critical component of the TANK-binding kinase 1-dependent innate immune response. *The EMBO journal*, 27(15), pp.2135–46.

Storz, P., 2013. Targeting the alternative NF-κB pathway in pancreatic cancer: a new direction for therapy? *Expert review of anticancer therapy*, 13(5), pp.501–4.

Sun, L. et al., 2013. Cyclic GMP-AMP synthase is a cytosolic DNA sensor that activates the type I interferon pathway. *Science (New York, N.Y.)*, 339(6121), pp.786–91.

Sun, M. et al., 2011. The role of DDX3 in regulating Snail. *Biochimica et biophysica acta*, 1813(3), pp.438–47.

Sun, S.-C., 2010. Controlling the fate of NIK: a central stage in noncanonical NF-kappaB signaling. *Science signaling*, 3(123), p.pe18.

Sun, S.-C., 2011. Non-canonical NF-κB signaling pathway. *Cell research*, 21(1), pp.71–85.

Sun, S.-C., 2012. The noncanonical NF-κB pathway. *Immunological reviews*, 246(1), pp.125–40.

Swamy, M. et al., 2007. A native antibody-based mobility-shift technique (NAMOS-assay) to determine the stoichiometry of multiprotein complexes. *Journal of immunological methods*, 324(1-2), pp.74–83.

Swamy, M., Siegers, G.M., et al., 2006. Blue native polyacrylamide gel electrophoresis (BN-PAGE) for the identification and analysis of multiprotein complexes. *Science's STKE : signal transduction knowledge environment*, 2006(345), p.pl4.

Swamy, M., Kulathu, Y., et al., 2006. Two dimensional Blue Native-/SDS-PAGE analysis of SLP family adaptor protein complexes. *Immunology letters*, 104(1-2), pp.131–7.

Takahasi, K. et al., 2009. Solution Structures of Cytosolic RNA Sensor MDA5 and LGP2 C-terminal Domains. *Journal of Biological Chemistry*, 284, pp.17465–17474.

Takaoka, A. et al., 2007. DAI (DLM-1/ZBP1) is a cytosolic DNA sensor and an activator of innate immune response. *Nature*, 448(7152), pp.501–5.

Tanner, N.K., The newly identified Q motif of DEAD box helicases is involved in adenine recognition. *Cell cycle (Georgetown, Tex.)*, 2(1), pp.18–9.

Tanner, N.K. et al., 2003. The Q motif: a newly identified motif in DEAD box helicases may regulate ATP binding and hydrolysis. *Molecular cell*, 11(1), pp.127–38.

Thompson, M.R. et al., 2011. Pattern recognition receptors and the innate immune response to viral infection. *Viruses*, 3(6), pp.920–40.

De Trez, C., 2012. Lymphotoxin-beta receptor expression and its related signaling pathways govern dendritic cell homeostasis and function. *Immunobiology*, 217(12), pp.1250–8.

Uematsu, S. et al., 2005. Interleukin-1 receptor-associated kinase-1 plays an essential role for Toll-like receptor (TLR)7- and TLR9-mediated interferon-{alpha} induction. *The Journal of experimental medicine*, 201(6), pp.915–23.

Unterholzner, L. et al., 2010. IFI16 is an innate immune sensor for intracellular DNA. *Nature immunology*, 11(11), pp.997–1004.

Unterholzner, L., 2013. The interferon response to intracellular DNA: Why so many receptors? *Immunobiology*, 218(11), pp.1312–21.

Vallabhapurapu, S. et al., 2008. Nonredundant and complementary functions of TRAF2 and TRAF3 in a ubiquitination cascade that activates NIK-dependent alternative NF-kappaB signaling. *Nature immunology*, 9(12), pp.1364–70.

Vashist, S. et al., 2012. Identification of RNA-protein interaction networks involved in the norovirus life cycle. *Journal of virology*, 86(22), pp.11977–90.

Ve, T. et al., 2012. Adaptors in toll-like receptor signaling and their potential as therapeutic targets. *Current drug targets*, 13(11), pp.1360–74.

Vollmer, J. et al., 2005. Immune stimulation mediated by autoantigen binding sites within small nuclear RNAs involves Toll-like receptors 7 and 8. *The Journal of experimental medicine*, 202(11), pp.1575–85.

Walker, J.E. et al., 1982. Distantly related sequences in the alpha- and beta-subunits of ATP synthase, myosin, kinases and other ATP-requiring enzymes and a common nucleotide binding fold. *The EMBO journal*, 1(8), pp.945–51.

Wang, C. et al., 2001. TAK1 is a ubiquitin-dependent kinase of MKK and IKK. *Nature*, 412(6844), pp.346–51.

Wang, H. & Ryu, W.-S., 2010. Hepatitis B virus polymerase blocks pattern recognition receptor signaling via interaction with DDX3: implications for immune evasion. *PLoS pathogens*, 6(7), p.e1000986.

Wang, R.-P. et al., 2008. Differential regulation of IKK alpha-mediated activation of IRF3/7 by NIK. *Molecular immunology*, 45(7), pp.1926–34.

Watters, T.M., Kenny, E.F. & O'Neill, L.A.J., Structure, function and regulation of the Toll/IL-1 receptor adaptor proteins. *Immunology and cell biology*, 85(6), pp.411–9.

Werler, S. et al., 2011. Expression of selected genes escaping from X inactivation in the 41, XX(Y)* mouse model for Klinefelter's syndrome. *Acta paediatrica (Oslo, Norway : 1992)*, 100(6), pp.885–91.

Werneburg, B.G. et al., 2001. Molecular characterization of CD40 signaling intermediates. *The Journal of biological chemistry*, 276(46), pp.43334–42.

Wesche, H. et al., 1997. MyD88: An Adapter That Recruits IRAK to the IL-1 Receptor Complex. *Immunity*, 7(6), pp.837–847.

Wietek, C. et al., 2006. IkappaB kinase epsilon interacts with p52 and promotes transactivation via p65. *The Journal of biological chemistry*, 281(46), pp.34973–81.

Wittig, I., Braun, H.-P. & Schägger, H., 2006. Blue native PAGE. *Nature protocols*, 1(1), pp.418–28.

Worm, M.M., Tsytsykova, A. & Geha, R.S., 1998. CD40 ligation and IL-4 use different mechanisms of transcriptional activation of the human lymphotoxin alpha promoter in B cells. *European journal of immunology*, 28(3), pp.901–6.

Wu, D.-W. et al., 2011. Reduced p21(WAF1/CIP1) via alteration of p53-DDX3 pathway is associated with poor relapse-free survival in early-stage human papillomavirus-associated lung cancer. *Clinical cancer research : an official journal of the American Association for Cancer Research*, 17(7), pp.1895–905.

Wu, J. et al., 2013. Cyclic GMP-AMP is an endogenous second messenger in innate immune signaling by cytosolic DNA. *Science (New York, N.Y.)*, 339(6121), pp.826–30.

Wu, R.-C. et al., 2002. Regulation of SRC-3 (pCIP/ACTR/AIB-1/RAC-3/TRAM-1) Coactivator activity by I kappa B kinase. *Molecular and cellular biology*, 22(10), pp.3549–61.

Wu, Y., 2012. Unwinding and rewinding: double faces of helicase? *Journal of nucleic acids*, 2012, p.140601.

Xiao, G., Fong, A. & Sun, S.-C., 2004. Induction of p100 processing by NF-kappaB-inducing kinase involves docking IkappaB kinase alpha (IKKalpha) to p100 and IKKalpha-mediated phosphorylation. *The Journal of biological chemistry*, 279(29), pp.30099–105.

Xiao, G., Harhaj, E.W. & Sun, S.C., 2001. NF-kappaB-inducing kinase regulates the processing of NF-kappaB2 p100. *Molecular cell*, 7(2), pp.401–9.

Xu, G. et al., 2011. Crystal structure of inhibitor of κB kinase β. *Nature*, 472(7343), pp.325–30.

Yamamoto, M. et al., 2002. Cutting edge: a novel Toll/IL-1 receptor domain-containing adapter that preferentially activates the IFN-beta promoter in the Toll-like receptor signaling. *Journal of immunology (Baltimore, Md. : 1950)*, 169(12), pp.6668–72.

Yamamoto, Y. et al., 2003. Histone H3 phosphorylation by IKK-alpha is critical for cytokine-induced gene expression. *Nature*, 423(6940), pp.655–9.

Yang, K. et al., 2005. Human TLR-7-, -8-, and -9-Mediated Induction of IFN-α/β and -λ Is IRAK-4 Dependent and Redundant for Protective Immunity to Viruses. *Immunity*, 23(5), pp.465–478.

Yang, P. et al., 2010. The cytosolic nucleic acid sensor LRRFIP1 mediates the production of type I interferon via a beta-catenin-dependent pathway. *Nature immunology*, 11(6), pp.487–94.

Ye, H. et al., 2002. Distinct molecular mechanism for initiating TRAF6 signalling. *Nature*, 418(6896), pp.443–7.

Yedavalli, V.S.R.K. et al., 2004. Requirement of DDX3 DEAD box RNA helicase for HIV-1 Rev-RRE export function. *Cell*, 119(3), pp.381–92.

Yedavalli, V.S.R.K.V.S.R.K. et al., 2008. Ring expanded nucleoside analogues inhibit RNA helicase and intracellular human immunodeficiency virus type 1 replication. *Journal of medicinal chemistry*, 51(16), pp.5043–5051.

Yoneyama, M. et al., 2004. The RNA helicase RIG-I has an essential function in double-stranded RNA-induced innate antiviral responses. *Nature immunology*, 5(7), pp.730–7.

You, L.R. et al., 1999. Hepatitis C virus core protein interacts with cellular putative RNA helicase. *Journal of virology*, 73(4), pp.2841–53.

Yu, M. et al., 2012. Critical role of B cell lymphoma 10 in BAFF-regulated NF-κB activation and survival of anergic B cells. *Journal of immunology (Baltimore, Md. : 1950)*, 189(11), pp.5185–93.

Yu, S. et al., 2010. Hepatitis B virus polymerase inhibits RIG-I- and Toll-like receptor 3-mediated beta interferon induction in human hepatocytes through interference with interferon regulatory factor 3 activation and dampening of the interaction between TBK1/IKKepsilon and . *The Journal of general virology*, 91(Pt 8), pp.2080–90.

Zarnegar, B.J. et al., 2008. Noncanonical NF-kappaB activation requires coordinated assembly of a regulatory complex of the adaptors cIAP1, cIAP2, TRAF2 and TRAF3 and the kinase NIK. *Nature immunology*, 9(12), pp.1371–8.

Zhang, Z., Kim, T., et al., 2011. DDX1, DDX21, and DHX36 helicases form a complex with the adaptor molecule TRIF to sense dsRNA in dendritic cells. *Immunity*, 34(6), pp.866–78.

Zhang, Z., Yuan, B., Lu, N., et al., 2011. DHX9 pairs with IPS-1 to sense double-stranded RNA in myeloid dendritic cells. *Journal of immunology (Baltimore, Md. : 1950)*, 187(9), pp.4501–8.

Zhang, Z., Yuan, B., Bao, M., et al., 2011. The helicase DDX41 senses intracellular DNA mediated by the adaptor STING in dendritic cells. *Nature immunology*, 12(10), pp.959–65.

Zhong, J. & Kyriakis, J.M., 2007. Dissection of a signaling pathway by which pathogen-associated molecular patterns recruit the JNK and p38 MAPKs and trigger cytokine release. *The Journal of biological chemistry*, 282(33), pp.24246–54.

Zou, J. et al., 2009. Origin and evolution of the RIG-I like RNA helicase gene family. *BMC evolutionary biology*, 9, p.85.

Züst, R. et al., 2011. Ribose 2'-O-methylation provides a molecular signature for the distinction of self and non-self mRNA dependent on the RNA sensor Mda5. *Nature immunology*, 12(2), pp.137–43.

6 Appendix

6.1 Publications

Fullam, A., Gu, L., Hoehn, Y., Schroeder, M.: DDX3 facilitates IKKα-mediated induction of type I interferon promoters. [In preparation] (2013)

Fullam A., Schröder M.: DExD/H-box RNA helicases as mediators of anti-viral innate immunity and essential host factors for viral replication. *Biochim Biophys Acta vol. 1829 854-865 (2013)*

Gu, L., Fullam, A., Brennan, R., Schroeder, M.: The human DEAD-box helicase 3 couples IKK-epsilon to IRF3 activation. *Mol Cell Biol vol.33 2004-15 (2013)*

6.2 DDX3 siRNA sequence

siRNA	Sequence	Identifier
DDX3-2	5'-UUCAACAAGAAGAUCCAACAAAUCC-3'	(HSS102713)

Table 6: siRNA sequence and Identifier (Invitrogen)